POWER QUALITY ENHANCEMENT USING ARTIFICIAL INTELLIGENCE TECHNIQUES

Ahmed S. Abbas, Adel Ali Mohamed Abou El-Ela,
Ragab A. El-Sehiemy, and Adel A. Elbaset

CRC Press
Taylor & Francis Group

Power Quality Enhancement Using Artificial Intelligence Techniques

This text discusses sensitivity parametric analysis for single-tuned filter parameters and presents an optimization-based method for solving the allocation problem of the distributed generation units and capacitor banks in distribution systems. It also highlights the importance of artificial intelligence techniques such as water cycle algorithms in solving power quality problems such as over-voltage and harmonic distortion.

Features:

- Presents a sensitivity parametric analysis for single-tuned filter parameters.
- Discusses optimization-based methods for solving the allocation problem of the distributed generation units and capacitor banks in distribution systems.
- Highlights the importance of artificial intelligence techniques (water cycle algorithm) for solving power quality problems such as over-voltage and harmonic distortion.
- Showcases a procedure for harmonic mitigation in active distribution systems using single-tuned harmonic filters.
- Helps in learning how to determine the optimal planning of single-tuned filters to mitigate harmonic distortion in distorted systems.

It will serve as an ideal reference text for graduate students and academic researchers in the fields of electrical engineering, electronics and communication engineering, and power systems planning and analysis.

Ahmed S. Abbas, Researcher, Electrical Engineering Department, Mechanical and Electrical Research Institute, NWRC, Egypt.

Adel Ali Mohamed Abou El-Ela, Professor of Electrical Power Systems, Electrical Engineering Department, Faculty of Engineering, Shebin El-Kom, Menoufia University.

Ragab A. El-Sehiemy, Professor of Electrical Power Systems, Electrical Engineering Department, Faculty of Engineering, Kafr El-Sheikh, Kafr El-Sheikh University.

Adel A. Elbaset, Professor of Electrical Power Systems, Electrical Engineering Department, Faculty of Engineering, Minia University, EL-Minia, Egypt; Professor of Electrical Power Systems, Department of Electromechanics, Engineering, Faculty of Engineering, Heliopolis University, Cairo, Egypt.

Power Quality Enhancement Using Artificial Intelligence Techniques

Ahmed S. Abbas
Adel Ali Mohamed Abou El-Ela
Ragab A. El-Sehiemy
Adel A. Elbaset

CRC Press
Taylor & Francis Group
Boca Raton London New York

CRC Press is an imprint of the
Taylor & Francis Group, an **informa** business

First edition published 2023
by CRC Press
6000 Broken Sound Parkway NW, Suite 300, Boca Raton, FL 33487-2742

and by CRC Press
4 Park Square, Milton Park, Abingdon, Oxon, OX14 4RN

CRC Press is an imprint of Taylor & Francis Group, LLC

Library of Congress Cataloging-in-Publication Data
Names: Abou El-Ela, Adel Ali Mohamed, author. | Abbas, Ahmed S., author. |
El-Sehiemy, Ragab A., author. | Elbaset, Adel A., author.
Title: Power quality enhancement using Artificial Intelligence techniques /
Adel Ali Mohamed Abou El-Ela, Ahmed S. Abbas, Ragab A. El-Sehiemy, Adel A. Elbaset.
Description: First edition. | Boca Raton : CRC Press, 2023. | Includes
bibliographical references and index. | Identifiers: LCCN 2022043201 (print) |
LCCN 2022043202 (ebook) | ISBN 9781032439228 (hardback) | ISBN 9781032439242 (paperback) |
ISBN 9781003369448 (ebook)
Subjects: LCSH: Electric power systems—Quality control—Data processing. |
Artificial intelligence.
Classification: LCC TK1010 .A25 2023 (print) | LCC TK1010 (ebook) |
DDC 621.31028563—dc23/eng/20221205
LC record available at https://lccn.loc.gov/2022043201
LC ebook record available at https://lccn.loc.gov/2022043202

ISBN: 9781032439228 (hbk)
ISBN: 9781032439242 (pbk)
ISBN: 9781003369448 (ebk)

DOI: 10.1201/9781003369448

Typeset in Times
by codeMantra

Contents

Preface

This book proposes two procedures for improving the power quality (PQ) of the distribution systems. The considered PQ parameters are voltage profile, voltage deviation, voltage stability index and harmonic distortion in smart distribution systems. One of the most important features of smart distribution systems is the presence of distributed generation units (DGs). Therefore, the positive and negative effects of the DGs on distribution system PQ are studied. The first proposed procedure is concerned with determining the optimal placement and sizing of DGs and CBs in distribution system for improving the system PQ besides other technical, economic, and environmental benefits. Also, this book proposes single-tuned filters (STFs) as an effective tool for mitigating the harmonic distortion in distribution systems. A parametric analysis is presented for determining the effect of different filter parameters on its performance, which helps system designers obtain the optimal filter design that can mitigate specific harmonic orders.

Moreover, the second proposed procedure is presented for determining the optimal design, placement and number of STFs to mitigate harmonic distortion in a system. The proposed procedure considers the harmonic content of the inverter-based DGs in the distribution system and its effect in increasing the harmonic distortion. The power quality problems are formulated as optimization problems, which can be solved using the optimization techniques. Therefore, water cycle algorithm (WCA) is formulated as an optimization technique for solving the considered optimization problems. The effectiveness of the WCA is assured through a comparative study with other well-known optimization techniques such as Bacterial Foraging Optimization Algorithm (BFOA), Crow Search Algorithm (CSA), etc. Moreover, fundamental and harmonic load flows with and without filters are formulated for analyzing a distribution system and studying its power quality problems.

Different IEEE standard radial distribution systems of 33-buses and 69-buses and a real distribution system of 30-buses are used to assure the effectiveness of the two proposed procedures. The software packages of MATLAB 2015 are used, while the AC fundamental and harmonic load flow studies are carried out and the WCA is formulated.

The salient critical contributions in this book can be summarized as follows:

1. Presenting a proposed procedure for simultaneously determining the optimal placement and sizing of both DGs and CBs in distribution systems to achieve technical, environmental and economic benefits using WCA.
2. Compared with other optimization algorithms, the effectiveness of the proposed WCA is proved.
3. Providing power flow analyses on the bases of backward/forward sweep method for normal and distorted radial distribution systems.
4. Studying the sensitivity of single-tuned filter parameters on filter performance via parametric analysis.

5. Proposing a harmonic mitigation procedure based on WCA considering the harmonic spectrum of inverter-based DGs integrated in the system.

Ahmed S. Abbas
Adel Ali Mohamed Abou El-Ela
Ragab A. El-Sehiemy
Adel A. Elbaset

Acknowledgments

First of all, we wish to express our deepest gratitude and indebtedness to

ALLAH, the Most Merciful, *who gave us everything we have and support us with patience and strength to complete this book.*

We would like to express our deepest gratitude to our wives for their help, encouragement and support all the time.

We would like to express our sincere gratitude to our families. We really appreciate their tolerance and support.

Authors

Dr. Ahmed S. Abbas currently works at the Department of Electrical Engineering, Mechanical and Electrical Research Institute, NWRC, Egypt. His main research topics are in electrical power systems engineering, renewable energies, optimization techniques applications. He earned his BSc, MSc, and PhD from Menoufia University, Egypt, in 2013, 2018, and 2022, respectively . He has 6 articles in peer-reviewed journals and conferences.

Prof. Dr. Adel Ali Mohamed Abou El-Ela earned his BSc, MSc, and PhD in Electrical Engineering from Menoufia University, Egypt, in 1977, 1980, and 1983, respectively. From 2006 to 2007, he was the head of the Electrical Engineering Department and a general supervisor of Strategic Studies and leader of the Development Center at Menoufia University, Egypt. From 2007 to 2008, he was the Vice-Dean of Faculty of Engineering at Menoufia University, Egypt. From 2008 to 2011, he was the Dean of Faculty of Engineering at Menoufia University, Egypt. Currently, he is the Dean of Alexandria High Institute for Engineering and Technology, Alexandria, Egypt. Professor Abou El-Ela published over 150 technical papers in international journals and conferences. He supervised and examined more than 110 MSc and PhD theses at Menoufia and other Egyptian universities.

Prof. Dr. Ragab A. El-Sehiemy earned his BSc, MSc, and PhD from Menoufia University, Egypt, in 1996, 2005, and 2008, respectively. He is currently a Professor with the Electrical Engineering Department, Faculty of Engineering, Kafrelsheikh University, Egypt. He received the Prof. Mahmoud Khalifa Award in Power System Engineering from the Academy of Research and Technology in 2016. He is the 2012 recipient of the El-Shorouk Academy for Computers & Information Technology in Industry from the Academy of Research and Technology. Professor El-Sehiemy is one of the top 2% of the effective scientists in 2020 according Elsevier data base. He is an editor of the *International Journal of Engineering Research in Africa* and an associate editor of *IEEE Access*. Professor El-Sehiemy has authored more than 150 articles in peer-reviewed journals and conferences. His research interests include smart grid and its applications, optimization and AI, and its application to power systems and renewable energies.

Adel A Elbaset, PhD, is a Full Professor with the Faculty of Engineering at Minia University, Egypt. He earned a BS, MSc, and PhD from Minia University in 1995, 2000, and 2006, respectively. Dr. Elbaset is also currently a Full Professor with the Faculty of Engineering at Heliopolis University where he also works as a Vice-Dean for Student Affairs and Head of the Department of Electromechanics. He has published over 120 technical papers in international journals and conferences proceedings and has supervised and examined more than 50 MSc and PhD theses at Minia and other Egyptian universities. His research interests are in the areas of wind energy systems, photovoltaics, renewable energy systems, power electronics, power system protection and control, power quality and harmonics, and applications of neural networks and fuzzy systems. Dr. Elbaset has published 13 international books in the field of renewable energy.

List of Abbreviations and Symbols Used

Symbol	Title
CO_2	Carbon dioxide
NOx	Nitrogen oxides
SO_2	Sulfur dioxide
DG	Distributed generation
PV	Photovoltaic
CB	Capacitor bank
LP	Linear programming
NLP	Nonlinear programming
SQP	Sequential quadratic programming
GA	Genetic algorithm
PSO	Particle swarm optimization
CSO	Cat swarm optimization
WCA	Water cycle algorithm
PQ	Power quality
PF	Power factor
S	Apparent power
P	Real power
IHD	Individual harmonic distortion
THD	Total harmonic distortion
UPS	Uninterruptible power supplies
AI	Artificial intelligence
RD	Raindrop
RP	Randomly generated matrix is given as (rows and columns are the number of population and the number of design variables, respectively)
HLF	Harmonic load flow
VD	Voltage deviation
VSI	Voltage stability index
EDN	East Delta Network
OFs	The objective functions
COF	Combined objective function
Ri	The line resistance
BFOA	Bacterial foraging optimization algorithm
BBO	Biogeography-based optimization
CSA	Crow search algorithm
STF	Single-tuned passive filters
Q_f	Quality factor
X	Vector of decision variables

C	The vector of the objective function coefficients
A	The matrix of the constraints coefficients with its elements
a_{ij}	The bounding vector
τ	The pheromone
η	The visibility
$J_k(r)$	The set of cities that remain to be visited by ant k positioned on city r
α and β	Two coefficients which make the pheromone information or the visibility information more important with respect to one another
$\Delta\tau_{rs}^{(k)}$	The contribution of the ant k to the pheromone trial between cities r and s
Q_0	A constant related to the amount of pheromone
L_k	The tour length of the kth ant
ff	The fitness function of a raindrop
N_{sr}	The summation of number of rivers (which is a user parameter) and a single sea
N_{Sn}	The flow intensity
d	Distance between the stream and the river
rand	A uniformly distributed random number between 0 and 1
$d$max	A small number (close to zero)
LB and UB	Lower and upper bounds defined by the given problem, respectively
μ	A coefficient which shows the range of searching region near the sea
$\sqrt{\mu}$	The standard deviation
e	A small nonnegative value defined as an allowable tolerance between the last results
i_i	Load current at bus i
i_c	Capacitor current
Q_C	Reactive power of the capacitor
S_i	Apparent power at bus i
Rand, r	Random number between 0 and 1
C	Constant
I_{n_m}	The current passing from node n to node m
I_{l_m}	Load current at bus m
I_{m_m+1}	The current passing from node m to node m+1
v_n	Voltage at bus n
$Z_{n\text{-}m}$	Impedance of line n-m
h_o	Harmonic order
v_{th}	Thevinin voltage
z_{th}	Thevinin equivalent impedance
i_{filter}	The current absorbed by the harmonic filter
C_{DG}	Cost function of the DG unit
C_{sub}	Cost function of the substation

C_{CB}	Cost function of the CBs
E_{DGi} and E_{Grid}	Emissions produced by the *i*th generation unit of both DGs and the grid
P_g	Real power produced by the ith generation
P_l, and Q_l	Active and reactive power losses
P_d, and Q_d	Active and reactive load demand, respectively
Q_G	Reactive power generated from any source
P_G	Active power generated from any source
Pr_{Grid}	Generated power cost at substations
e_i, and C_{ci}	The coefficients of capacitor cost function
t_f	The tuned harmonic frequency
Q_C	Filter size
Z_f	The equivalent impedance of the single-tuned filter
X_c	The capacitive reactance
$Z_{\min}$	The filter impedance at the tuned frequency
$Z_{\text{system}}^{\min}$	The minimum load impedance in the system
V_{hi}	The harmonic (h) voltage at bus i
N	The total number of buses
v_1	The fundamental bus voltage
v_i^{spec}	The specified voltage magnitude (1.0 p.u)
$v_i^{\max}$, $v_i^{\min}$	Maximum and minimum voltage at bus i
k_C, k_L, and k_R	The cost coefficients of the filter capacitor, inductor, and resistor, respectively
FF	Normalized fitness function
$k1$, $k2$ and $k3$	Priorities factors which are as 0.5, 0.25 and 0.25, respectively
N_{pop}	Number of populations
P_{best}	The personal best data
m_1, m_{i}	Slack bus, Bus number (2, 3,..., nbus)
Gr	Annual rate of benefit ($/h)
LF	Load factor of DGs
e_i, C_{ci}	CBs installation and purchase cost
Q_{Ci}	Reactive power of the CBs
Life time	Investment years of DGs/CBs

1 Introduction

1.1 GENERAL

Distribution system power quality is one of the most important issues of electrical power systems. In recent years, the deterioration in the power quality of a distribution system, such as the aggravation of voltage sag, voltage swell, voltage deviation, and the increase of harmonic distortion, has been apprehended [1]. It is thought to be causally related to the diversification of load by the progress of power electronics technology and the rapid increase in nonlinear loads. These problems are responsible for deteriorating consumer appliances. In order to enhance the behavior of the power system, power quality problems should be eliminated.

Nowadays, conventional distribution systems are being transferred into smart systems for their benefits and to overcome the issues of the conventional ones. One of the most important features of the smart distribution systems is the presence of distributed generation units (DGs) especially those based on inverters such as photovoltaic (PV) and wind generators [2]. So the effect of the smart distribution system on the power quality should be studied to determine its positive and negative effects. The quality of the power delivered to the end user is very important as the performance of the consumer's equipment is heavily dependent on it. Poor power quality can cause malfunction and failure of many devices.

The power quality of the smart distribution systems with DGs attracts great attention due to its importance. The optimal integration of DGs and capacitor banks (CBs) in distribution systems should be addressed to enhance the system power quality and achieve other technical, environmental and economic merits. To do this, the distribution system performance should be analyzed. So, various power flow methods have been introduced [3–5] for analyzing the distribution system. Every power flow method fits specific system conditions; in other words, some power flow methods are suitable for radial systems and others are suitable for meshed systems. Therefore, the proper power flow method must be able to find all of the nodes voltages, branches currents, power flows, system losses, and other steady state quantities.

Determining the optimal location and size of the DGs and CBs in the distribution system can achieve many merits. This process can be formulated as an optimization problem taking into consideration the operational equality and inequality constraints. Therefore, many optimization techniques are used for solving optimization problems such as conventional and artificial intelligence optimization techniques [6, 7]. Conventional optimization techniques include linear programming, nonlinear programming, sequential quadratic programming, etc. These methods are fast and accurate in getting the optimal solution, but they may fail with complex and multi-objective optimization problems. Artificial intelligence techniques are more suitable for complex and multi-objective optimization problems, but they are slower than

DOI: 10.1201/9781003369448-1

the conventional ones. Artificial intelligence techniques include genetic algorithm (GA), particle swarm optimization, cat swarm optimization, etc. Water cycle algorithm (WCA) [8] is considered as one of the modern artificial intelligence techniques that emulate the behavior of the water cycle in nature. WCA has been successfully applied in various areas in optimization problems and it is selected and formulated to be used in this book.

One of the most serious power quality problems is harmonic distortion, as it can result in excessive losses and system equipment overheating and damage. To keep distribution systems reliable and working in high performance, harmonics levels should be kept within the allowable limits approved in the IEEE 519 standard [9]. Therefore, harmonic mitigation in distribution systems becomes a persistent need to decrease distortion levels and enhance system performance. On the other hand, huge efforts have been exerted for increasing the percentage of DGs in distribution systems, especially renewable-sources-based DGs that are dependent on inverters such as PV and wind generation sources [10]. The presence of DGs in distribution systems can provide many technical, environmental, and economic merits [11]; on the other hand, the harmonic content of inverter-based DGs may increase harmonic distortion in distribution systems [12]. Therefore, various harmonic load flow studies have been presented to analyze a system's harmonic distortion [13, 14]. In [14], the authors presented a harmonic load flow method based on the backward/forward sweep method for analyzing the harmonics in distribution systems. Also, various tools were used to reduce harmonic distortion in distribution systems [15–17]. Among these tools, single-tuned harmonic filters (STFs) are considered as an effective tool for mitigating harmonic distortion. STFs have various parameters that affect their performance and the harmonic pass band that the filter can eliminate, therefore a parametric analysis of the STF is a useful way to analyze the filter performance by varying the values of these parameters. Also, parametric analysis can help in determining the effectiveness of each parameter on filter performance during harmonic mitigation; this helps the designer in the proper selection of the parameters without depending only on their experience.

The planning of harmonic filters in the distribution system has a huge effect on the system harmonic mitigation. The authors in [18] presented a method for STF placement in small distribution system based on GA to reduce harmonic distortion. In [19], the authors presented two sensitivity indices as a guide for passive filter placement problem that can determine the sensitive buses for filter placement. In [20], a multi-objective optimization problem was considered for solving the optimal planning problem of passive filter considering specific harmonic orders. Many of the filter placement studies haven't considered the harmonic distortion resulting from DG units and their effect on exceeding the harmonic allowable levels.

1.2 BOOK OBJECTIVES

This book proposes two procedures for improving the power quality (PQ) of distribution systems. The considered PQ parameters are voltage profile, voltage deviation, voltage stability index, and harmonic distortion in smart distribution systems. One of the most important features of smart distribution systems is the presence of DGs.

Therefore, the positive and negative effects of DGs on distribution system PQ are studied. The first proposed procedure is concerned with determining the optimal placement and sizing of DGs and CBs in a distribution system for improving the system PQ besides other technical, economic, and environmental benefits. Also, this book proposes the STF as an effective tool for mitigating harmonic distortion in distribution systems. A parametric analysis is presented for determining the effect of different filter parameters on their performance, which helps system designers obtain the optimal filter design that can mitigate specific harmonic orders.

Moreover, the second proposed procedure is presented for determining the optimal design, placement and number of STFs to mitigate the harmonic distortion in the system. The proposed procedure considers the harmonic content of the inverter-based DGs in the distribution system and its effect in increasing the harmonic distortion. The PQ problems are formulated as optimization problems that can be solved using optimization techniques. Therefore, WCA is formulated as an optimization technique for solving the considered optimization problems. The effectiveness of the WCA is assured through a comparative study with other well-known optimization techniques such as bacterial foraging optimization algorithm, crow search algorithm, etc. Moreover, fundamental and harmonic load flows with and without filters are formulated for analyzing the distribution system and studying its PQ problems.

Different IEEE standard radial distribution systems of 33-buses and 69-buses and a real distribution system of 30-buses, as shown in Appendix A, are used to assure the effectiveness of the two proposed procedures. The software packages of MATLAB 2015 are used, while the AC fundamental and harmonic load flow studies are carried out and the WCA is formulated.

1.3 BOOK CONTRIBUTIONS

The salient critical contributions in this book can be summarized as follows:

1. Presenting a proposed procedure for determining simultaneously the optimal placement and sizing of both DGs and CBs in distribution systems in order to achieve technical, environmental, and economic benefits using WCA.
2. Comparing between the proposed optimization algorithm and other well-known optimization techniques for solving the optimal placement and sizing problem to prove the effectiveness of the proposed algorithm.
3. Formulating both fundamental and harmonic power flows based on the backward/forward sweep method for radial distribution systems.
4. Determining the effect of STF parameters on filter performance and their effectiveness on harmonic mitigation through a parametric analysis of the filter.
5. Proposing a harmonic mitigation procedure based on WCA. The proposed procedure aims to determine the optimal sizing, number, and placement of the STFs considering the harmonic spectrum of inverter-based DGs integrated in the system. Two cases studied to obtain the effect of the DG harmonics on the system harmonic distortion are considered.

6. Applying the proposed procedures on different distribution systems to prove their effectiveness compared to other techniques.

1.4 BOOK OUTLINES

This book consists of eight chapters followed by two Appendices for the test systems data and the published papers. In addition, a references list is presented. These contents can be summarized as follows:

Chapter 1: Presents a brief introduction of the PQ problems and their effects on the distribution system voltage, with an introduction to the proposed approach for mitigating these problems. Hence, it summarizes the objectives and contributions of the book.

Chapter 2: Presents a literature review about the PQ in the smart distribution system and its most common problems. Also, a literature review about the different types of DGs and their integration into distribution systems is presented.

Chapter 3: Presents a brief discussion about the different types of optimization techniques including the conventional and artificial intelligence optimization techniques and the characteristics of each type.

Chapter 4: Presents the fundamental and harmonic load flow calculations that are formulated for analyzing the different configurations of radial distribution systems. These load flow calculations are based on the backward/forward sweep power flow.

Chapter 5: Presents the first proposed procedure for optimal placement and sizing of both DGs and CBs using the WCA. A comparison between the presented optimization algorithm and other well-known algorithms is presented to ensure the effectiveness of the proposed procedure, which will be used in the next chapters.

Chapter 6: Presents an analytical study of the STF parameters to show their effects on changing the filter performance to help designers in selecting the proper values of these parameters, which achieve specific characteristics.

Chapter 7: Presents a proposed harmonic mitigation method for distribution systems with inverter-based DGs. The second proposed procedure is based on WCA for simultaneously determining the optimal number, sizing and placement of STFs in the presence of inverter-based DGs. Two cases studied are considered to determine the effect of DGs harmonic spectrum on system distortion.

Chapter 8: Presents the conclusions of the book and related future work that can be carried out.

2 Power Quality in Smart Distribution Systems

2.1 INTRODUCTION

Power distribution systems are part of power systems that have a direct impact on customers. Because of the hierarchical topology of its assets, the existing electricity grid suffers from many problems and failures. Now with the infusion of the *smart grid* [2, 21, 22] technology, new challenges and opportunities are emerging. Smart grid initiatives accelerated activities related to distributed generations and smart metering. The smart grid provides utility companies with full visibility and pervasive control over their assets and services. In addition, one of the most important features of the smart grid is the existence of the distributed generation units, either renewable or nonrenewable types. Power quality issues are considered as a remarkable challenge in distribution systems, which has increased in recent years. According to the huge improvement and high sensitivity of electronic and power electronic equipment, power quality in distribution systems has been affected by the steady increase in nonlinear loads. Therefore, power quality deserves more attention, as low power quality can lead to catastrophic damage or malfunction of many electrical equipment and loads that may cause huge economical losses.

2.2 SMART DISTRIBUTION SYSTEMS

The concept of a smart distribution system (smart grid) combines a number of technologies, and customer solutions. Also, it addresses several policies and regulatory drivers. Smart grid does not have a single, obvious definition. The European Technology Platform [23] defines smart grid as follows: "An electricity network that can intelligently integrate the actions of all users connected to it. Generators, consumers and those that do both in order to efficiently deliver sustainable, economic and secure electricity supplies."

According to Smarter Grids [24], "A smart grid uses sensing, embedded processing and digital communications to enable the electricity grid to be observable (able to be measured and visualized), controllable (able to be manipulated and optimized), automated (able to adapt and self-heal), fully integrated (fully interoperable with existing systems and with the capacity to incorporate a diverse set of energy sources)."

From the aforementioned definitions, the smart grid can be described as the transparent, seamless, and instantaneous two-way delivery of energy, enabling the electricity industry to better manage energy delivery, transmission and empowering consumers to have more control over energy decisions. A number of studies

DOI: 10.1201/9781003369448-2

have concluded that, when viewed at a high level, the benefits of a smart grid far outweigh its costs. Recognizing these many attributes, the American Recovery and Reinvestment Act of 2009 (ARRA) was designed to provide additional stimulus to accelerate the smart grid transition, and thereby realize the benefits sooner.

According to the EAC, the smart grid is expected to have economic and environmental benefits over the conventional grids [25]. First of all, the automated and self-healing functions of the smart grid will reduce the overall amount of outage time. Smart distribution systems have a bidirectional power flow that improves system performance and enhances its reliability. Advanced metering will also allow consumers to manage their energy usage based on price or on perceived environmental impact. Distributed generation integrated with distribution systems is an important property for the transition from conventional to smart distribution systems as it enables the power in the system to flow bidirectionally, and this property is a main advantage in smart grids. Therefore, the impact of DGs on system power quality should be evaluated.

2.3 DISTRIBUTED GENERATION UNITS (DGS)

DG applications in the vicinity of the load had shown greater operational and power quality advantages, in addition to transmission loss reduction. DGs are highly appropriate for any specific site or application as they require a short period for construction and low investment. They can be defined on the basis plant size, which may vary from a few KW to MW (10–100 MW). DGs can be classified based on their fuel source, renewable or nonrenewable [26]. There are many definitions that suggest size limits for distributed generation systems, as shown in Table 2.1.

However, no general definition of power rating can be given to a DG as the rating will depend basically on the design and the application of a specific system. The categories of clearly defined DG capacities are described as follows [26]:

- Micro distributed generation: 1 W to <5 kW
- Small distributed generation: 5 kW to <5 MW
- Medium distributed generation: 5 MW to <50 MW
- Large distributed generation: 50 MW to <300 MW

TABLE 2.1
Different Definitions of Distributed Generation Capacity [7]

Source	Definition
Electric Power Research Institute	A few kW to 50 MW
Gas Research Institute	25 W to 25 MW
Preston and Rastler	A few kW to over 100 MW
International Conference on Large High Voltage Electric Systems	Less than 100 MW
English and Welsh markets	Less than 100 MW
Sweden	Less than 1.5 MW

As DGs are generation sources located at or near load centers, they are recognized as an environment friendly, reliable, and secure source of power that not only have minimal negative social impacts but also serve to promote social welfare. For large and dispersed rural countries, decentralized power generation systems, where electricity is generated at the consumer end and thereby avoids transmission and distribution costs, offer a better solution toward smart distribution systems. DGs can be classified into conventional and nonconventional types and this classification is clearly shown with the help of Figure 2.1.

Some of the most common DG types according to the previous classification are discussed briefly as follows:

1. **Reciprocating Engines:** Reciprocating engines are the most common technology used as DGs. They are a proven technology with low capital cost, large size range, relatively high electric conversion efficiency, and good operating reliability. These characteristics, combined with the engines' ability to start up rapidly, make them the main choice for emergency or standby power supplies. They are by far the most commonly used power generation equipment under 1 MW. The main drawbacks of reciprocating engines are noise, costly maintenance and high emissions, particularly of nitrogen oxides.
2. **Gas Turbines:** Small industrial gas turbines of 1–20 MW are commonly used in combined heat and power applications. The maintenance cost is slightly lower than that for reciprocating engines, also its electrical conversion efficiency is higher. Emissions are somewhat lower than that of reciprocating engines, as nitrogen oxide emissions control technology is commercially available and is cost-effective. The most important drawbacks of gas turbines are that they are noisy and depend on fossil fuels.
3. **Fuel Cells:** Fuel cells are compact and quiet power generators that use hydrogen and oxygen to generate electricity. The transportation sector is the major potential market for fuel cells, and car manufacturers are making

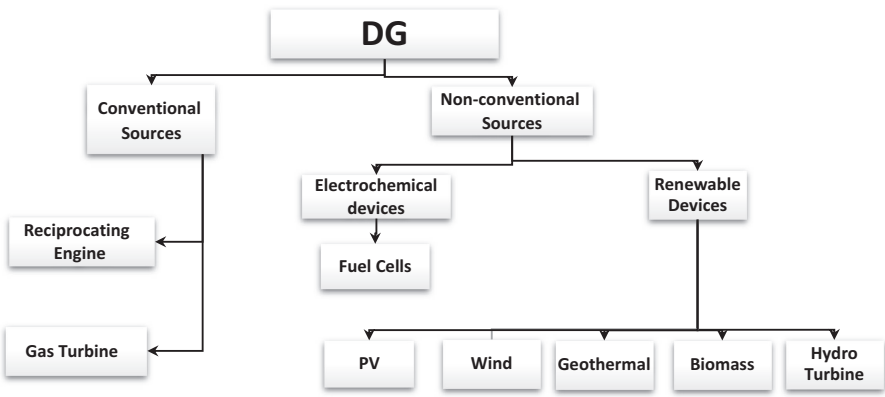

FIGURE 2.1 Classification of DG technologies.

substantial investments in research and development in this field. Fuel cells can convert fuels to electricity at very high efficiencies (35%–60%), compared with conventional technologies.

4. **Photovoltaic (PV) Systems:** Unlike the other DG technologies discussed above, PV systems are a capital-intensive, renewable technology with very low operating costs as there are no fueling costs. PV systems also are widely used in developing countries, serving rural populations that have no other access to basic energy services. PV systems can be used to provide electricity for a variety of isolated applications in households, community lighting, small businesses, agriculture, healthcare, and water supply. The other type of existing PV is the on-grid type, mostly as distributed generation.
5. **Wind Turbines:** Wind generation is rapidly growing as a share of worldwide electricity supply. About 14.158 GW of electricity was installed during the year 2011.Wind power is sometimes considered to be distributed generation, because the size and location of some wind farms make it suitable for connection at distribution voltages. One of the most popular DG types is wind generation since it is the cheapest of all renewable energy sources.
6. **Hydroelectric Resources:** Water constantly moves through a vast global cycle, in which it evaporates from oceans, seas, and other water reservoirs, forms clouds, precipitates as rain or snow, then flows back to the ocean. The energy of this water cycle, which is driven by the sun, is tapped most efficiently with hydropower.

   It can be concluded from the mentioned types that each DG type has advantages over the other types; these advantages make each type suitable for specific applications.

2.4 POWER QUALITY IN DISTRIBUTION SYSTEMS

2.4.1 Power Quality Definition

There are different definitions of electrical power quality, depending on one's frame of reference. Utilities may define power quality as those characteristics of power supply that enable the equipment to work properly. Power quality is ultimately a customer-driven issue, such as any power problem manifested in voltage, current or frequency deviations that results in failure or malfunction of customer equipment.

The IEEE organization defined power quality as [27]: the concept of powering and grounding sensitive equipment is a matter that is suitable for the operation of that equipment. The quality of electric power has become an important issue for electric utilities and their customers. As a result, power quality studies are gaining increasing interest, as degradation in the quality of electric power normally causes problems such as malfunctions, instabilities, short lifetime, failure of electrical equipment, … etc. In an electric distribution network, the use of solid-state switching devices, nonlinear loads and power electronic switched loads such as rectifiers or inverters may cause harmonic distortion and notching in the voltage and current waveforms. Also, the use of arc furnaces may lead to flickers and many types of harmonics.

Ferro-resonance, transformer energization or capacitor switching may cause transients and harmonics.

2.4.2 Power Quality Parameters

There is a need for common terminology in order to avoid confusion from many different terms that have similar meanings, develop standards for characterizing and categorizing monitoring and measurement results, and permit statistical analysis of data obtained from different sources. So the power quality parameters can be classified as follows [28].

2.4.2.1 Voltage Sag

Voltage sag is defined according to the IEEE-1100 standard as: an RMS reduction in the ac voltage, at the power frequency for durations from 0.01 second to a (minute) as shown in Figure 2.2. The magnitude of voltage sag is between 0.1 and 0.9 PU.

2.4.2.2 Voltage Swell

Voltage swell is defined according to the IEEE 1100 standard as: an increase in RMS voltage or current at the power frequency for durations from (a half cycle) to 1 minute as shown in Figure 2.3. The magnitude of voltage swell is between 1.1– and 1.8 pu.

2.4.2.3 Over-Voltage

Over-voltage is defined according to the IEEE-1100 standard as: an RMS increase in the ac voltage at the power frequency for a period of time greater than 1 minute as shown in Figure 2.4.

2.4.2.4 Under Voltage

Under voltage is defined according to IEEE-1100 standard as: an RMS decrease in the ac voltage at the power frequency for a period of time greater than 1 minute as shown in Figure 2.5.

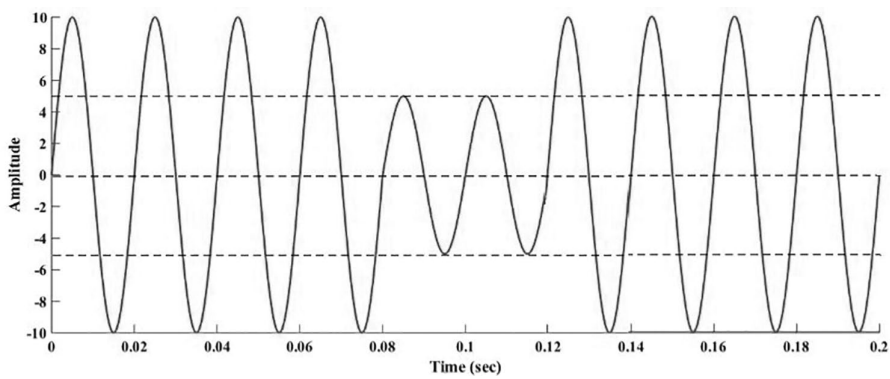

FIGURE 2.2 Phase voltage with voltage sag.

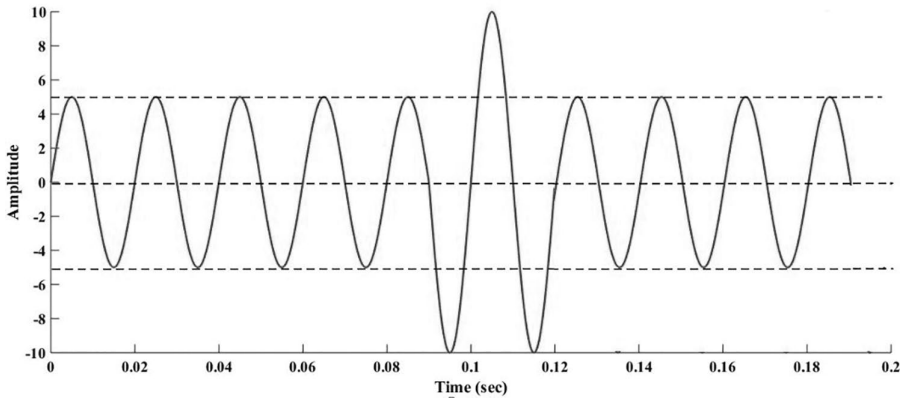

FIGURE 2.3 Phase voltage with voltage swell.

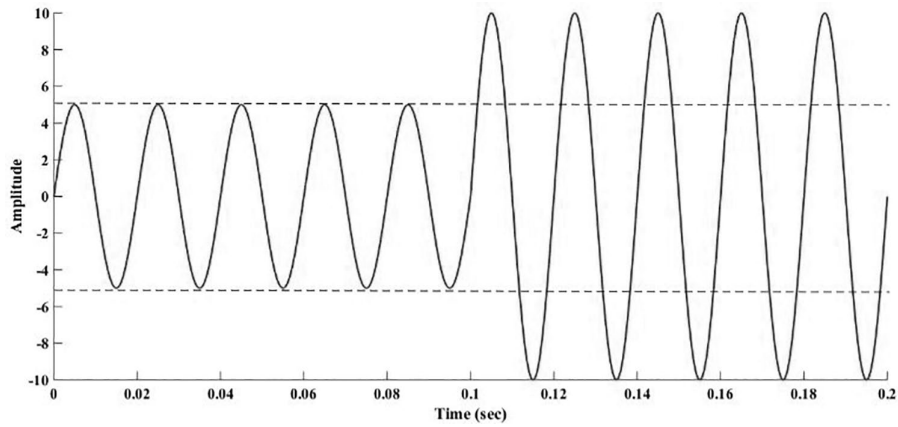

FIGURE 2.4 Phase voltage with over-voltage.

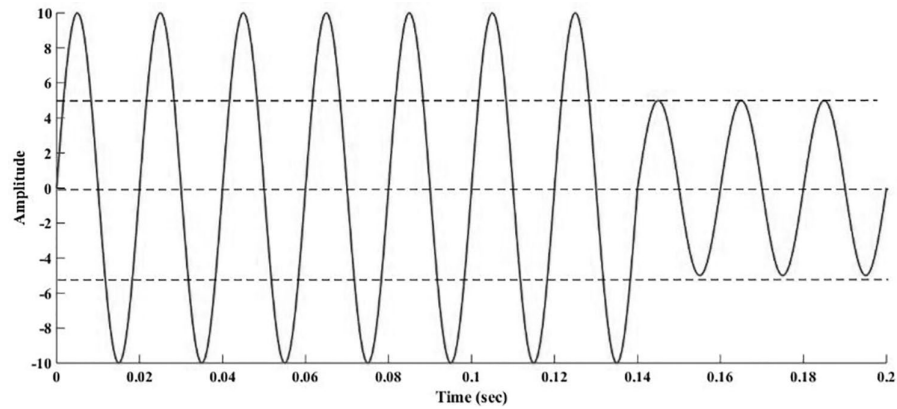

FIGURE 2.5 Phase voltage with under voltage.

2.4.2.5 Voltage Fluctuation

Voltage fluctuation is a series of voltage changes or a cyclic variation of the voltage envelope as shown in Figure 2.6.

2.4.2.6 Transient Voltage

IEEE-1100-1999 standard defines transient voltage as: a sub-cycle disturbance in the ac waveform that is evidenced by a sharp, brief discontinuity of the waveform that may be of either polarity and may be additive to, or subtractive from, the nominal waveform as shown in Figure 2.7.

2.4.2.7 Noise Disturbance

Noise is any electromagnetic disturbance that interrupts, obstructs or otherwise degrades or limits the effective performance of electronics and electrical equipment. The IEEE 1100 standard defines noise as: unwanted electrical signals that produce undesirable effects in the circuits of the control systems in which they occur, as shown in Figure 2.8.

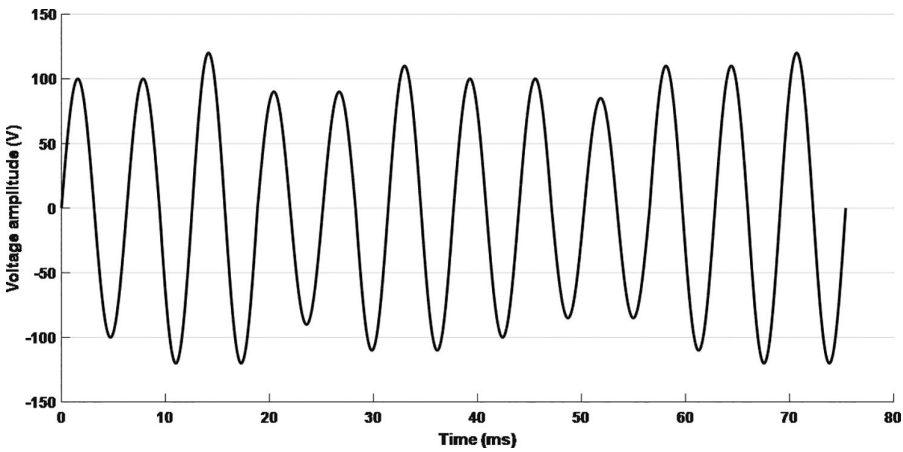

FIGURE 2.6 Phase voltage with voltage fluctuation.

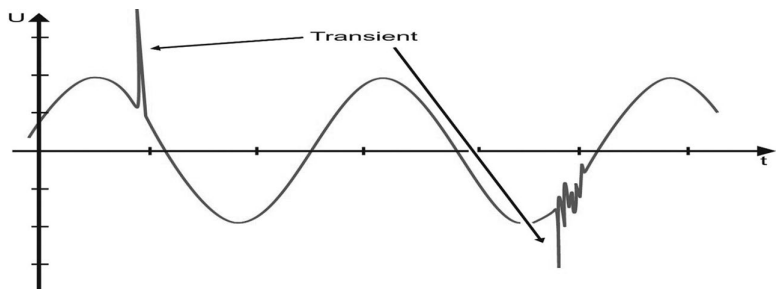

FIGURE 2.7 Phase voltage with voltage disturbance.

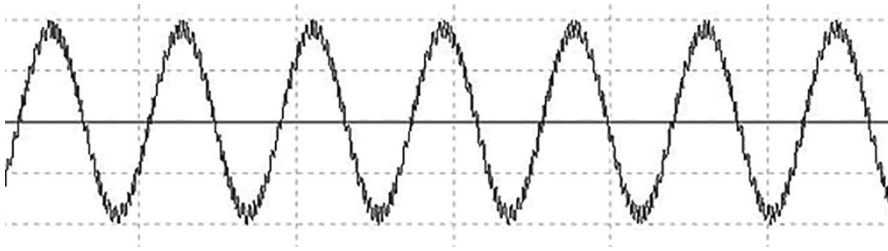

FIGURE 2.8 Phase voltage with noise.

2.4.2.8 Voltage Unbalance

A three-phase power system is called balanced or symmetrical if the three-phase voltages and currents have the same amplitude and are phase-shifted by 120° with respect to each other. If one or both of these conditions are not met, the system is called unbalanced or asymmetrical, as shown in Figure 2.9. It is implicitly assumed that the waveforms are sinusoidal and thus do not contain harmonics. In most practical cases, the asymmetry of the loads is the main cause of the unbalance.

2.4.2.9 Power Factor

Power factor (PF) may be viewed as the percentage of the total apparent power (S) that is converted to real or useful power (P). PF is a power quality issue in that low power can sometimes cause equipment to fail. In many instances, the cost of low PF can be high; utilities penalize facilities that have low PF because they find it difficult to meet the resulting demands for electrical energy. PF can be expressed as

$$PF = P / S \tag{2.1}$$

2.4.2.10 Harmonics

One of the urgent problems in power quality aspects is the harmonics content in electrical systems. Harmonics can be generated by either the source or the load side. Harmonics generated by load are caused by nonlinear operation of devices, including power converters, arc furnaces, gas discharge lighting devices, etc. Load harmonics can cause overheating of the magnetic cores of transformers and motors. On the other hand, source harmonics are mainly generated by power supply with non-sinusoidal voltage waveform. Voltage and current source harmonics imply power losses, electromagnetic interference and pulsating torque in AC motor drives [29].

EN 50160 standards [30] define harmonics as a sinusoidal voltage with a frequency equal to an integer multiple of the fundamental frequency of the supply voltage, as shown in Figure 2.10.

Harmonic pollution on a power line can be quantified by means of Total Harmonic Distortion (THD). High harmonic distortion can negatively impact a facility's electric

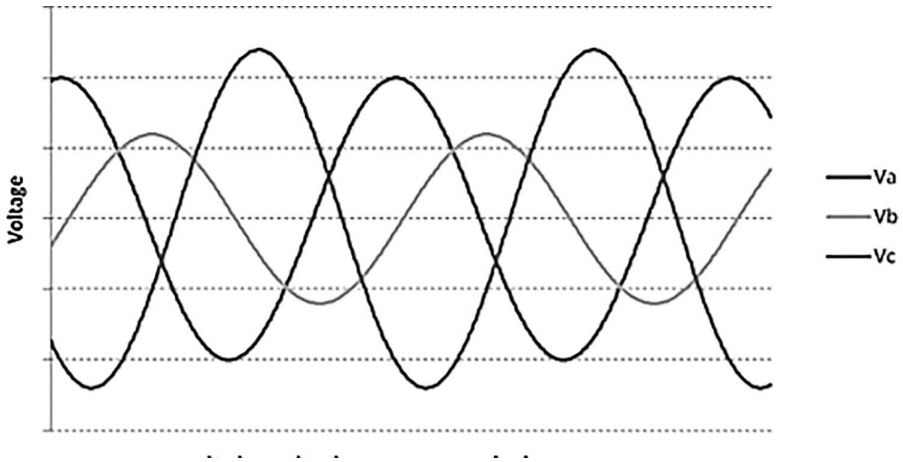

FIGURE 2.9 Unbalanced three phases voltage.

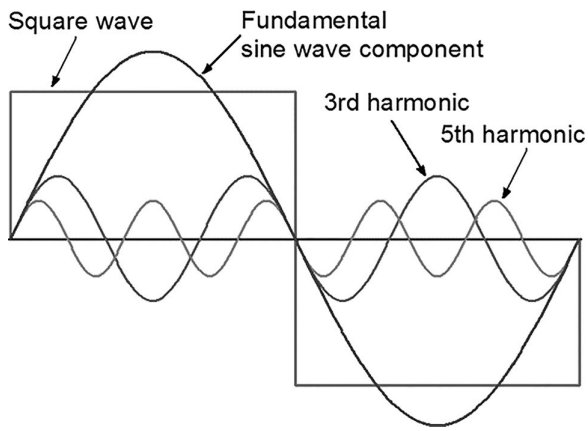

FIGURE 2.10 Harmonic analysis of a square wave.

distribution system and can generate excessive heat in motors, causing early failures. Heat also builds up in wire insulation causing breakdown and failure. Increased operating temperatures can affect other equipment as well, resulting in malfunctions and early failure. Harmonic distorted waveform is clearly not a sine wave and that means the normal measurement equipment, such as average reading RMS-calibrated multi-meters, will give inaccurate readings [31]. Note that there could also be many zero crossing points per cycle instead of two, so any equipment that uses zero crossing as a reference will malfunction. Such a waveform contains nonfundamental frequencies, and the equipment should be capable of identifying them.

2.4.3 Impacts of Power Quality Issues

The effects of power quality problems vary from one type of equipment to another and with the age of the equipment. The quality of electric power is vital for both electric utilities and their customers. The major issues faced by the stakeholders are:

A. **Consumer Side**
- Intermittent failure of computer equipment
- Interference with data communication equipment
- Malfunction of process controllers
- Stalling of motors on start up
- Inaccurate power metering
- Constant risk of fatal electrical shock

B. **Utility Side**
- Increased transmission and distribution losses
- Overloading of cables, transformers, and switchgears
- Tripping of circuit breakers and residual current devices
- Incorrect operation of solid-state relays

2.4.4 Power Quality Solutions

Solving power quality problems depends on acquiring meaningful data at the optimum location or locations and within an expedient time frame. In order to acquire useful and relevant data, instruments most suited for a particular application should be utilized. The wide range of power quality solutions employed at present and found in literature can be categorized as follows:

- Harmonic filters
- PWM-based higher power compensators
- FACTS controller, custom power devices
- Voltage regulators
- Transformer tap changer
- Energy storage devices

2.4.5 Harmonic Standards

Power quality problems ultimately impact the end user. However, there are many other parties involved in creating, propagating, and solving power quality problems. Power quality standards must provide guidelines, recommendations, and limits to help assure compatibility between end use equipment and the system where it is applied. The harmonic standard, IEEE 519-1992 [31], has proposed a two-way responsibility for controlling harmonic levels on the power system. End users must limit the harmonic currents injected onto the power system. The power supplier will control harmonic voltage distortion by making sure the system resonant conditions

do not cause excessive magnification of the harmonic levels. Harmonic distortion levels can be characterized by the complete harmonic spectrum with magnitudes and phase angles of each individual harmonic component. It is also common to use a single quantity, the THD, as a measure of the magnitude of harmonic distortion. Harmonic evaluations on the utility system involve procedures to make sure that the quality of the voltage supplied to all customers is acceptable. IEEE 519-1992 provides guidelines for acceptable levels of voltage distortion on the utility system, as listed in Table 2.2.

2.4.6 Harmonic Elimination Techniques

To avoid the harmful effects of harmonics on the operation of sensitive equipment, it is necessary to keep harmonic contents below the safety limit by using one or more types of harmonic elimination techniques [32]. One of the most common techniques for eliminating harmonics of different orders is to install harmonic filters at specific locations.

2.4.6.1 Passive Filters

These filters are inductive capacitive (LC) resonating or parallel resonance circuits that offer very high or low impedance at tuning frequency. These filters are resistive at the tuned frequencies, capacitive at below tuned frequencies, and inductive beyond tuned frequencies. Passive filters can be classified as described in Table 2.3.

2.4.6.2 Active Filters

When the number of harmonics to be filtered is large, a large number of branches of passive filters will be required. The actual number of branches will depend upon the number of harmonic levels to be compensated. Hence, the use of passive filters for the filtration of a large number of harmonic orders results in large size and more cost. The subsequent design of active filters resulted in low cost and high performance suitable for eliminating the harmonics of different orders to overcome the drawbacks of passive filters. Active filters compensate the voltage of the current harmonic signal measured. The injected voltage or current harmonic signal into the power system network has the same magnitude and is opposite in phase with the measured harmonic signal. It comprises power converter and control loop, which control the harmonics injection from the filter as a function of the harmonic signal measured. Active harmonic filters have many types, as shown in Table 2.4.

TABLE 2.2
Recommended Voltage Distortion Limits for General Systems [31]

Bus Voltage	Maximum Individual Harmonic Component (%)	Maximum THD (%)
69 kV and below	3.0	5.0
115–161 kV	1.5	2.5
Above 161 kV	1.0	1.5

TABLE 2.3
Types of Passive Filters [32]

Series Passive Filters	Shunt Passive Filters
Connected in series with power system network.	Connected between line and earth.
Offer high impedance at turning frequencies.	Offer very low impedance at the tuned frequency.
The drawback of series filters are high cost, because the rating of filter component required is rated full load current.	High pass shunt filters are connected to the point of common coupling.

TABLE 2.4
Types of Active Filters [32]

Shunt Type Active Filters	Series Type Active Filters
1. These devises are designed to constantly monitor the harmonics in the load current and same harmonic equal in magnitude and opposite in phase, thus cancel the original harmonics.	1. These are connected in series with network and nonlinear load.
2. These filters are connected in parallel with harmonic generating nonlinear load.	2. They introduce a suitable voltage through a matching transformer; the voltage introduced by series filter is in such a way that the supply sees a very high impedance for harmonic and low impedance for fundamental.

A comparison between active and passive harmonic filters is described in Table 2.5.

2.4.6.3 Harmonic Cancellation

The phase cancellation or cancellation technique is used in the case of static power converters to eliminate lower harmonics. To use the above technique the following conditions must be satisfied:

1. Transformer ratio and impedance must be equal.
2. The delay angle of each pulse must be exactly the same.
3. The loads must be equal.

2.4.6.4 Isolation Transformer

These transformers are used in isolating the third harmonics that are common when delta to star configuration is used.

2.4.6.5 Harmonic Blocking

When harmonic content is low, then the harmonic blocking technique is used to protect the most effected equipment, e.g., capacitor banks used for PF correction offer very low impedance to high frequency harmonics and may get damaged because of large current drawn due to thermal break down. In this case, inductor or damping resistor is connected in series to protect the capacitor bank.

TABLE 2.5
Comparison between Active and Passive Harmonic Filters

	Passive Filters	Active Filters
Advantages	1. Simple in construction, less costly and efficient. 2. Serve dual purpose harmonic filtration and power factor correction of load.	1. No loading problems. 2. Small in size and weight. 3. Generally easier to tune.
Disadvantages	1. Cannot function under saturated condition. 2. Connection of passive filters necessitates a specific analysis of each installation. 3. Nonadaptability to system variations.	1. Complex and costlier. 2. Need more components. 3. Power supply required.

The THD expresses harmonics as a percent of fundamental (50/60 Hz) current at the time of measurement. Some loads such as drives have higher THD at light load even though they draw less total harmonic current in amperes and thus cause less harmonic voltage distortion. The consideration of minimizing harmonic current production during equipment design has gained greater importance, as reflected by technological improvements in fluorescent lamp ballasts, adjustable speed drives, battery chargers, and uninterruptible power supplies (UPS).

DG units in smart distribution systems may supply active and/or reactive power to the grid, which may affect the voltage profile of the system. Also, DG units may be considered as a source of harmonics that increase the harmonic distortion of the system. These effects will be studied in detail in the next chapters.

3 Optimization Techniques

3.1 INTRODUCTION

Optimization is defined as "the operation of getting the conditions that give the minimum or maximum value of a specific function." Optimization problems can be classified into unconstrained and constrained optimization problems. Constrained optimization is much harder than unconstrained optimization because it requires finding the best value of the objective function, in addition to verifying various constraints of the problem. There is no specific method available for solving all optimization problems efficiently. However, a number of optimization techniques have been improved for solving different types of optimization problems [6]. The optimum-seeking methods are also known as mathematical programming techniques and are generally studied as a part of operations research. Operations research is a branch of mathematics concerned with the application of scientific methods and techniques to decision-making problems and with establishing the best or optimal solutions. Mathematical programming techniques are useful in finding the minimum value of a specific function with several variables under a prescribed set of constraints. In recent years, modern optimization methods have emerged as powerful and popular methods for solving complex engineering optimization problems. The main elements of any constrained optimization problem are defined in Table 3.1.

TABLE 3.1
Constrained Optimization Problem Elements [6]

Parameter	Definition
Optimization problem	A computational problem in which the objective is to find the best of all possible solutions. More formally, find a solution in the feasible region that has the minimum (or maximum) value of the objective function. The formulation of particular optimization problem consists of three basic components, namely, control variables, objective functions, and constraints.
Control variables	The variables usually represent things that can be adjusted or controlled, where the goal is to find values of the variables that provide the best value of the objective function.
Objective function	This mathematical expression combines the variables to express the goal, which will be required to either maximize or minimize the objective function.
Constraints	These mathematical expressions combine the variables to express limits on the possible solutions
Variable bounds	Most of the variables in an optimization problem are permitted to take on any value between the minimum and maximum limit.

DOI: 10.1201/9781003369448-3

3.2 OPTIMIZATION TECHNIQUES CLASSIFICATION

Optimization techniques can be classified into conventional optimization techniques and artificial intelligence (AI) techniques.

3.2.1 Conventional Optimization Techniques

Many of the existing conventional types of optimization techniques such as linear programming [33] and quadratic programming [7], accept only changes that yield immediate improvement, which are effective for the optimization problems with deterministic objective function that has only one minimum. However, it often induces local optimal rather than global optimal and sometimes results in divergence when minimizing both objective functions at the same time. As a result, these techniques usually achieve local optimal rather than global optimal.

3.2.1.1 Linear Programming

Linear programming (LP) is the most common optimization technique applied for constrained optimization problems, where entire objective functions and equality and inequality constraints are linear. It is widely used because many practical problems can be formulated as LP problems; there are noniterative, simplex and efficient methods for solving optimization problems [34]. The classical LP problem is to obtain the optimal decision variables values that maximize the linear objective function under linear equality and inequality constraints. Specifically, the standard form of LP problem in vector form is:

$$\left.\begin{array}{ll} \text{Maximize} & C \cdot X \\ \text{Subject to} & A\,X \le b \\ & X \ge 0 \end{array}\right\} \tag{3.1}$$

where $X = [x_1,\ldots\ldots, x_n]^T$ is the vector of the decision variables to be determined, $C = [C_1,\ldots\ldots, C_n]$ is the vector of the objective function coefficients, $A = [a_{ij}] \in R^{mxn}$ is the matrix of the constraints coefficients with its elements, and a_{ij}, $b = [b_1, b_2,.., b_m]^T$ is the bounding vector.

3.2.1.2 Quadratic Programming

Quadratic programming (QP) [7] is a linearly constrained optimization problem with a quadratic objective function. The objective function is minimized subject to linear equality and inequality constraints. The general quadratic program can be written as:

$$\left.\begin{array}{ll} \text{Minimize} & C \cdot X + \dfrac{1}{2} X^T \cdot Q \cdot X \\ \text{Subject to} & A\,X \le b \\ & X \ge 0 \end{array}\right\} \tag{3.2}$$

where C is an n-dimensional row vector describing the coefficients of the objective function and $Q \in R^{nxn}$ is a symmetric matrix describing the coefficients of the quadratic terms.

3.2.2 Artificial Intelligence Techniques

The conventional optimization techniques are unable to globally optimize a system effectively. They are generally single path search algorithms, starting from an initial condition and improving the control variables in every iteration [35]. These techniques require more time for execution and generally get trapped in a local optimal. Conventional methods are also unable to handle the complex nature of electrical power systems. In recent times, AI techniques have been implemented to overcome the abovementioned demerits of conventional optimization techniques. Different AI techniques are considered for solving the optimization problems in electrical power systems, such as genetic algorithm (GA), ant colony optimization, tabu search, simulated annealing, etc. Improvements in these AI techniques have also been suggested over the years.

AI techniques present a better, faster, and accurate solution to an optimization problem than conventional techniques. AI techniques generally make use of multiple approaches to obtain an optimal solution, as they can remember past findings, learn and adapt their performance, plan their path forward, and act intelligently according to human or social intelligence. One of the recent AI optimization techniques is water cycle algorithm (WCA).

3.2.2.1 Genetic Algorithm

It is an optimization and search technique based on the basics of genetic and natural selection. GA was created by John Holland in 1975. Holland presented GA as a heuristic method depending on "survival of the fittest." GA can be considered as an evolution and evolutionary programming. It is based on the idea of emulating the evolution of individual structures by steps of selection, reproduction, and mutation. The operations are based on the realized properties of the individual construction as defined by the environment problem.

The functional block diagram of a GA is represented in Figure 3.1. It is assumed that an efficient issue to a problem can be represented as a parameter set. Those parameters are called genes, which combine together to create a string called a

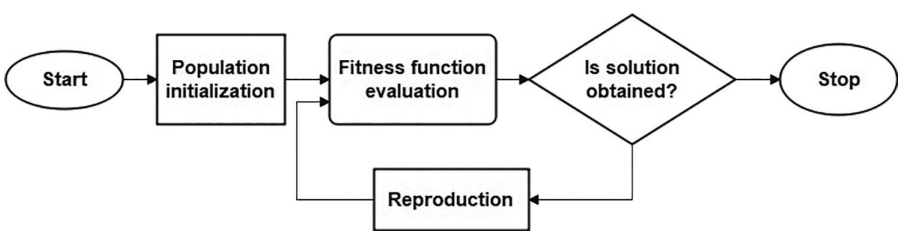

FIGURE 3.1 Flowchart of genetic algorithm iteration.

chromosome. A gene, indicates for feature and explains specified option that is coded inside the chromosome [35].

The encoding process provides a solution in a chromosome and there is no unique method for solving the problems. A fitness function should be prepared for the problem that needs to be solved. For a definite single chromosome, the fitness function provides a single numerical fitness, which will define and determine the ability of the individual that the chromosome represents in the optimization operation.

3.2.2.2 Ant Colony Optimization Algorithm

Ant colony optimization algorithm depends on the foraging behavior of ant colonies. While searching for food, ants first explore the area surrounding their nest in a random mode. As soon as an ant detects a source of food, it evaluates quality and quantity of the food and takes some of the detected food to the nest. During the return trip, the ant deposits a pheromone trail on its path. The pheromone deposited quantity, which may be based on the quality and quantity of the food, will lead other ants to the food source. This indirect communication operation between ants via the pheromone trail helps them to discover the shortest paths between food sources and their nest. This functionality of real ant colonies is used in artificial ant colonies to solve global optimization searching problems when the closed-form optimization technique cannot be applicable [7].

Each ant generates a complete tour throughout selecting the cities by using a probabilistic state rule. Mathematically, the probability with which ant k in city r selects to move to the city s is [36]

$$P_k(r,s) = \frac{\left(\sum_{i=1}^{r}\left[\gamma^{r-1}.\tau(i,s)\right]\right)^{\alpha}.\left[\eta(i,s)\right]^{\beta}}{\sum_{v\in J_k(r)}\left(\left(\sum_{i=1}^{r}\left[\gamma^{r-1}.\tau(i,v)\right]\right)^{\alpha}.\left[\eta(i,v)\right]^{\beta}\right)} \tag{3.3}$$

where, τ is the pheromone; η is the visibility, which is the inverse of the distance $\delta(r, s)$; $J_k(r)$ is the set of cities that remain to be visited by ant k positioned on city r; α and β are two coefficients which make the pheromone information or the visibility information more important with respect to one another and the parameter $\gamma > 0$.

The best solutions found so far and in the immediate generation are used to update the pheromone information. However, before that, some portion of pheromone is able to evaporate according to

$$\tau_{rs}(t+n) = \rho.\tau_{rs} + \sum_{k=1}^{m}\Delta\tau_{rs}^{(k)} \tag{3.4}$$

where $\Delta\tau_{rs}^{(k)}$ is the contribution of ant k to the pheromone trail between cities r and s, and is usually calculated as

$$\Delta\tau_{rs}^{(k)} = \frac{Q_o}{L_k} \tag{3.5}$$

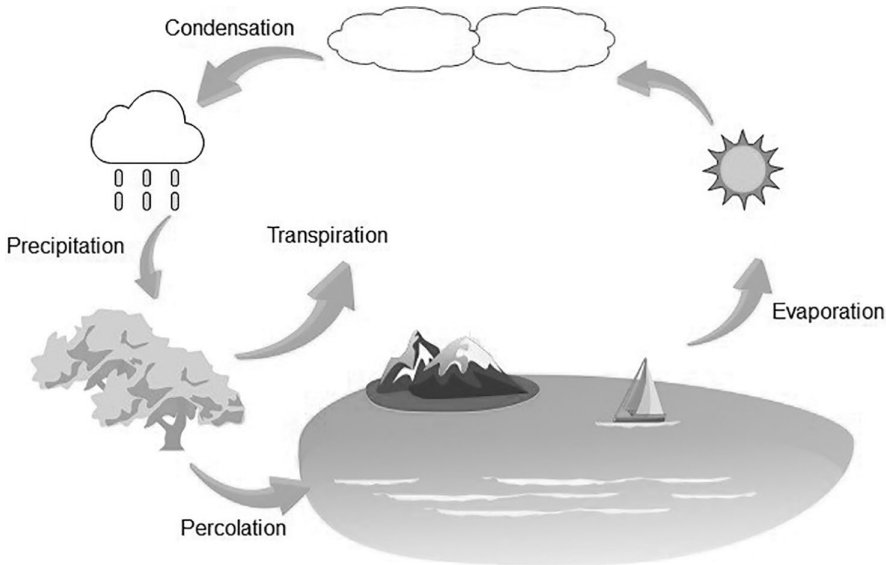

FIGURE 3.2 A simplified diagram of the water cycle.

where, Q_O is a constant related to the amount of pheromone laid by ants and L_k is the tour length of the kth ant. The process is then iterated and the algorithm runs until some stopping criterion is met [36].

3.2.2.3 Proposed Water cycle algorithm

The idea of the WCA is inspired from nature and based on the observation of water cycle and how rivers and streams flow downhill toward the sea in the real world. A river, or a stream, is formed whenever water moves downhill from one place to another. Rivers always flow downhill. On its downhill journey and eventually ending up in a sea, water is collected from rain and other streams.

Water in rivers and lakes is evaporated while plants transpire water during photosynthesis. The evaporated water is carried into the atmosphere to generate clouds which then condenses in the colder atmosphere, releasing the water back to the earth in the form of rain or precipitation. This process is called the water cycle [36]. In the real world, as snow melts and rain falls, most of the water enters the groundwater (aquifer). The underground water may be discharged into a stream (marsh or lake). Water evaporates from the streams and rivers, in addition to being transpired from the trees and other greenery, hence bringing more clouds and thus more rain as this cycle continues, as shown in Figure 3.2.

3.3 MATHEMATICAL FORMULATION OF WCA

Similar to other metaheuristic algorithms, WCA begins with an initial population called the raindrops. First, it is assumed that there is rain or precipitation. The best individual (best raindrop) is chosen as a sea. Then, a number of good raindrops are

chosen as a river and the rest of the raindrops are considered as streams which flow to the rivers and the sea. Depending on their magnitude of flow, which will be described in the following subsections, each river absorbs water from the streams. In fact, the amount of water in a stream entering a river and/or sea varies from other streams. In addition, rivers flow to the sea, which is the most downhill location.

3.3.1 Creation of the Initial Population

In order to solve an optimization problem using population -based metaheuristic methods, it is necessary that the values of problem variables be formed as an array. In WCA this array is called raindrop (RD) for a single solution. In an N_{var} dimensional optimization problem,

$$RD = [x_1, x_2, x_3, ..., x_N] \tag{3.6}$$

To start the optimization algorithm, a candidate representing a matrix of raindrops of size N_{pop}*N_{var} is generated (i.e., population of raindrops). Hence, the matrix RP, which is generated randomly, is given as follows (rows and columns are the number of population and the number of control variables, respectively):

$$RP = \left\{ x_k^j : j = 1 : N_{\text{pop}} \text{ and } k = 1 : N_{\text{var}} \right\} \tag{3.7}$$

The fitness function of a raindrop is obtained by the evaluation of (ff), given as

$$ff_i = f(x_1^i, x_2^i, x_3^i, ..., x_{N\,\text{var}}^i), i = 1, 2, 3, ...N_{\text{pop}} \tag{3.8}$$

Individuals (minimum values) are selected as sea and rivers. The raindrop which has the minimum value among others is considered as a sea. In fact, N_{sr} is the number of rivers (which is a user parameter) and a single sea, as given in Eq. (3.9):

$$N_{sr} = \text{rivers} + 1 \tag{3.9}$$

The rest of the population (raindrops form the streams which flow to the rivers or may directly flow to the sea) is calculated using Eq. (3.10):

$$N_{\text{raindrops}} = N_{\text{pop}} - N_{sr} \tag{3.10}$$

Eq. (3.11) calculates the streams that flow to a sea or a river depending on the flow intensity as

$$NS_n = \text{round}\left\{ \left| \frac{ff_n}{\sum_{i=1}^{N_{sr}} ff_i} \right| \times N_{\text{pop}} \right\} \qquad n = 1, 2, 3, ..., N_{sr} \tag{3.11}$$

The streams are created from the raindrops and join each other to form new rivers. Some of the streams may also flow directly to the sea. All rivers and streams end up in the sea (best optimal point). Figure 3.3 shows the schematic view of a stream's flow toward a specific river. As illustrated in Figure 3.3, a stream flows to the river along the connecting line between them using a randomly chosen distance, given as follows:

$$X \in (0, \mathrm{C} \times d), C \succ 1 \tag{3.12}$$

where, C is a value between 1 and 2. The best value of C is chosen to be 2. The current distance between the stream and the river is represented as (d). The value of X in Eq. (3.12) corresponds to a distributed random number between 0 and ($C \times d$). The value of C being greater than 1 enables streams to flow in different directions toward the rivers.

This concept may also be used in the rivers' flow to the sea. Therefore, the new position for streams and rivers can be given as

$$X_{\text{stream}}^{i+1} = X_{\text{stream}}^{i} + \text{rand} * U * (X_{\text{river}}^{i} - X_{\text{stream}}^{i}) \tag{3.13}$$

$$X_{\text{river}}^{i+1} = X_{\text{river}}^{i} + \text{rand} * U * (X_{\text{sea}}^{i} - X_{\text{river}}^{i}) \tag{3.14}$$

where rand is a uniformly distributed random number between 0 and 1. If the solution given by a stream is better than its connecting river, the positions of the river and the stream are exchanged (i.e., stream becomes river and river becomes stream). Such an exchange can similarly happen for rivers and sea. Figure 3.4 depicts the exchange of a stream, which is the best solution among other streams and the river.

3.3.2 Evaporation Condition

Evaporation is one of the most important factors that can prevent the algorithm from rapid convergence (immature convergence). As it can be seen in nature, water evaporates from rivers and lakes while plants transpire water during photosynthesis.

The evaporated water is carried into the atmosphere to form clouds which then condenses in the colder atmosphere, releasing the water back to earth in the form of rain. The rain creates new streams and the new streams flow to the rivers which flow to the sea [37].

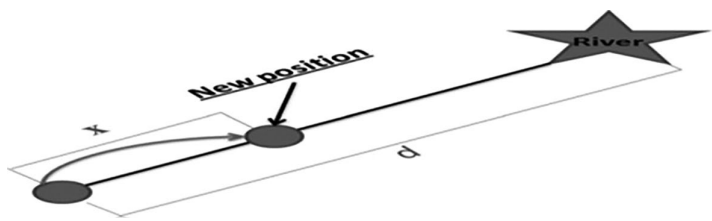

FIGURE 3.3 Schematic view of a stream's flow to a specific river.

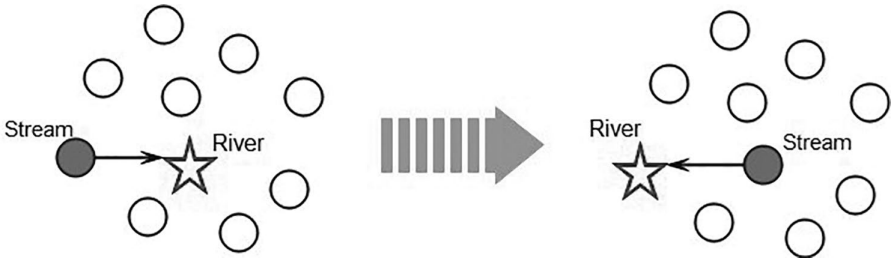

FIGURE 3.4 Position exchanging process.

In WCA, the evaporation process causes the sea water to evaporate as rivers/streams flow to the sea. This assumption has been proposed in order to avoid getting trapped in local optimal. The following criteria show how to determine whether or not a river flows to the sea.

$$\left|X_{\text{sea}}^{i} - X_{\text{river}}^{i}\right| < d_{\max}, i = 1,2,3,....,N_{sr} - 1 \tag{3.15}$$

where $d_{\max}$ is a small number (close to zero). Therefore, if the distance between a river and the sea is less than $d_{\max}$, it indicates that the river has reached the sea. In this situation, the evaporation process is applied, and, as seen in nature, after some adequate evaporation rain (precipitation) will start. A large value for $d_{\max}$ reduces the search while a small value encourages the search intensity near the sea. Therefore, $d_{\max}$ controls the search intensity near the sea (the optimum solution). The value of $d_{\max}$ adaptively decreases as

$$d_{\max}^{i+1} = d_{\max}^{i} - (d_{\max}^{i} / \text{maxiteration}) \tag{3.16}$$

3.3.3 Raining Process

After satisfying the evaporation process, the raining process is applied. In the raining process, the new raindrops form streams in different locations for specifying the new locations of the newly formed streams, and the following equation is used:

$$X_{\text{stream}}^{\text{new}} = LB + \text{rand} \times (UB - LB) \tag{3.17}$$

where, LB and UB are lower and upper bounds defined by the given problem, respectively.

Again, the best newly formed raindrop is considered as a river flowing to the sea. The rest of new raindrops are assumed to form new streams which flow to the rivers or may directly flow to the sea.

In order to enhance the convergence rate and computational performance of the algorithm for constrained problems, Eq. (3.18) is used only for the streams which directly flow to the sea. This equation aims to encourage the generation of streams

which directly flow to the sea in order to improve the exploration near sea (the optimal solution) in the feasible region for constrained problems.

$$X_{\text{stream}}^{\text{new}} = X_{\text{sea}} + \sqrt{\mu} \times \text{r and } n(1, N_{\text{var}}) \tag{3.18}$$

where μ is a coefficient that shows the range of the searching region near the sea. The larger value for μ increases the possibility to exit from the feasible region. On the other hand, the smaller value for μ leads the algorithm to search in a smaller region near the sea. A suitable value for μ is set to 0.1. From the mathematical point of view, the term $\sqrt{\mu}$ in Eq. (3.18) represents the standard deviation and, accordingly, μ defines the concept of variance. Using these concepts, the generated individuals with variance μ are distributed around the best obtained optimum point (sea).

3.3.4 Constraint Handling

In the search space, streams, and rivers may violate either the problem-specific constraints or the limits of the design variables. In the current work, a modified-feasibility-based mechanism is used to handle the problem-specific constraints based on the following four rules [37]:

Rule 1: Any feasible solution is preferred to any infeasible solution.
Rule 2: Infeasible solutions containing slight violation of the constraints (from 0.01 in the first iteration to 0.001 in the last iteration) are considered as feasible solutions.
Rule 3: Between two feasible solutions, the one having the better objective function value is preferred.
Rule 4: Between two infeasible solutions, the one having the smaller sum of constraint violation is preferred.

Using the first and fourth rules, the search is oriented to the feasible region rather than the infeasible region. Applying the third rule guides the search to the feasible region with good solutions [38]. For most structural optimization problems, the global minimum locates on or close to the boundary of a feasible design space. By applying rule 2, the streams and rivers approach the boundaries and can reach the global minimum with a higher probability [8].

3.3.5 Convergence Criteria

For termination criteria, as commonly considered in metaheuristic algorithms, the best result is calculated where the termination condition may be assumed as the maximum number of iterations, CPU time, or (e) which is a small nonnegative value and is defined as an allowable tolerance between the last two results.

The WCA proceeds until the maximum number of iterations as a convergence criterion is satisfied. The schematic view of the proposed method is illustrated in Figure 3.5 where circles, stars, and the diamond correspond to streams, rivers, and sea, respectively.

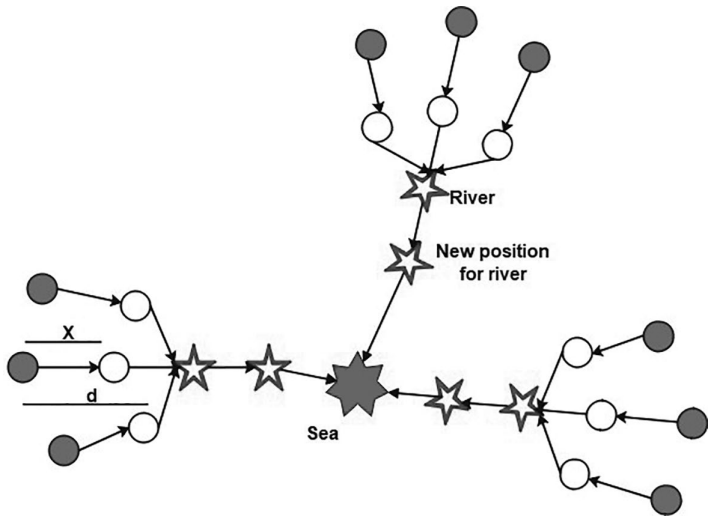

FIGURE 3.5 Schematic view of WCA

3.3.6 Steps of WCA

The steps of WCA are summarized as follows:

Step 1: Choose the initial parameters of the WCA: N_{sr}, d_{max}, N_{pop}, maxiteration.

Step 2: Generate random initial population and form the initial streams (raindrops), rivers, and sea using Eqs. (3.7), (3.9), and (3.10).

Step 3: Calculate the value (fitness) of each raindrop using Eq. (3.8).

Step 4: Determine the intensity of flow for rivers and sea using Eq. (3.11).

Step 5: Determine the streams' flow to the rivers by Eq. (3.13).

Step 6: Determine the rivers' flow to the sea which is the most downhill place using Eq. (3.14).

Step 7: Exchange positions of a river with a stream that gives the best solution, as shown in Figure 3.3.

Step 8: Apply exchange positions between rivers and sea similar to Step 7, if a river finds better solution than the sea, the position of river is exchanged with the sea.

Step 9: Check the evaporation condition using Eqs. (3.15) and (3.16).

Step 10: If the evaporation condition is satisfied, the raining process will occur using Eqs. (3.17) and (3.18).

Step 11: Reduce the value of d_{max}, which is user defined parameter, using Eq. (3.16).

Step 12: Check the convergence criteria. If the stopping criterion is satisfied, the algorithm will be stopped, otherwise return to Step 5.

3.4 CONCLUSION

Different optimization techniques have been described in this chapter, especially the proposed WCA optimization that will be applied in the next chapters. The salient points in this chapter can be summarized as follows:

- Deterministic optimization methods are basically used for single objective, and not with multi-objective, optimization due to its method of operation.
- AI optimization techniques are suitable for multi-objective optimization and overcome the local minimum and maximum for solving the optimization problems in the following chapters.
- The WCA mathematical model is very simple, since it has fewer parameters.
- WCA uses "evaporation and raining conditions," which may resemble the mutation operator in GA. The evaporation and raining conditions can prevent WCA algorithm from getting trapped in local solutions.

4 Harmonic Load Flow Analysis for Radial Distribution Systems

4.1 INTRODUCTION

A load flow analysis involves finding all of the node voltages. After that it is possible to compute currents, power flows, system losses, and other steady-state quantities under given load conditions. These analyses are essential for the continuous evaluation of the existing power system and effective planning of alternatives for system expansion to meet increased load demand in the future. Load flow studies are helpful to confirm selected transformer, capacitor banks, and cable sizing. These studies should also be used to confirm the adequate voltage profiles during different operating conditions, such as heavily loaded and lightly loaded system conditions. Load flow studies can help in determining the optimal size and location of capacitor banks and distributed generation units. The results of load flow studies are also the starting points for other power system studies.

Distribution systems have characteristics different from transmission systems such as radial or weakly meshed structure, large number of branches, and wide-ranging resistance and reactance values. These characteristics make the traditional load flow methods such as fast-decoupled and Newton–Raphson methods [3] not suitable for distribution systems. Therefore several load flow methods have been presented especially for distribution systems. In [4], the authors presented a compensation-based method to solve the load flow problems in distribution systems. In [39], a simple algorithm based on Kirchhoff's current and voltage laws had been presented for analyzing a three-phase radial distribution network. In [40], Chen and Yang proposed an iterative direct branch impedance matrix load flow method based on nontraditional branch-oriented data. Basic graph theory and injection current techniques are also applied. In [5], Das et al. presented a method for solving balanced radial networks based on the utilization of the radial characteristics to develop a numbering scheme for buses and branches. Most recent methods are based on the concept of doing backward/forward sweeps, and these take into account the radial structure of distribution systems. Such methods usually result in faster convergence and a reduced number of equations.

Also harmonic load flow (HLF) is one of the most important tools for distribution system analysis and design. It can be used to quantify the harmonic distortion in voltage and current waveforms at various buses for a given power system. Various harmonic analysis techniques have been presented based on either steady-state

DOI: 10.1201/9781003369448-4

analysis [41,42,43] or transient-state analysis, such as wavelet and time domain analysis [44–46]. In [47], a harmonic load flow method was presented for distribution systems analysis. This method is based on frequency-scan formulation and forward/backward sweep technique. The mathematical formulation of the proposed load flow analysis in this book is described in the following sections.

4.2 FUNDAMENTAL LOAD FLOW

To analyze load flow in a radial distribution system at the fundamental frequency, an iterative technique called backward/forward sweep is specifically designed. The general procedure of the backward/forward sweeps technique is discussed below in detail for the distribution test feeder shown in Figure 4.1.

Step 1: Numbering the nodes of the feeder in ascending form starting from the substation toward the end of the feeder, as shown in Figure 4.1.

Step 2: Preparing the system data matrix, where each row describes one line section, so the matrix consists of six columns as follows:

1. Line section number
2. Number of the node that the line section starts from
3. Number of the end node of this line section
4. The impedance of the line section
5. Load real Power
6. Load reactive Power

Step 3: Determining the end nodes (7, 10, and 11). Also, determining the branched nodes (5, and 9).

Step 4: Determining the main path nodes (1–5, 8, 9, and 11).

Step 5: Determining the nodes in each branch. For example nodes 6 and 7 in the first branch, and node 10 in the second branch.

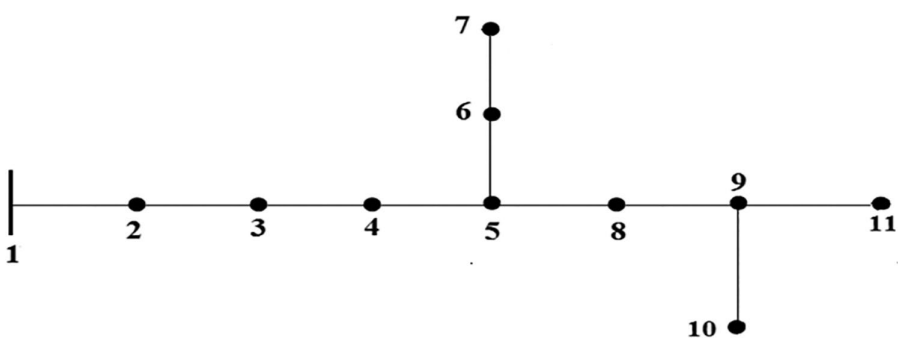

FIGURE 4.1 11-bus radial distribution test feeder.

Step 7: Assuming the voltages at all nodes are nominal.

Step 8: At each node, computing the summation of currents due to shunt components such as load currents, capacitor banks, and distributed generators.

The loads are considered as constant complex power loads, since the load current is calculated as follows:

$$i_i = \left(\frac{s_i}{v_i} \right)^* \tag{4.1}$$

The same equation is used for distributed generators, but the sign of current is negative.

Capacitor currents can be calculated as follows:

$$i_{c_i} = jB_i * v_i \tag{4.2}$$

where,

$$B = \frac{Q_c}{v_{\text{rated}}^2} \tag{4.3}$$

Step 9: Doing backward sweep in each branch starting from the end node downstream to the starting node of this branch, as shown in Figure 4.2. At each line section calculate the current entering this line section, and also calculate the voltages at the node that line section starts from, as follows:

Considering one line section starting from node (n) to node (m), as shown in Figure 4.3. The current entering the line section can be calculated from the following equation:

$$I_{n\_m} = I_{m\_m+1} + I_{l_m} \tag{4.4}$$

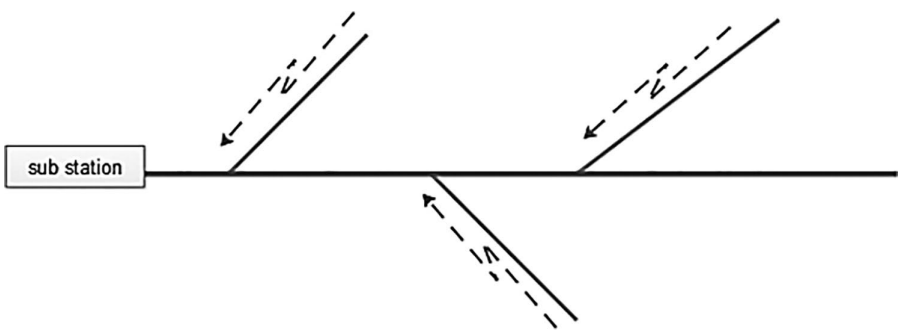

FIGURE 4.2 Backward sweep in each branch.

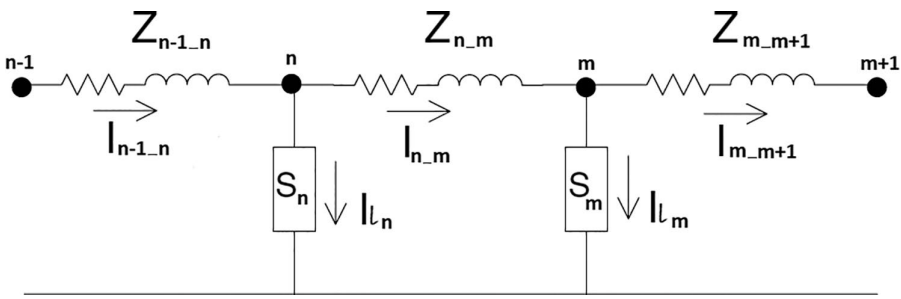

FIGURE 4.3 One line section of radial distribution system.

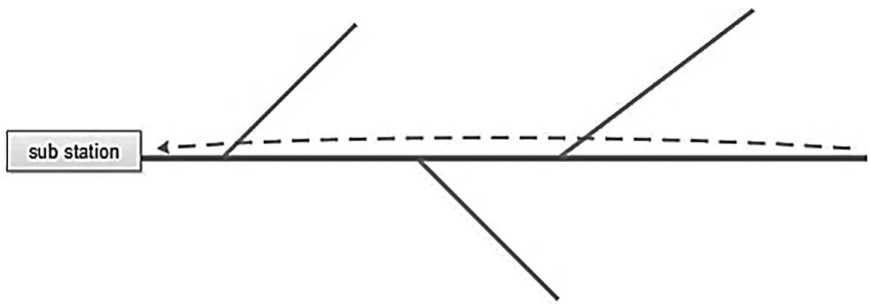

FIGURE 4.4 Backward sweep in the main path.

The voltages at node (n) can be calculated from the following equation:

$$v_n = v_m + I_{n\_m} * Z_{n\_m} \tag{4.5}$$

Step 10: Doing backward sweep in the main path of the feeder starting from the end node downstream up to the starting node of the main path, as shown in Figure 4.4. Also, calculating the voltages and the currents that enter each line section.

Step 11: Calculating the error between the calculated voltage at the first node of the feeder and the specified source voltage.

Step 12: Doing forward sweep in the main path of the feeder starting from the starting node upstream up to the end node as in Figure 4.5. Also, calculating the voltage at the end of each line section by the following equation:

$$v_m = v_n - I_{n\_m} * Z_{n\_m} \tag{4.6}$$

Step 13*:* Doing forward sweep in each branch starting from the start node of this branch upstream up to the end node of the branch as in Figure 4.6. Also, calculating the voltages at the end of each line section.

Step 14*:* Repeating steps 8–13 until the error in step 11 indicates that the first node of the feeder is within a good specified tolerance of the source voltage.

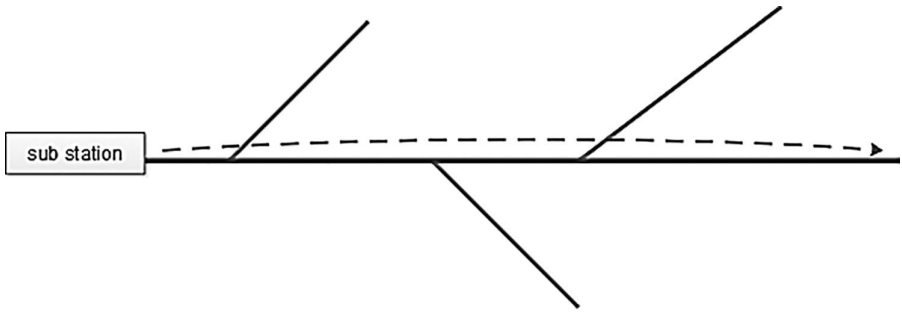

FIGURE 4.5 Forward sweep in the main path.

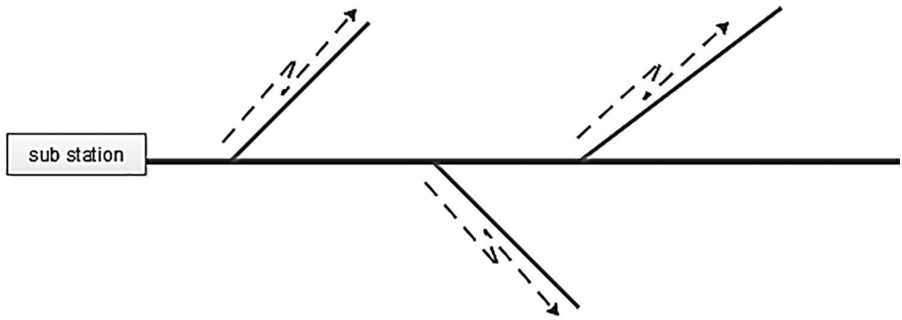

FIGURE 4.6 Forward sweep in each branch.

Numerical Example 4.1

Use the backward/forward sweep power flow method to calculate the voltages and currents of the simple radial distribution system shown in Figure 4.7. The data of the given system is described in Table 4.1. Assume $V_{sub}=V_1=V_2=V_3=V_4=11$ kV initially. Do only one iteration.

Solution:

$Z_{12} = 0.493 + J_0.2511$, $S_2 = 100 + J60$ KVA
$Z_{23} = 0.366 + J_0.1864$, $S_3 = 90 + J40$ KVA
$Z_{34} = 0.3159 + J_0.1635$, $S_4 = 120 + J80$ KVA
$V_1 = V_2 = V_3 = V_4 = 11$ kV
The load current at Node 2 is calculated as

$$I_2 = \left(\frac{S_2}{V_2}\right)^* = \left(\frac{100 + J60}{11}\right)^* = 10.6\angle -30.96 \text{ A}$$

The load current at Node 3 is calculated as

$$I_3 = \left(\frac{S_3}{V_3}\right)^* = \left(\frac{90 + J40}{11}\right)^* = 8.95\angle -23.96 \text{ A}$$

FIGURE 4.7 Single line diagram of a 4-bus radial distribution system.

TABLE 4.1
Data of a 4-Bus Radial Distribution System

Line Number	From	To	R (ohm)	X (ohm)	P_{load} (MW)	Q_{load} (MVAR)
1	1	2	0.4930	0.2511	0.1000	0.0600
2	2	3	0.3660	0.1864	0.0900	0.0400
3	3	4	0.3159	0.1635	0.1200	0.0800

The load current at Node 4 is calculated as

$$I_4 = \left(\frac{S_4}{V_4}\right)^* = \left(\frac{120 + J80}{11}\right)^* = 13.11\angle -33.69 \text{ A}$$

The current flowing in line 3–4 is calculated as

$I_{34} = 13.11\angle -33.69$ A

The current flowing in line 2–3 is calculated as

$I_{23} = I_3 + I_{34} = 21.98\angle -29.74$ A

The current flowing in line 1–2 is calculated as

$I_{12} = I_2 + I_{23} = 32.58\angle -30.14$ A

The voltage at Node 2 is calculated to be

$V_2 = V_1 - Z_{12} * I_{12} = 11000\angle 0 - (0.493 + J0.2511) * 32.58\angle -30.14 = 10982\angle 0.0051$ V

The voltage at Node 3 is calculated to be

$V_3 = V_2 - Z_{23} * I_{23} = 10982\angle 0.0051 - (0.366 + J0.1864) * 21.98\angle -29.74 = 10972\angle 0.0073$ V

The voltage at Node 4 is calculated to be

$V_4 = V_3 - Z_{34} * I_{34} = 10972\angle 0.0073 - (0.3159 + J0.1635) * 13.11\angle -33.69 = 10967.4\angle 0.0099$ V

Based on the obtained voltage values, the system currents are recalculated as follows:

The load current at Node 4 is

$$I_4 = \left(\frac{S_4}{V_4}\right)^* = \left(\frac{120 + J80}{10.967}\right)^* = 13.15\angle -33.69 \ A$$

$$I_{34} = I_4 = 13.15\angle -33.69 \ A$$

$$V_3 = V_4 + Z_{34} * I34 = 10967.4\angle 0.0099 + (0.3159 + J0.1635) * 13.15\angle -33.69 = 10972.05\angle 0.0072 \ V$$

The load current at Node 3 is calculated as

$$I_3 = \left(\frac{S_3}{V_3}\right)^* = \left(\frac{90 + J40}{10.97205\angle 0.0072}\right)^* = 8.976\angle -23.955 \ A$$

$$I_{23} = I_3 + I_{34} = 19.489\angle -10.793 \ A$$

$$V_2 = V_3 + Z_{23} * I_{23} = 10972.05\angle 0.0072 + (0.366 + J0.1864) * 19.489\angle -10.793 = 10979.74\angle 0.0188 \ V$$

The load current at Node 2 is calculated as

$$I_2 = \left(\frac{S_2}{V_2}\right)^* = \left(\frac{100 + J60}{10.97974\angle 0.0188}\right)^* = 10.621\angle -30.945 \ A$$

$$I_{12} = I_2 + I_{23} = 29.686\angle -17.873 \ A$$

The calculated substation voltage is

$$V_1 = V_2 + Z_{12} * I_{12} = 10979.74\angle 0.0188 + (0.493 + J0.2511) * 29.686\angle -17.873 = 10995.95\angle 0.032 \ V$$

At this point the magnitude of the computed voltage at the substation is compared to the magnitude of the calculated substation voltage:

Error = $|V_{1spec} - V_{1cal}|$=11000-10995.95 = 4.05 V

$$\text{Error\%} = \frac{4.05}{11000} \times 100 = 0.0368$$

If the error is greater than the tolerance (typically 0.001 per unit), more iterations are done until the error becomes smaller than the tolerance.

Numerical Example 4.2

Use the backward/forward sweep power flow method to analyze the IEEE 33-bus distribution system shown in Figure A.2, and compute the voltage for all the system buses. Also, calculate the currents in all the system branches. The IEEE 33-bus system data is shown in Appendix A.

Solution:

By applying the illustrated steps for the backward/forward sweep, the MATLAB M-file code for analyzing the IEEE 33-bus distribution system is developed as follows:

```
clc
clear all
%=====================================================================
%                              LINE DATA [Ohm]
%=====================================================================
%branch no sending  reciving  R(Ohm)     X(Ohm)
%=====================================================================
LD=[
    1   1   2   0.0922  0.0470      400;
2   2   3   0.4930  0.2511      400;
3   3   4   0.3660  0.1864      400;
4   4   5   0.3811  0.1941      400;
5   5   6   0.8190  0.7070      400;
6   6   7   0.1872  0.6188      400;
7   7   8   0.7114  0.2351      400;
8   8   9   1.0300  0.7400      400;
9   9   10  1.0440  0.7400      400;
10  10  11  0.1966  0.0650      200;
11  11  12  0.3744  0.1238      200;
12  12  13  1.4680  1.1550      200;
13  13  14  0.5416  0.7129      200;
14  14  15  0.5910  0.5260      200;
15  15  16  0.7463  0.5450      200;
16  16  17  1.2890  1.7210      200;
17  17  18  0.7320  0.5739      200;
18  2   19  0.1640  0.1565      200;
19  19  20  1.5042  1.3554      200;
20  20  21  0.4095  0.4784      200;
21  21  22  0.7089  0.9373      200;
22   3  23  0.4512  0.3083      200;
23  23  24  0.8980  0.7091      200;
24  24  25  0.8960  0.7011      200;
25  6   26  0.2030  0.1034      200;
26  26  27  0.2842  0.1447      200;
27  27  28  1.0590  0.9337      200;
28  28  29  0.8042  0.7006      200;
29  29  30  0.5075  0.2585      200;
30  30  31  0.9744  0.9630      200;
31  31  32  0.3105  0.3619      200;
32  32  33  0.3410  0.5302      200;
];
% Bus No   PloadKW    QLoadKVAR      Qc   pg  Qg
BD=[
    1.0000     0     0     0   0   0;
    2.0000    100    60     0   0   0;
    3.0000    90     40     0   0   0;
    4.0000    120    80     0   0   0;
    5.0000    60     30     0   0   0;
    6.0000    60     20     0   0   0;
    7.0000    200    100    0   0   0;
    8.0000    200    100    0   0   0;
    9.0000    60     20     0   0   0;
   10.0000    60     20     0   0   0;
```

```
    11.0000    45     30     0    0    0;
    12.0000    60     35     0    0    0;
    13.0000    60     35     0    0    0;
    14.0000    120    80     0    0    0;
    15.0000    60     10     0    0    0;
    16.0000    60     20     0    0    0;
    17.0000    60     20     0    0    0;
    18.0000    90     40     0    0    0;
    19.0000    90     40     0    0    0;
    20.0000    90     40     0    0    0;
    21.0000    90     40     0    0    0;
    22.0000    90     40     0    0    0;
    23.0000    90     50     0    0    0;
    24.0000    420    200    0    0    0;
    25.0000    420    200    0    0    0;
    26.0000    60     25     0    0    0;
    27.0000    60     25     0    0    0;
    28.0000    60     20     0    0    0;
    29.0000    120    70     0    0    0;
    30.0000    200    600    0    0    0;
    31.0000    150    70     0    0    0;
    32.0000    210    100    0    0    0;
    33.0000    60     40     0    0    0;
];
%=====================================================


br=length(LD);
no=length(BD);
%=========================================================================
MVAb=100;
KVb=12.66;
Zb=(KVb^2)/MVAb;
%=========================================================================
%                              Per Unit Values
%=========================================================================

for i=1:br
    R(i,1)=(LD(i,4))/Zb;
    X(i,1)=(LD(i,5))/Zb;
end
for i=1:no
    P(i,1)=((BD(i,2))/(1000*MVAb));
    Q(i,1)=((BD(i,3))/(1000*MVAb));
end
R;
X;
P;
Q;
%=========================================================================
%             Code for  bus-injection to branch-current matrix [BIBC]
%=========================================================================
bibc=zeros(size(LD,1),size(LD,1));
for i=1:size(LD,1)
    if LD(i,2)==1
      bibc(LD(i,3)-1,LD(i,3)-1)=1;
    else
       bibc(:,LD(i,3)-1)=bibc(:,LD(i,2)-1);
       bibc(LD(i,3)-1,LD(i,3)-1)=1;
    end
end
```

```
S=complex(P,Q);                                                    % complex power
Vo=ones(size(LD,1),1);% initial bus votage% 10 change to specific data value
S(1)=[];
VB=Vo;
iteration=100;
%=========================================================================
for i=1:iteration
    %=====================================================================
    %                          Backward Sweep Calculation
    %=====================================================================
    I=conj(S./VB);                                          % injected current
    Z=complex(R,X);                                          %branch impedance
    ZD=diag(Z);                                            %makeing it diagonal
    IB=bibc*I;                                               %branch current
    %=====================================================================
    %                          Forward Sweep Calculation
    %=====================================================================
    TRX=bibc'*ZD*bibc;
    VB=Vo-TRX*I;
end
%=========================================================================
Vbus=[1;VB];
V_bus=abs(Vbus)
I_Line=abs(IB)
```

TABLE 4.2
Load Flow Results for the IEEE 33-Bus Distribution System

Bus	Bus Voltage (pu)	Line Current (kA)	Bus	Bus Voltage (pu)	Line Current (kA)
1	1	0.0461	18	0.9131	0.0040
2	0.9970	0.0410	19	0.9965	0.0030
3	0.9829	0.0295	20	0.9929	0.0020
4	0.9755	0.0280	21	0.9922	0.0010
5	0.9681	0.0274	22	0.9916	0.0106
6	0.9497	0.0128	23	0.9794	0.0096
7	0.9462	0.0104	24	0.9727	0.0048
8	0.9413	0.0081	25	0.9694	0.0143
9	0.9351	0.0074	26	0.9477	0.0137
10	0.9292	0.0067	27	0.9452	0.0131
11	0.9284	0.0061	28	0.9337	0.0125
12	0.9269	0.0054	29	0.9255	0.0111
13	0.9208	0.0046	30	0.9220	0.0051
14	0.9185	0.0031	31	0.9178	0.0033
15	0.9171	0.0025	32	0.9169	0.0008
16	0.9157	0.0018	33	0.9166	
17	0.9137	0.0011			

By applying the backward/forward sweep load flow on the IEEE 33-bus distribution system, the following results are obtained (Table 4.2).

Numerical Example 4.3

Use the backward/forward sweep power flow method to analyze the IEEE 69-bus distribution system shown in Figure A.4, and compute the voltage for all the system buses. Also, calculate the currents in all the system branches. The IEEE 69-bus system data is shown in Appendix A.

Solution:

By applying the illustrated steps for the backward/forward sweep, the MATLAB M-file code, for analyzing the IEEE 69-bus distribution system, is developed as follows:

```
%=========================================================================
%            Load flow calculation for the IEEE-69 BUS SYSTEM
%=========================================================================
clc
clear all
%=========================================================================
%                              LINE DATA [Ohm]
%=========================================================================
%branch no sending  reciving  R(Ohm)     X(Ohm)
%=========================================================================
LD=[
    1   1   2   0.0005  0.0012  400 ;
2   2   3   0.0005  0.0012  400 ;
3   3   4   0.0015  0.0036  400 ;
4   4   5   0.0251  0.0294  400 ;
5   5   6   0.366   0.1864  400 ;
6   6   7   0.381   0.1941  400 ;
7   7   8   0.0922  0.047   400 ;
8   8   9   0.0493  0.0251  400 ;
9   9   10  0.819   0.2707  400 ;
10  10  11  0.1872  0.0619  200 ;
11  11  12  0.7114  0.2351  200 ;
12  12  13  1.03    0.34    200 ;
13  13  14  1.044   0.345   200 ;
14  14  15  1.058   0.3496  200 ;
15  15  16  0.1966  0.065   200 ;
16  16  17  0.3744  0.1238  200 ;
17  17  18  0.0047  0.0016  200 ;
18  18  19  0.3276  0.1083  200 ;
19  19  20  0.2106  0.069   200 ;
20  20  21  0.3416  0.1129  200 ;
21  21  22  0.014   0.0046  200 ;
22  22  23  0.1591  0.0526  200 ;
23  23  24  0.3463  0.1145  200 ;
24  24  25  0.7488  0.2475  200 ;
25  25  26  0.3089  0.1021  200 ;
```

```
    26  26  27  0.1732  0.0572  200 ;
    27  3   28  0.0044  0.0108  200 ;
    28  28  29  0.064   0.1565  200 ;
    29  29  30  0.3978  0.1315  200 ;
    30  30  31  0.0702  0.0232  200 ;
    31  31  32  0.351   0.116   200 ;
    32  32  33  0.839   0.2816  200 ;
    33  33  34  1.708   0.5646  200 ;
    34  34  35  1.474   0.4873  200 ;
    35  3   36  0.0044  0.0108  200 ;
    36  36  37  0.064   0.1565  200 ;
    37  37  38  0.1053  0.123   200 ;
    38  38  39  0.0304  0.0355  200 ;
    39  39  40  0.0018  0.0021  200 ;
    40  40  41  0.7283  0.8509  200 ;
    41  41  42  0.31    0.3623  200 ;
    42  42  43  0.041   0.0478  200 ;
    43  43  44  0.0092  0.0116  200 ;
    44  44  45  0.1089  0.1373  200 ;
    45  45  46  0.0009  0.0012  200 ;
    46  4   47  0.0034  0.0084  300 ;
    47  47  48  0.0851  0.2083  300 ;
    48  48  49  0.2898  0.7091  300 ;
    49  49  50  0.0822  0.2011  300 ;
    50  8   51  0.0928  0.0473  200 ;
    51  51  52  0.331   0.1114  200 ;
    52  9   53  0.174   0.0886  300 ;
    53  53  54  0.203   0.1034  300 ;
    54  54  55  0.2842  0.1447  300 ;
    55  55  56  0.2813  0.1433  300 ;
    56  56  57  1.59    0.5337  300 ;
    57  57  58  0.7837  0.263   300 ;
    58  58  59  0.3042  0.1006  300 ;
    59  59  60  0.3861  0.1172  300 ;
    60  60  61  0.5075  0.2585  300 ;
    61  61  62  0.0974  0.0496  300 ;
    62  62  63  0.145   0.0738  300 ;
    63  63  64  0.7105  0.3619  300 ;
    64  64  65  1.041   0.5302  300 ;
    65  11  66  0.2012  0.0611  200 ;
    66  66  67  0.0047  0.0014  200 ;
    67  12  68  0.7394  0.2444  200 ;
    68  68  69  0.0047  0.0016  200 ;
    ];

    % Bus No   PloadKW    QLoadKVAR      Qc   pg  Qg
    BD=[
        1   0   0   0   0   0   ;
    2   0   0   0   0   0   ;
    3   0   0   0   0   0   ;
    4   0   0   0   0   0   ;
    5   0   0   0   0   0   ;
    6   2.6 2.2 0   0   0   ;
    7   40.4    30  0   0   0   ;
    8   75  54  0   0   0   ;
    9   30  22  0   0   0   ;
    10  28  19  0   0   0   ;
    11  145 104 0   0   0   ;
    12  145 104 0   0   0   ;
    13  8   5   0   0   0   ;
```

```
    14  8    5.5 0    0    0    ;
    15  0    0   0    0    0    ;
    16  45.5     30  0    0    0    ;
    17  60   35  0    0    0    ;
    18  60   35  0    0    0    ;
    19  0    0   0    0    0    ;
    20  1    0.6 0    0    0    ;
    21  114  81  0    0    0    ;
    22  5    3.5 0    0    0    ;
    23  0    0   0    0    0    ;
    24  28   20  0    0    0    ;
    25  0    0   0    0    0    ;
    26  14   10  0    0    0    ;
    27  14   10  0    0    0    ;
    28  26   18.6     0    0    0    ;
    29  26   18.6     0    0    0    ;
    30  0    0   0    0    0    ;
    31  0    0   0    0    0    ;
    32  0    0   0    0    0    ;
    33  14   10  0    0    0    ;
    34  19.5     14  0    0    0    ;
    35  6    4   0    0    0    ;
    36  26   18.55   0    0    0    ;
    37  26   18.55   0    0    0    ;
    38  0    0   0    0    0    ;
    39  24   17  0    0    0    ;
    40  24   17  0    0    0    ;
    41  1.2  1   0    0    0    ;
    42  0    0   0    0    0    ;
    43  6    4.3 0    0    0    ;
    44  0    0   0    0    0    ;
    45  39.22    26.3     0    0    0    ;
    46  39.22    26.3     0    0    0    ;
    47  0    0   0    0    0    ;
    48  79   56.4     0    0    0    ;
    49  384.7    274.5    0    0    0    ;
    50  384.7    274.5    0    0    0    ;
    51  40.5     28.3     0    0    0    ;
    52  3.6  2.7 0    0    0    ;
    53  4.35     3.5 0    0    0    ;
    54  26.4     19  0    0    0    ;
    55  24   17.2     0    0    0    ;
    56  0    0   0    0    0    ;
    57  0    0   0    0    0    ;
    58  0    0   0    0    0    ;
    59  100  72  0    0    0    ;
    60  0    0   0    0    0    ;
    61  1244     888 0    0    0    ;
    62  32   23  0    0    0    ;
    63  0    0   0    0    0    ;
    64  227  162 0    0    0    ;
    65  59   42  0    0    0    ;
    66  18   13  0    0    0    ;
    67  18   13  0    0    0    ;
    68  28   20  0    0    0    ;
    69  28   20  0    0    0    ;

    ];
    %=====================================================


    br=length(LD);
```

```
no=length(BD);
%=========================================================================
MVAb=100;
KVb=12.66;
Zb=(KVb^2)/MVAb;
%=========================================================================
%                              Per Unit Values
%=========================================================================

for i=1:br
    R(i,1)=(LD(i,4))/Zb;
    X(i,1)=(LD(i,5))/Zb;
end
for i=1:no
    P(i,1)=((BD(i,2))/(1000*MVAb));
    Q(i,1)=((BD(i,3))/(1000*MVAb));
end
R;
X;
P;
Q;
%=========================================================================
%            Code for  bus-injection to branch-current matrix [BIBC]
%=========================================================================
bibc=zeros(size(LD,1),size(LD,1));
for i=1:size(LD,1)
    if LD(i,2)==1
      bibc(LD(i,3)-1,LD(i,3)-1)=1;
    else
       bibc(:,LD(i,3)-1)=bibc(:,LD(i,2)-1);
       bibc(LD(i,3)-1,LD(i,3)-1)=1;
    end
end
S=complex(P,Q);                                          % complex power
Vo=ones(size(LD,1),1);%initial bus votage% 10 change to specific data value
Vo=ones(size(LD,1),1);%initial bus votage% 10 change to specific data value
S(1)=[];
VB=Vo;
iteration=100;
%=========================================================================
for i=1:iteration
    %=====================================================================
    %                            Backward Sweep Calculation
    %=====================================================================
    I=conj(S./VB);                                        % injected current
    Z=complex(R,X);                                        %branch impedance
    ZD=diag(Z);                                           %makeing it diagonal
    IB=bibc*I;                                               %branch current
    %=====================================================================
    %                            Forward Sweep Calculation
    %=====================================================================
    TRX=bibc'*ZD*bibc;
    VB=Vo-TRX*I;
end
%=========================================================================
Vbus=[1;VB];
V_bus=abs(Vbus)
I_Line=abs(IB)
%=========================================================================
```

TABLE 4.3
Load Flow Results for the IEEE 69-Bus Distribution System

Bus	Bus Voltage (pu)	Line Current (kA)	Bus	Bus Voltage (pu)	Line Current (kA)	Bus	Bus Voltage (pu)	Line Current (kA)
1	1.0000	0.0490	25	.9564	0.0004	49	0.9947	0.0048
2	1.0000	0.0490	26	0.9564	0.0002	50	0.9942	0.0006
3	0.9999	0.0456	27	0.9563	0.0011	51	0.9785	0.0
4	0.9998	0.0352	28	0.9999	0.0008	52	0.9785	0.0231
5	0.9990	0.0352	29	0.9999	0.0005	53	0.9747	0.0230
6	0.9901	0.0351	30	0.9997	0.0005	54	0.9714	0.0227
7	0.9808	0.0346	31	0.9997	0.0005	55	0.9669	0.0224
8	0.9786	0.0331	32	0.9996	0.0005	56	0.9626	0.0224
9	0.9774	0.0097	33	0.9993	0.0003	57	0.9401	0.0224
10	0.9724	0.0093	34	0.9990	0.0001	58	0.9290	0.0224
11	0.9713	0.0070	35	0.9989	0.0023	59	0.9248	0.0210
12	0.9682	0.0045	36	0.9999	0.0019	60	0.9197	0.0210
13	0.9653	0.0044	37	0.9997	0.0016	61	0.9123	0.0043
14	0.9624	0.0043	38	0.9996	0.0016	62	0.9121	0.0039
15	0.9595	0.0043	39	0.9995	0.0013	63	0.9117	0.0039
16	0.9590	0.0037	40	0.9995	0.0010	64	0.9098	0.0008
17	0.9581	0.0030	41	0.9988	0.0010	65	0.9092	0.0005
18	0.9581	0.0023	42	0.9986	0.0010	67	0.9713	0.0002
19	0.9576	0.0023	43	0.9985	0.0009	68	0.9713	0.0007
20	0.9573	0.0022	44	0.9985	0.0009	69	0.9679	0.0004
21	0.9568	0.0008	45	0.9984	0.0005	70	0.9679	
22	0.9568	0.0007	46	0.9984	0.0105			
23	0.9568	0.0007	47	0.9998	0.0105			
24	0.9566	0.0004	48	0.9985	0.0095			

By applying the backward/forward sweep load flow on the IEEE 69-bus distribution system, the following results are obtained (Table 4.3).

4.3 HARMONIC LOAD FLOW

Let us consider a simple radial distribution system consisting of six buses and two nonlinear loads in buses 3 and 5, as shown in Figure 4.7. These nonlinear loads inject harmonic currents into the system. These currents' frequencies are multiples of the normal frequency of the system. These currents distort the voltage of the system, which is called harmonics. Harmonic order (h_o) is the ratio between the harmonic frequency and the fundamental frequency. For each harmonic order, backward/forward load flow calculation will be done with the same sequence of fundamental load flow with the following considerations.

- All loads will be constant impedance load; its impedance is calculated at the specified harmonic frequency.

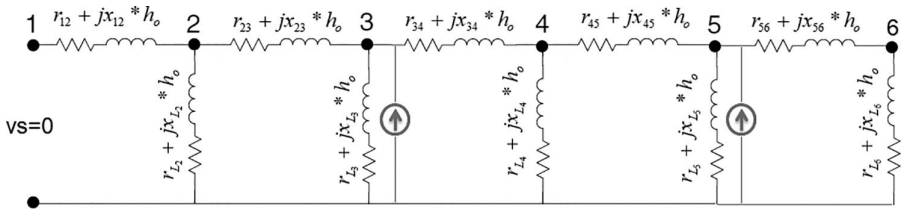

FIGURE 4.8 Simple radial distribution feeder with nonlinear loads.

- Substation voltage will be zero.
- The imaginary part of the line section impedances between buses will be multiplied with the harmonic order.
- Any nonlinear load will be represented by constant impedance load in parallel with a current source which injects current equal to the load current at normal frequency multiplied with the harmonic ratio of this harmonic order, as shown in Figure 4.8.

After doing harmonic load flows at the harmonic orders, the total harmonic distortion (*THD*) at bus (*i*) can be calculated as follows:

$$THD_i = \frac{\sqrt{\sum_{h_o=2}^{\infty} v_{i_{h_o}}{}^2}}{v_{i_1}} \tag{4.7}$$

4.4 SINGLE-TUNED FILTER REPRESENTATION IN LOAD FLOW

The resonance caused after installing the filter may represent a problem while doing harmonic load flow due to the very low impedance (short circuit) of the filter branch, especially at the tuned harmonic order. If the filter impedance is high, the filter is modeled as constant impedance load, as shown in Figure 4.9. If the filter is in resonance case, it is modeled as a constant current source with negative polarity (absorb constant current), as shown in Figure 4.10. The value of this constant current is calculated from the Thevenin equivalent circuit shown in Figure 4.11 as follows:

$$i_{\text{filter}} = \frac{v_{th}}{z_{th}} \tag{4.8}$$

where v_{th} is Thevenin voltage and Z_{th} is Thevenin equivalent impedance.

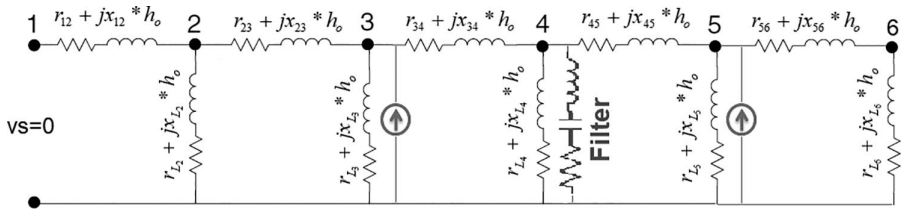

FIGURE 4.9 Filter representation as a constant impedance load in the system.

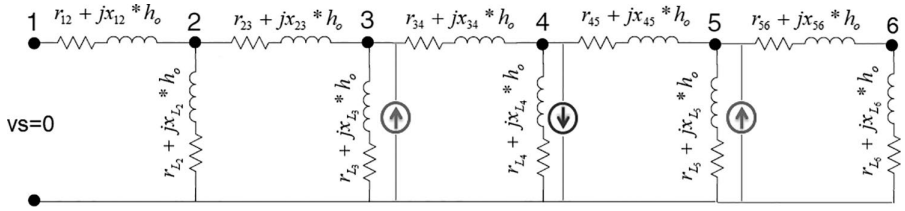

FIGURE 4.10 Filter representation as a constant current source in the system.

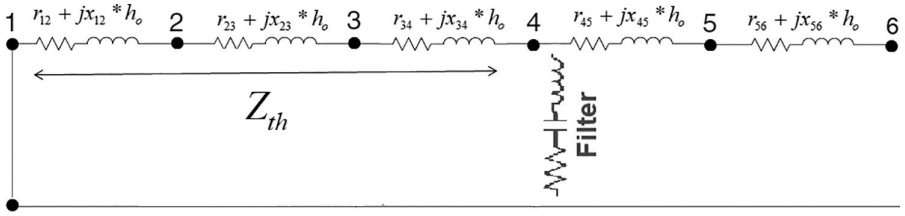

FIGURE 4.11 Thevenin equivalent circuit of the system at resonance conditions.

4.5 CONCLUSION

From this chapter, it can be concluded that

- Conventional iterative power flow methods such as Newton–Raphson and fast decoupled are not suitable for radial distribution feeders.
- The backward/forward sweeps power flow technique is suitable for solving the load flow problem of radial distribution systems.
- The backward/forward sweep method can be formulated to solve harmonic power flow problems in distribution systems.
- Single-tuned harmonic filter representation has been introduced in fundamental and harmonic power flow.

5 Optimal Placement and Sizing of Distributed Generation and Capacitor Banks in Distribution Systems

5.1 INTRODUCTION

5.1.1 Distributed Generation Units Placement

Installation and integration of DGs in distribution systems can provide several technical, economic, and environmental benefits. The technical benefits are power loss reduction, voltage profile improvement, and power quality enhancement [48]. The environmental benefits are the reduction of pollution and emission levels in the system. The economic benefits aim to reduce the operational costs as much as possible and to increase the profits of all system participants.

DG placement has been studied using several techniques. The authors in [49] studied the insertion of the DGs into distribution systems and the effect of their placement on protective device settings. In [50], a cat swarm optimization method was presented for finding the optimal placement and sizing of DGs in the network to reduce total power loss, total generation cost, and emissions. Injeti and Kumar [51] presented a particle swarm optimization (PSO) algorithm to find the optimal placement and sizing of the DGs in distribution systems to minimize power loss. Ref. [52] considered different load levels while finding the optimal placement of the DG using a multi-objective optimization technique. Amini et al. [53] utilized a two-stage optimization method for getting the optimal allocation of DGs and electric vehicles stations.

5.1.2 Capacitor Banks Placement

Installation of CBs in distribution systems can support the reactive power that can improve load-bus voltage and reduce distribution power losses [54]. Thus, the required reactive power demand from the main grid is reduced [55]. Added to that, the voltage fluctuations caused by some types of DGs can be reduced by using (fixed-switched) CBs [56]. Optimal placement and sizing of CBs can offer several benefits

DOI: 10.1201/9781003369448-5

such as minimizing power loss cost and harmonic distortion level [57]. Optimization techniques for CBs placement and sizing problem can be classified into many categories [58]: numerical methods and heuristic and other optimization techniques. A review of CBs placement and sizing techniques has been presented in [59]. In [60], the iterative allocation method of CBs was introduced for reactive power planning problem.

5.1.3 Hybrid DGs/CBs Placement

Therefore, it is expected that a hybrid penetration of DGs and CBs reduces distribution power losses, improves voltage profile, and therefore enhances the overall distribution system performance. But, to achieve these benefits and to decrease voltage deviation problems, placement and sizing of DGs and CBs need to be investigated using proper optimization tools [59]. Saonerkar and Bagde [60] presented a genetic algorithm for achieving the optimal placement and sizing of combined DGs and CBs in distribution systems. Jannat and Savic [61] presented a method for solving the placement and sizing problem considering the effect of renewable energy uncertainty.

5.1.4 Chapter Contribution

The procedure using the WCA to obtain the optimal DGs/CBs placement and sizing in distribution systems proposed in this chapter aims to realize the following benefits:

1. Studying the impact of the DGs and CBs penetration on the technical, environmental, and economic issues of distribution systems.
2. The placement of combined DGs and CBs is simulated as a multi-objective optimization problem.
3. Three technical objectives are satisfied: power loss reduction, voltage profile improvement, and stability index enhancement. While, two economic issues, namely, minimizing the costs of generated power and capacitor banks, are considered. In the viewpoint of environmental benefit, reducing emission is considered for achieving a clean operation.
4. Providing a controllable power factor strategy for flexible operation of distribution systems.
5. Three operational cases of DGs/CBs are considered with single objective optimization to find the effectiveness of the proposed WCA compared with other techniques.
6. Two additional multi-objective cases are considered to estimate the technical, economic, and environmental impacts of the optimal placement and sizing of DGs/CBs.
7. To meet the above feature, the proposed procedure is applied on standard and real radial distribution systems.
8. Simultaneous penetration of DGs and CBs can enhance the distribution system operation by merging the benefits that were defined for each of them.

5.2 PROBLEM FORMULATION

The objective functions (OFs) and the equality and inequality constraints are introduced for optimal placement and sizing of DGs and CBs in distribution systems as follows.

5.2.1 Objective Functions

The DGs/CBs allocation problem aims to achieve three types of OFs: technical, economic, and environmental OFs.

1. **Technical OF:** Three technical OFs are considered in this section.

The first one aims to minimize the distribution power losses (f_1), which can be expressed as [62]

$$f_1(x) = \min \sum_{i=1}^{nL} R_i * |I_i|^2 \tag{5.1}$$

The second technical OF aims to improve the voltage profile and to preserve better voltage profile. This function can be described as [63]

$$f_2(x) = \min \sum_{i=0}^{N} \left(\frac{v_i - v_i^{\text{spec}}}{v_i^{\max} - v_i^{\min}} \right)^2 \tag{5.2}$$

Voltage stability is one of the most significant indices. The third OF (f_3) for voltage stability index can be described as follows [63]:

$$f_3(x) = \min \left(\frac{1}{VSI(m_2)} \right) \tag{5.3}$$

$$\begin{aligned} VSI(m_2) = ABS(&|V(m_1)|^4 - 4 * \left[P(m_2) * X_{ij} - Q(m_2) * R_{ij} \right]^2 \\ &-4 * \left[P(m_2) * R_{ij} + Q(m_2) * X_{ij} \right] * |V(m_1)|^2) \end{aligned} \tag{5.4}$$

2. **Economical Objective Functions:** The economical OF (f_4) aims to minimize the power generation costs. The cost function (f4), which has three components, can be expressed as [51, 64]

$$f_4(x) = \min \sum_{i=1}^{N_{DG}} (C_{DG_i} + C_{\text{sub}} + C_{CB}) \tag{5.5}$$

where the cost of generated power from DG is computed from

$$C_{DG_i} = a + b * PG_i \tag{5.6}$$

The cost coefficients are obtained from

$$a = \frac{\text{capital cost}(\$ / kW) * \text{capacity}(kW) * Gr}{\text{lifetime(year)} * 8760 * LF} \quad (\$) \tag{5.7}$$

$$b = O \,\&\, M \text{ cost}(\$ / kWh) + \text{fuel cost}(\$ / kWh) \tag{5.8}$$

The second cost function is expressed as

$$C_{\text{sub}} = P_{\text{grid}} * Pr_{\text{grid}} \tag{5.9}$$

The cost of CBs is computed from

$$C_{CB} = \frac{\sum_{i=1}^{N_C} (e_i + C_{ci} |Q_{ci}|)}{\text{lifetime} * 8760} \tag{5.10}$$

3. **Environmental Objective Function**: (Minimization of Generation Units' Emissions (f_5)):CO_2, SO_2, and NO_x are considered as most effective pollutants in power generation sources. The mathematical formulation of this objective function can be described as follows [50]:

$$f_5(x) = \sum_{i=1}^{N_{DG}} E_{DG_i} + E_{\text{Grid}} \tag{5.11}$$

where, the emissions produced by the DGs are obtained from

$$E_{DG_i} = (CO_2^{DG} + NO_x^{DG} + SO_2^{DG}) \times PG_i \tag{5.12}$$

The emissions produced by the grid are obtained from

$$E_{\text{Grid}} = (CO_2^{\text{Grid}} + NO_x^{\text{Grid}} + SO_2^{\text{Grid}}) \times P_{\text{Grid}} \tag{5.13}$$

5.2.2 System Constraints

1. Equality operational constraints: The constraints for active and reactive power balance requirements are expressed as

$$\sum_{i=1}^{NG} PG_i - P_L = P_d \;,\; \sum_{i=1}^{NG} QG_i - Q_L = Q_d \tag{5.14}$$

2. Inequality operational constraints: Maximum admissible generated power from DGs/CBs shouldn't exceed their permissible limitations of the distribution systems, which is calculated as
   a. Generation operating limits:

$$PG_i^{\min} \le PG_i \le PG_i^{\max}, QG_i^{\min} \le QG_i \le QG_i^{\max} \tag{5.15}$$

   b. Installed capacitors limits:

$$Q_{\text{total}}^{CB} < Q_d \tag{5.16}$$

   c. Bus voltage limits:

$$0.95 \le V_i \le 1.05, i = 1,2,....nbus \tag{5.17}$$

   d. DG power factor limit:

$$0.8 \le PF \le 1 \tag{5.18}$$

Numerical Example 5.1

It is required to determine the optimal placement and sizing of two capacitor banks that should be installed in the IEEE 33-bus distribution system to minimize the system power loss according to the following assumptions:

- Use the objective function as shown in Eq. (5.1), and according to the constraints in Eqs. (5.14–5.17).
- Total number of populations of WCA equals 100, no. of iterations equals 50.
- The capacitor banks' capacity ranges between 0 and 1500 kVAr.

Solution:
The steps for determining the optimal placement and sizing of the capacitor banks using WCA follows the procedure shown in Figure 5.1. The MATLAB M-file code for the optimal placement and sizing of CBs on the IEEE 33-bus distribution system is developed as shown in the figure.

```
%optimal placement and sizing of capacitor banks using WCA
% objective function= min ploss
% applied on ieee 33-bus)
clc;
clear all
% index  sending  reciving  R(Ohm)     X(Ohm)   Imax(A)
LD1=[
1   1   2   0.0922  0.0470     400;
2   2   3   0.4930  0.2511     400;
3   3   4   0.3660  0.1864     400;
4   4   5   0.3811  0.1941     400;
```

```
5   5   6   0.8190  0.7070     400;
6   6   7   0.1872  0.6188     400;
7   7   8   0.7114  0.2351     400;
8   8   9   1.0300  0.7400     400;
9   9   10  1.0440  0.7400      400;
10  10  11  0.1966  0.0650      200;
11  11  12  0.3744  0.1238      200;
12  12  13  1.4680  1.1550      200;
13  13  14  0.5416  0.7129      200;
14  14  15  0.5910  0.5260      200;
15  15  16  0.7463  0.5450      200;
16  16  17  1.2890  1.7210      200;
17  17  18  0.7320  0.5739      200;
18  2   19  0.1640  0.1565      200;
19  19  20  1.5042  1.3554      200;
20  20  21  0.4095  0.4784      200;
21  21  22  0.7089  0.9373      200;
22   3  23  0.4512  0.3083      200;
23  23  24  0.8980  0.7091      200;
24  24  25  0.8960  0.7011      200;
25  6   26  0.2030  0.1034      200;
26  26  27  0.2842  0.1447      200;
27  27  28  1.0590  0.9337      200;
28  28  29  0.8042  0.7006      200;
29  29  30  0.5075  0.2585      200;
30  30  31  0.9744  0.9630      200;
31  31  32  0.3105  0.3619      200;
32  32  33  0.3410  0.5302      200;
];
% Bus No    PloadKW     QLoadKVAR       Qc   pg  Qg
BD=[
   1.0000     0     0     0   0   0;
    2.0000    100    60    0   0   0;
    3.0000    90     40    0   0   0;
    4.0000    120    80    0   0   0;
    5.0000    60     30    0   0   0;
    6.0000    60     20    0   0   0;
    7.0000    200    100   0   0   0;
    8.0000    200    100   0   0   0;
    9.0000    60     20    0   0   0;
   10.0000    60     20    0   0   0;
   11.0000    45     30    0   0   0;
   12.0000    60     35    0   0   0;
   13.0000    60     35    0   0   0;
   14.0000    120    80    0   0   0;
   15.0000    60     10    0  0   0;
   16.0000    60     20    0   0   0;
   17.0000    60     20    0 0  0;
```

```
   18.0000    90     40    0  0   0;
   19.0000    90     40    0   0   0;
   20.0000    90     40    0  0   0;
   21.0000    90     40    0   0   0;
   22.0000    90     40    0   0   0;
   23.0000    90     50    0   0   0;
   24.0000    420    200   0   0   0;
   25.0000    420    200   0   0   0;
   26.0000    60     25    0   0   0;
   27.0000    60     25    0   0   0;
   28.0000    60     20    0   0   0;
   29.0000    120    70    0  0   0;
   30.0000    200    600   0   0   0;
   31.0000    150    70    0   0   0;
   32.0000    210    100   0   0   0;
   33.0000    60     40    0  0   0;
];
 dr(1,1)=0;%booo
 dmax=1*10^-3;%evaporation and raining process factor
 W1=1;
 npop=100;  %number of raindrops
 itt=50;  %number of itterations
 n_run=2;  %number of program runs
 run(itt,n_run)=0; % store matrix personal pest fitness function for all itt
 ploss_best(itt,n_run)=0;
for run_number=1:n_run
 % assume the ploss and qloss in the first itt is same for all cats and taki
 average_ploss= .2027*1000;   % KW
 average_Qloss= .2027*1000;   % KW
 % calculate pload and qload from the bus matrix of the system and losses
 bb=BD(:,2);
 pload_system=sum(bb);
 qload_system=sum(BD(:,3));
 pload=ones(npop,1)*(pload_system+average_ploss);
 Qloadtt=ones(npop,1)*(qload_system+average_Qloss);
 pload;
 Qloadtt;
 min_bus_voltage(npop,1)=0;
 bus_num_vmin(npop,1)=0;
 %=============================================================================
  % pbest(itt,1)=0;  %matrix of personal pest fitness function of cats
   r11=rand(1);          %a random number with the range of [0, 1]
   c11=2;                %the acceleration constant
   %matrix of fitness functions
  total_losses(npop,1)=0;
  fitness(npop,1)=0;
   %---------------
  gbest=inf;   %min ploss of fitness function matrix
```

```
u(npop,1)=0; ratio=100;
for i=1:npop
   u(i,1)=1;
end;

 CB_location(npop,ng-1)=0;   %matrix of CBs location
databest(1,2*ng)=0;    % data of best raindrops solution (pgi,qgi)
c(npop,2*ng)=0;       %matrix of solutions data of all raindrops in each itt
n_branch=length(LD1);   %no of lines on the system
n_bus=length(BD);       % no of buses on the system
mbccli(n_branch,1)=0;
vdi(n_bus,1)=0;
% step1  Randomly initialize the initial set of raindrops of size Npop,
%where each rains is of dimensions [ pg1 pg2 .....pgng, qg1 qg2 .....qgng]
%~~~~~~~~~~~~~~~~~~~~~~~~~~~~~~~~~~~~~~~~~~~~~~~~~~~~~~~~~~~~~~~~~~~~~~~~~~~~
for z=1:itt
    z;
      %%mak sum pg,qg =load
 if(z>1)
    for ja=1:npop
      if  (ploss(ja,1)==inf)
      ploss(ja,1)=average_ploss;
      end
    end
 ploss ;
last_ploss=ploss;
last_qloss=Qloss;

pload=ones(npop,1)*pload_system+last_ploss;
Qloadtt=ones(npop,1)*qload_system+last_qloss;
end
for jj=1:npop
    for i=2:ng
        if(c(jj,i)<ming(i))
           c(jj,i)=ming(i);
        end
        if(c(jj,i)>maxg(i))
           c(jj,i)=maxg(i);
        end
     suma(jj,1)=suma(jj,1)+c(jj,i);
     sumar1(jj,1)=sumar1(jj,1)+(c(jj,i)-ming(i));
     sumar2(jj,1)=sumar2(jj,1)+(maxg(i)-c(jj,i));

    end

c(jj,1)= pload(jj,1)-suma(jj,1);

    if (c(jj,1)<ming(1))
       rs1(jj,1)=ming(1)-c(jj,1);
       c(jj,1)=ming(1);
        for i=2:ng
        c(jj,i)=c(jj,i)-rs1(jj,1)*(c(jj,i)-ming(i))/sumar1(jj,1);
        end
    end
```

```
    if (c(jj,l)>maxg(l))
        rs2(jj,l)=-maxg(l)+c(jj,l);
        c(jj,l)=maxg(l);
         for i=2:ng
          c(jj,i)=c(jj,i)+rs2(jj,l)*(maxg(i)-c(jj,i))/sumar2(jj,l);
         end
    end
 for ii=1:ng-1
  if(CB_location(jj,ii)<2)
     CB_location(jj,ii)=2;
  end
  if(CB_location(jj,ii)>33)
     CB_location(jj,ii)=33;
  end
 end
%step3      Evaluate the fitness of each cat and keep the position of
%           the pop that has the highest fitness value.
 ploss=zeros(npop,1);
 Qloss=zeros(npop,1);
for j=1:npop
 BD(:,5)=zeros(n_bus,1);
 BD(:,6)=zeros(n_bus,1);
 BD(1,5)=c(j,1);
 BD(1,6)=c(j,ng+1);
 for ndg=1:ng-1
  q2=CB_location(j,ndg);
 BD(q2,5)=c(j,ndg+1);
 BD(q2,6)=c(j,ng+ndg+1);
 end
%====================================================================
%                    power flow
%====================================================================
for abc=1:1...
for w9=1:n_branch...
vdi=1*ones(n_bus,1)-voltage;
min_bus_voltage(j,1)=min(voltage);
for w66=1:n_bus...


%====================================================================
%                   end power flow
%--------------------------------------------------------------------
ploss(j,1)=0;
Qloss(j,1)=0;
 ploss(j,1)=sum(Plosskw);
 Qloss(j,1)=sum(Qlosskw);
  %*************************************************************************
  % fittness function
  %min power loss *************************
  total_losses(j,1)=ploss(j,1);
  %*************************************************************************

  fitness(j,1)=total_losses(j,1);
  %*************************************************************************
```

```
  %cheek the constrain of voltage on buses
 VM=voltage;
 for ww=1:n_bus
 if ((VM(ww) >1.05) || (VM(ww) <0.95 ))
  fitness(j,1) = inf;break;
 end;
 end
 IBASE=MVAb/(KVb/1000);
 for www=1:n_branch
 if( (Ibrp(www,1)*IBASE) >LD1(www,6))
  fitness(j,1) = inf;break;
 end;
 end

% start WCA xxxxxxxxxxxxxxxxxxxxxxxxxxxxxxxxxxxxxxxxxxxxxxxxxxxxxxxxxxxxxxx
% xxxxxxxxxxxxxxxxxxxxxxxxxxxxxxxxxxxxxxxxxxxxxxxxxxxxxxxxxxxxxxxxxxxxxxxx
% End WCA xxxxxxxxxxxxxxxxxxxxxxxxxxxxxxxxxxxxxxxxxxxxxxxxxxxxxxxxxxxxxxxx
c=rd(1:npop,1:2*ng);
CB_location=round(rd(1:npop,2*ng+1:3*ng-1));
%xxxxxxxxxxxxxxxxxxxxxxxxxxxxxxxxxxxxxxxxxxxxxxxxxxxxxxxxxxxxxxxxxxxxxxx
if(z==itt)
    break;
end

end
last_sol=databest
min_ploss=ploss_best(itt,1)
min_bus_voltage=bus_Vmin
min_bus_voltge_value=min_bus_voltage1
last_placement=best_buses
it=[1:itt];
run(:,run_number)=pbest(:,1);


end
best_run=min(run(itt,:))
 for j7=1:n_run
     if(run(itt,j7)==best_run)
         k3=j7;
     end
 end
best_run_data=k3
```

The results of applying the described code results in selecting two CBs to be installed at bus 13 and 31 with capacities equal to 0.8708 kVAr and 0.9392 kVAr, respectively, where, this solution reduces the power loss from 202.67 kW to 143.48 kW.

5.3 APPLICATIONS

5.3.1 Test Distribution Systems

The proposed procedure using WCA is applied to three distribution systems. These systems are IEEE 33-bus distribution system [65], IEEE 69-bus distribution system [8],

and the EDN as a real part of the Egyptian distribution network [66]. The total real and reactive loads of the three systems are 3.715+j2.3 MVA, 3.802+j2.694 MVA, and 22.441+j14.162 MVA, respectively. The power flow calculations are carried out using backward/forward sweeping [66, 67]. The total real power losses for the three distribution systems in the initial case are 202.67 kW, 225 kW, and 805.73 kW, respectively.

5.3.2 WCA for Allocating DGs and CBs in the System Problem

The allocation of combined DGs and CBs is considered as an optimization problem which can be solved using the proposed procedure by loading the distribution system data and defining the power limits of DGs and CBs in the system, and then applying the WCA steps stated in Chapter 3. The flow chart of the proposed procedure is shown in Figure 5.1.

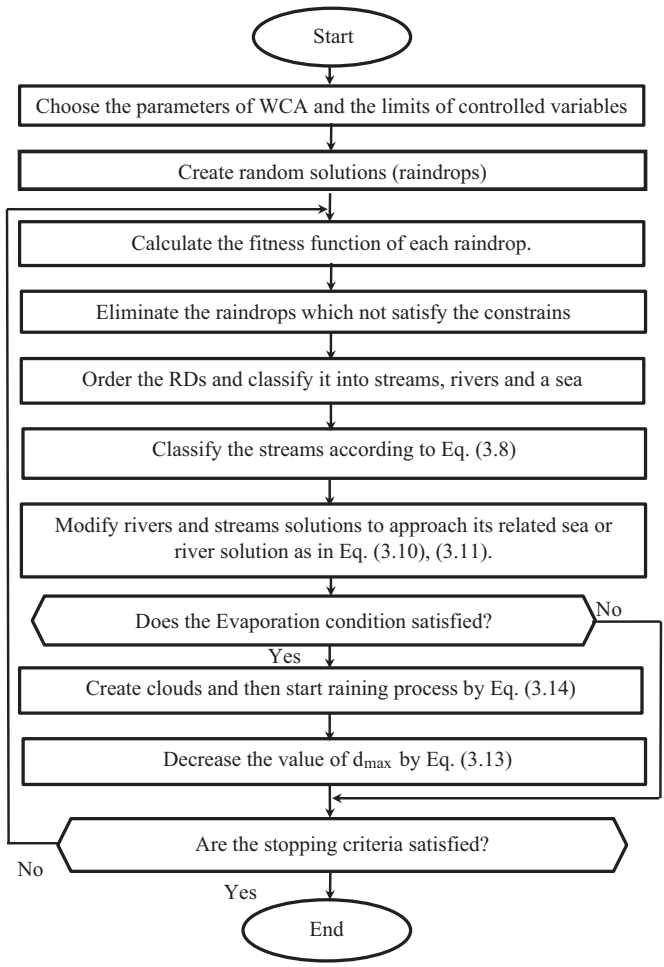

FIGURE 5.1 Flow chart of the proposed procedure.

5.3.3 Cases Studied

Five operational cases are introduced to show the effectiveness of the proposed procedure and to study the impact of DGs and CBs installation on system performance:

Case 1: Single OF, power loss minimization, is considered for placement and sizing of CBs alone.

Case 2: Single OF, power loss minimization, is considered for placement and sizing of DGs that operate at unity PF.

Case 3: Single OF, power loss minimization, is considered for optimal placement and sizing combination of CBs/DGs.

Case 4: Multi-objective optimal placement and sizing of CBs/DGs. The DGs are operated with controllable PF. Three technical objectives (f_1, f_2, f_3) are considered. The multi-OF is implemented by using the weighting factors approach. The OF can be expressed as follows:

$$OF = \min(k_1 f_1 + k_2 f_2 + k_3 f_3) \tag{5.19}$$

Case 5: Multi-objective optimal placement and sizing of multi-CBs/DGs. DGs are controllable units to supply active and reactive power. The technical, economic, and environmental objectives (f_1, f_4, f_5) are optimized. Therefore, the combined objective function (COF) can be written as

$$COF = \min(k_1 f_1 + k_2 f_4 + k_3 f_5) \tag{5.20}$$

The economic and environmental properties of DGs are dependent on their type. Table 5.1 shows the characteristics of the considered DGs, which are customized from [50, 64].

In order to increase the DGs penetration levels, three types of DGs are considered (PV, WT, GT). Generated power costs at substations are considered to be 0.044 $/kWh [64]. The coefficients e_i and C_{ci} are taken equal to 1,000 and 30,000 $/MVAr, respectively [54]. The generated power cost in the EDN grid is (0.0625+0.72 P_{rsub}) $/h according to [68].

TABLE 5.1
Characteristics of DGs

DG Type	Rated Capacity (MW)	Life Time (year)	Capital Cost ($/kW)	O&M Costs ($/kWh)	Fuel Cost ($/kWh))	Emission Factors (lb/MWh)		
						NO_X	SO_2	CO_2
Grid	25	25	—	—	0.044	5.06	11.6	2031
PV	1	20	3985	0.01207	—	—	—	—
WT	5	20	1822	0.00952	—	—	—	—
GT	3	12	1224	0.06481	0.0667	0.279	0.93	1239.2

5.4 RESULTS AND COMMENTS

5.4.1 Results of 33-Bus Network

Results of case 1 are shown in Table 5.2 where the optimal placement and sizing of CBs is determined using the proposed procedure. The results of this case are compared with other algorithms (bacterial foraging optimization algorithm (BFOA) [69], crow search algorithm (CSA) [70], and PSO [71]). Three capacitors are installed at buses 14, 24, and 30. The results show that the proposed procedure is efficient to find the optimal solution with the lowest real power losses of 130.91 kW and the total installed CBs capacity equals 1.8484 MVAR. The lowest voltage (0.951 p.u.) is found at bus 18.

Table 5.3 presents the optimal solution for case 2. It shows the effectiveness of the proposed procedure for finding the optimal placement and sizing of DGs only. The obtained results are assessed comparing with that of BFOA in [69, 71–73]. The proposed procedure gives a significant reduction in total active power loss to be 71.052 kW with a reduction of 64.9% referred to the initial case of 202.67 kW. Three DGs are installed at buses 14, 24, and 29 with penetration power equal to 0.8546,

TABLE 5.2
Optimal Placement and Sizing of CBs for the 33-Bus System (Case 1)

Method	Power Loss (kW)	CBs Size (MVAR) and Location	Min. Voltage (p.u.)
BFOA[23]	144.04	0.349 (18), 0.821 (30), 0.277 (33)	0.936*
CSA [24]	131.5	0.6(11), 0.3(33), 0.45(24), 0.6(30)	0.943*
PSO [24]	132.48	0.9(2),0.45(7),0.45(31),0.3(15), 0.45(29)	0.945*
WCA	130.91	0.3973(14),0.4511(24), 1.0(30)	0.951(18)

**The bus number which had minimum voltage has not been mentioned.*

TABLE 5.3
Optimal Placement and Sizing of DGs for the 33-Bus System (Case 2)

Method	Power Loss (kW)	DG Size (MW) and Location	Min. Voltage (p.u.)
FWA [16]	88.68	0.5897(14),0.189(18),1.0146(32)	0.968*
BFOA [23]	98.3	0.633 (17),0.09 (18),0.9470 (33)	0.964*
HSA [25]	96.76	0.5724(17),0.107(18),1.0462(33)	0.967 (29)
TM[26]	91.305	0.5876(15),0.1959(25),0.783(33)	0.958 (30)
GA/PSO [27]	103.4	0.9250(11),0.8630(16),1.2(32)	0.980 (25)
PSO [27]	105.35	1.1768(8),0.9816(13),0.8297(32)	0.980 (30)
GA [27]	106.3	1.50(11),0.4228(29),1.0714(30)	0.981 (25)
WCA	71.052	0.8546(14),1.1017(24),1.181(29)	0.973 (33)

**Placement of minimum bus voltage has not been mentioned.*

1.017, and 1.181 MW, respectively. The minimum voltage level (0.973) is obtained at bus 33.

Table 5.4 presents the results of case 3. In case 3, the proposed procedure gives superior power loss reduction compared with cases 1 and 2. Case 3 suggests installing three DGs at buses 11, 25, and 29 and three CBs at buses 14, 23, and 30. A significant power loss reduction (24.688 kW) is achieved compared to GA (71.25 kW) and BFOA (41.41 kW). The minimum voltage level of 0.98 p.u. is obtained at bus 33.

From the results of case 4 that is shown in Table 5.5, it is clear that the optimal placement and sizing of DGs (with controllable PF (and CBs will be very effective to minimize system power loss, improve voltage stability index, and minimize voltage deviation. A comparison between bus voltage profiles of different cases can be seen in Figure 5.2. The convergence curves for the IEEE 33-bus distribution system are presented in Figure 5.3. The evaporation process for the proposed procedure using WCA leads to optimal solutions with fewer number of iterations. Table 5.6 presents the technical, economic, and environmental benefits of simultaneous placement of DGs and CBs in 33-bus distribution system. Results show that the total emission is reduced by 58% due to the penetration of renewable DGs (PV with 0.7149 and 0.6397; WT with 0.6476; and GT with 0.2008 MW). Also, the generated power cost is reduced by 18%, while the distribution power loss is reduced to 28.962 kW.

TABLE 5.4
Placement and Sizing of DGs and CBs for the 33-Bus System (Case 3)

Method	Power Loss (kW)	DG Size (MW) and Location	Capacitor Size (MVAR) and Location	Min. Voltage (p.u.)
GA [14]	71.25	0.25 (16), 0.25 (22), 0.50 (30)	0.30 (15) , 0.30 (18) 0.30 (29), 0.60 (30), 0.30 (31)	0.971*
BFOA [23]	41.41	0.542 (17), 0.160 (18), 0.895 (33)	0.163 (18), 0.338 (33), 0.541 (30)	0.978*
WCA	24.688	0.973(25), 1.04 (29), 0.563(11)	0.465 (23), 0.565 (30) 0.535(14)	0.980 (33)

**Placement of minimum bus voltage has not been mentioned.*

TABLE 5.5
Multi-objective Placement and Sizing for the 33-Bus System (Case 4)

Method	DG		Capacitor Size (MVAR) and Location	Min. Voltage (p.u.)
	Power Factor	Size (MW) and Location		
WCA	0.905	0.9917(11)	0.325(19)	0.989(18)
	0.985	0.9823(31)	0.3116(23)	
	0.959	1.652(24)	0.5432(30)	
OF	f1=19.848	f2=0.041	f3=0.015	

TABLE 5.6
Multi-objective Placement and Sizing for the 33-Bus System (Case 5)

	Location	Active Power (MW)	Reactive Power (MVAR)
Grid	1	1.5410	0.6572
PV	32, 27	0.7149, 0.6397	0.4385, 0.2776
WT	25	0.6476	0.1467
GT	18	0.2008	0.0516
CB	15, 26, 19	0, 0, 0	0.3, 0, 0.45
OFs	**Power losses (kW)**	**Cost ($/h)**	**Emission (lb/h)**
Before	202.6	304.8966	8.0267e+006
After	28.9615	249.3429	3.4045e+006

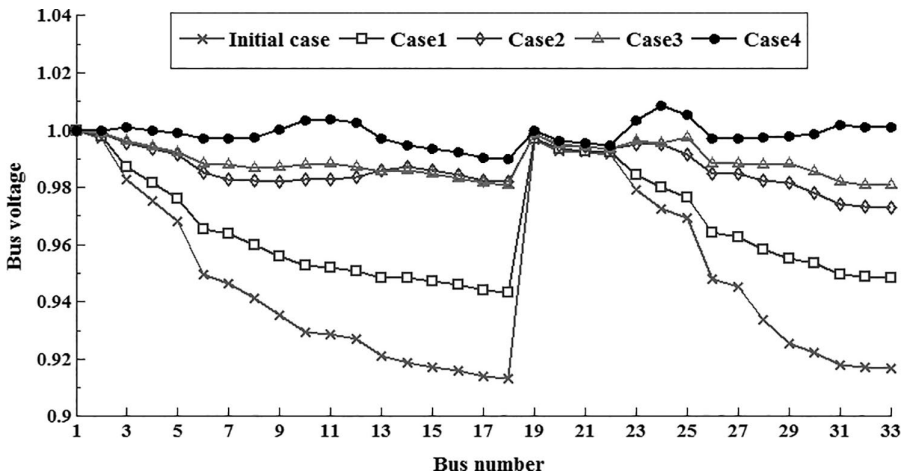

FIGURE 5.2 Voltage profiles of different cases for the 33-bus system.

5.4.2 Results of 69-Bus Network

Tables 5.7 and 5.8 present the results of cases 1 and 2 for the 69-bus standard network, respectively. It can be observed that the power loss obtained by WCA is better than those obtained by other competition methods. The power loss obtained by WCA is decreased to 144.53 kW and 71.5 kW for cases 1 and 2, respectively. Add to that, the voltage profiles have the lowest voltage levels at node 65 for cases 1 and 2 (0.95, 0.979 p. u.), respectively. Table 5.9 shows the placement of DGs and CBs for cases 3 and 4. In case 3 the power loss is 33.339 kW, which is the smallest value compared to cases 1 and 2, with DGs at nodes 69, 61, and 17 using active power penetration levels of 1.159, 2, and 0.541 MW, respectively. Also, three CBs at nodes 2, 62, and 69 are used with reactive power penetration levels of 1.188, 1.237, and 0.27 MVAR, respectively. Therefore, the DGs/CBs placement enhances the power loss reduction and maximizes the energy utilization of the distribution system. Multi-objective optimal

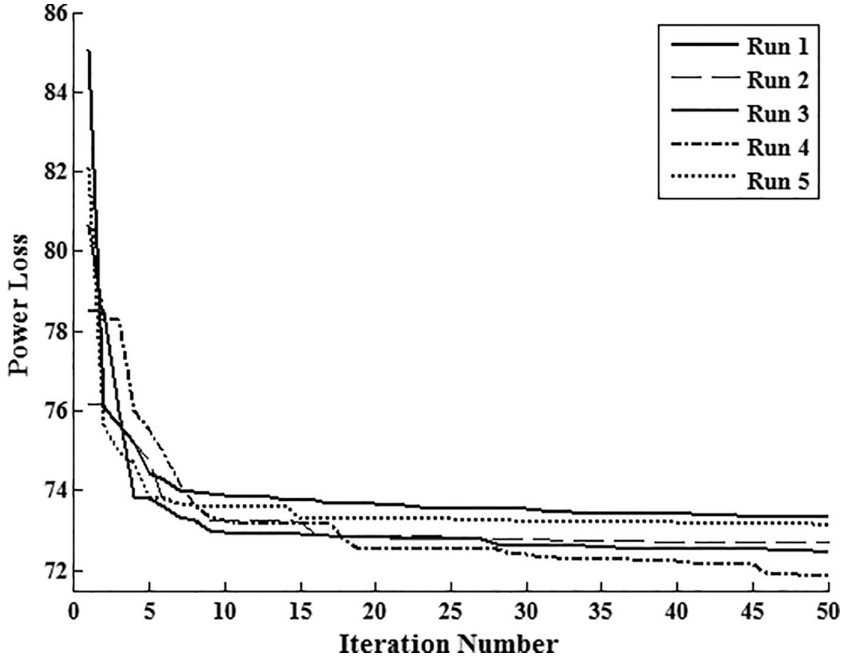

FIGURE 5.3 Convergence curves of case 2 for the first five runs of the 33-bus distribution system.

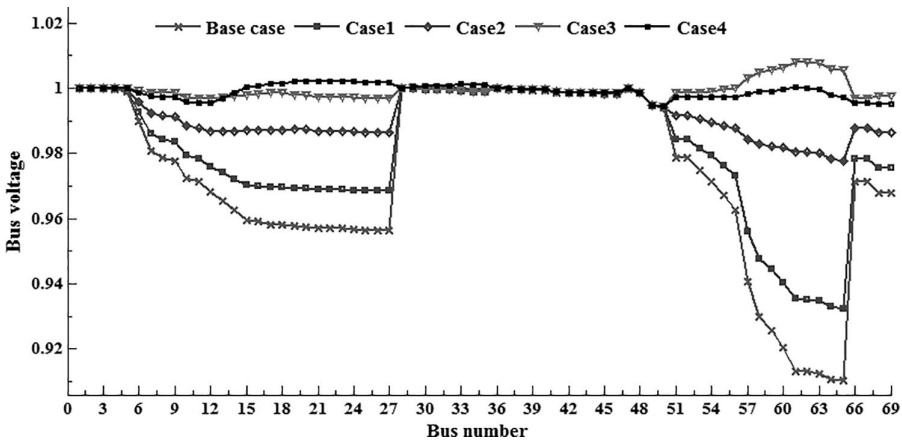

FIGURE 5.4 Voltage profiles of different cases for the 69-bus distribution system.

placement and sizing of CBs and DGs with controllable PF (case 4) give better results than using DG with unity PF as shown in Table 5.9. Also, the voltage profile of the system in case 4 is better than that of the other cases as shown in Figure 5.4. Table 5.10 shows the application of case 5 for the 69-bus distribution system. A high reduction in power loss (22.36 kW) is obtained. Added to that, significant economic

TABLE 5.7
Optimal Placement and Sizing of CBs for the 69-Bus System (Case 1)

Method	Power loss (kW)	Capacitor size (MVAR) and location	Min. voltage (p.u.)
PSO [65]	156.14	1.015(59),0.241(61), 0.365(65)	0.934*
DE [74]	149.55	0.2(16), 0.7(60), 0.5(61)	0.928*
(DE-PS) [75]	146.13	0.95(61),0.2(64), 0.05(65), 0.15(95), 0.3(21)	0.931*
CSO [76]	147.95	1.2(62), 0.25(21)	0.930*
TLBO [77]	146.35	0.6 (12) ,1.050(61),0.150(64)	NR
GSA [78]	145.9	0.15(26),0.15(13), 1.050(15)	0.952*
DSA [79]	147	0.9(61), 0.45(15), 0.45(60)	NR
WCA	144.53	1.2882(61),0.2134(69), 0.27(18)	0.95 (65)

**Placement of minimum bus voltage has not been mentioned.*

TABLE 5.8
Placement and Sizing of DGs Only for the 69-Bus System (Case 2)

Method	Power loss (kW)	DG size (MW) and location	Min voltage (p.u)
FWA [63]	77.85	0.2258 (27), 1.1986 (61), 0.4085 (65)	0.974(62)
HSA [78]	86.77	1.7732	0.967*
GA [80]	88.5	1.9471	0.969*
RGA [81]	87.65	1.7868	0.968*
CVSI [82]	83.18	1.895 (61)	0.968(27)
WCA	71.5	0.775(61), 1.105(62), 0.4380(23)	0.987(65)

**Placement of minimum bus voltage has not been mentioned.*

and environmental benefits are satisfied in case 5. However, economic benefits are achieved by reducing production costs from 309.7134 $/h to 297.47 $/h, while the emissions pollution is reduced from $82.508*10^5$ lb/h to $4.247*10^5$ lb/h.

5.4.3 Results of the Real Distribution System

The results of the proposed procedure using WCA for cases 1–4 applied to EDN are shown in Table 5.11. Results show a significant improvement in system performance (VSI and VD). A comparison between bus voltage profiles of each case is shown in Figure 5.5 for EDN. The highest reduction in power losses (47.1369 kW) is obtained with the placement of DGs and CBs in case 4. Also, case 4 has the best voltage profile with the lowest voltage deviation of 0.0029 p.u. compared to cases 1–3. Cases 3 and 4 present acceptable levels of VSI compared with cases 1 and 2.

TABLE 5.9
Placement and Sizing of DGs and CBs for the 69-Bus System for Cases 3 and 4

	DGs			CBs		Min. voltage (p.u.)
Cases	Location	Size (MW)	Power factor	Location	Size (MVAR)	
Case 3	17	0.5408	1.0	2	1.1879	0.994 (50)
	61	2	1.0	62	1.2373	
	69	1.1592	1.0	69	0.2697	
	OF: f_1=33.339 kW					
Case 4	61	1.8247	0.877	15	0.0188	0.994 (50)
	36	1.0414	0.916	33	0.4578	
	19	0.1063	0.904	22	0.5586	
OFs	f_1=18.7048 kW		f2=0.0092		f_3= 0.0313	

TABLE 5.10
Multi-objective Placement and Sizing Solution for the 69-Bus System (Case 5)

	Location	Active power (MW)	Reactive power (MVAR)
Grid	1	1.7467	0.2946
PV	58	0.1024	0.0352
	66	0.7314	0.2913
WT	63	0.7030	0.2742
GT	64	0.5405	0.3130
CB	23, 62, 42	0, 0, 0	0.6, 0.6, 0.3
OFs	Power losses (kW)	Cost ($/h)	Emission (lb/h) × 10^6
Before	225	309.7134	8.2508
After	22.36	297.47	4.247

TABLE 5.11
Placement and Sizing of DGs and CBs of EDN for Cases 1–4

Method	Case1	Case2	Case3	Case4
DG size	____	0.59(21)	3.5586 (24)	7.49, 2.74 (16)
(MW,MVAR) and		0.59(6)	7.5307 (5)	6.11, 1.99 (22)
location		0.726(16)	6.537 (19)	5.06, 3.393 (7)
CB size (MVAR)	3.302 (22)	____	5.119(14)	3.61 (17)
and location	3.736 (6)		5.825 (18)	2.35 (2)
	5.047 (16)		2.472(11)	
Min. voltage (p.u.)	0.957(30)	0.983(30)	0.995(15)	0.997(30)
Power loss (kW)	581.368	250.18	53.836	47.1367
VD	0.698	0.328	0.0071	0.0029
VSI	0.039	0.036	0.035	0.035

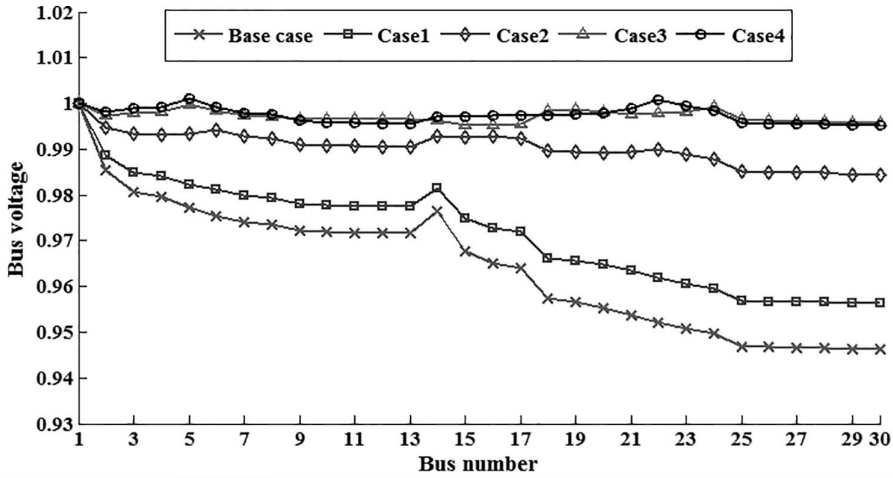

FIGURE 5.5 Voltage profiles of different cases for EDN system.

TABLE 5.12
Multi-objective Solution of EDN for Case 5

DG type	Location	Active Power (MW)	Reactive Power (MVAR)
Grid	1	12.663	4.251
PV	30, 7	1.0, 1.0	0. 006, 0.001
WT	19	5	3.750
GT	28	3	2.250
CB	3	0	4.050
OF	**Power losses (kW)**	**Cost ($/h)**	**Emission (lb/h) × 10^6**
Before	805.7327	16870	47.602
After	257.4912	9717.4	32.146

Simulation results obtained by multi-objective optimization of the technical, economic, and environmental objectives are shown in Table 5.12. The PV and WT have active roles in emission reduction, and both DGs and CBs have active roles in power loss and power generation cost reduction. For case 5 a large reduction in power loss (257.49 MW) is obtained. Significant economic and environmental benefits are satisfied in case 5. Economic benefits are achieved by reducing production cost from 16870 $/h to 9717.4 $/h. while the emissions pollution is reduced from 47.602 Mb/h to 32.146 Mlb/h.

The above results for different test systems assure the capability of the proposed procedure to achieve significant technical, economic, and environmental benefits. The power losses of the different cases for the test systems are shown in Figure 5.6.

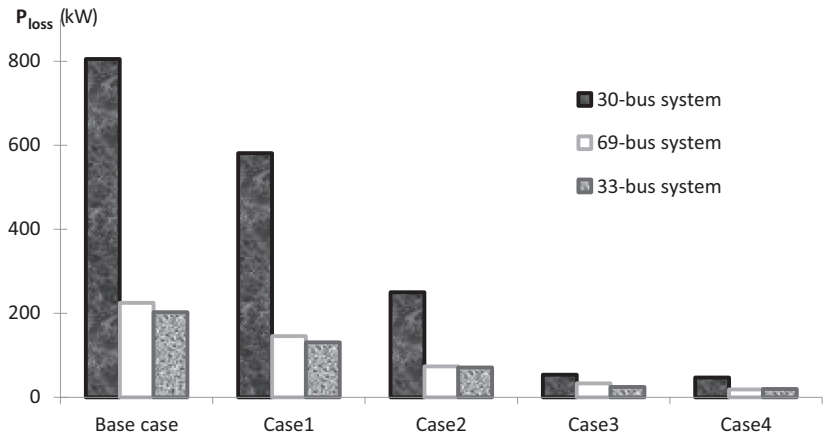

FIGURE 5.6 Power losses for different cases of the three test systems.

5.5 CONCLUSION

A proposed procedure using WCA has been presented for solving single and multi-objective frameworks of optimal placement and sizing of combined DGs/CBs in distribution networks. It aims at maximizing technical, economic, and environmental benefits. In this regard, five operational cases of DGs and CBs have been applied to three different distribution systems and compared with other optimization algorithms. The salient findings of the simulation results are summarized as follows:

- More effectiveness of the proposed procedure using the WCA have been obtained for solving the optimal placement and sizing problem, compared with other optimization algorithms.
- System power losses have been minimized using the placement of CBs alone or DGs alone, but major reduction in power losses have been obtained using the optimal placement and sizing of combined DGs and CBs.
- Simultaneous DGs and CBs placement achieve substantial technical, economic, and environmental benefits.
- More emission reduction up to 58%, more power loss reduction up to 86%, more energy cost reduction up to 18%, as in case 5 for 33-bus system, have been achieved using the proposed procedure.
- Good convergence characteristics of the proposed WCA have been noticed.
- More improvement in distribution system performance has been achieved using DGs with controllable power factor.

6 Parametric Analysis of Single-Tuned Harmonic Filter

6.1 INTRODUCTION

There are various types of shunt passive filter configurations such as single- and double-tuned, band pass filters. These filters provide a low impedance branch to trap the harmonic orders that the filter is tuned to mitigate. Theoretically, these filters have zero impedance at the tuning frequency thus absorbing the harmonic of interest. The most common type of shunt passive filters is the STF because of their lower cost, simple structure, low maintenance, and simple principle. However, the design of their effective parameters that determine the filter impedance–frequency characteristics curve is an important issue. Filter parameters such as filter size (Qc), quality factor (Q_f), and tuned frequency (t_f) are the basics to determine and design the filter components (R, L, C). Practically, the effective parameters of STF are determined based on the designer experience [83]. In recent years, many researchers have done various research studies to get the optimal design of the filter components to overcome the drawbacks of the traditional method of design to achieve various goals. Many of the filter design methods are based on artificial intelligence techniques such as genetic algorithm [84–86] and simulated annealing [87]. In [88], a filter designing method was presented to reduce power loss and increase the transformer loading capability. In [89] an optimal design method of passive filter based on quadratic programming was presented to minimize the total harmonic distortion (THD) of the system. In [90], a hybrid passive filter designing method was presented to reduce the THD and improve the power factor of the load using constrained optimization. In [91], a passive filter components calculation method was presented based on analytical expressions of the load current harmonic components to reduce the harmonic distortion in the system.

It is noticed that none of the STF design research studies studied the effect of the filter parameters or the system parameters on filter performance to get a better and effective filter design. However, the optimal selection of these parameters' values can help in increasing the passband that the filter can mitigate and achieve superior filtering characteristics.

DOI: 10.1201/9781003369448-6

6.2 SINGLE-TUNED FILTER DESIGN

STF is efficient in most harmonic mitigation cases if it is optimally designed and implemented in the system. STF construction consists of capacitor (C), reactor (L), and resistor (R) connected in series as shown in Figure 6.1. STF is usually connected in parallel in the system and represents a very low impedance path for the harmonic current at the tuned harmonic frequency. The equivalent impedance of the STF can be calculated from the following:

$$Z_f = R_f + j(X_L - X_C) \tag{6.1}$$

where Z_f is the filter impedance, R_f is the filter resistance, and X_L and X_C are the inductive and capacitive reactances of the filter.

6.2.1 Single-Tuned Filter Designing Steps

STF design is the process of determining the values of its components (R, L, and C) as follows [84].

Step 1: Determining the tuned harmonic order (t_f), which is the harmonic frequency that the filter is designed to mitigate, such as (3rd, 5th, 7th ….) harmonic order. Practically, the value of t_f is selected empirically slightly below the concerned harmonic frequency to minimize the possibility of unwanted harmonic resonance, which may take place if the filter components are derated or the system parameters are changed.

Step 2: Determining the value of the capacitor reactive power rating or the filter size (Qc) in kVArs. The value of Qc not only affects in mitigating the harmonic distortion but also in improving the power factor.

Step 3: Calculating the capacitance (C) of the capacitor and inductance (L) of the inductor from the determined Qc as follows:

$$X_c = \frac{V_L{}^2}{Q_c} \tag{6.2}$$

FIGURE 6.1 STF configuration.

$$C = \frac{1}{2\pi f X_C} \tag{6.3}$$

$$X_L = \frac{X_c}{t_f^2} \tag{6.4}$$

$$L = \frac{X_L}{2\pi f} \tag{6.5}$$

where V_L is the RMS value of the line voltage (kV).

Step 4: Selecting the quality factor (Q_F) value of the filter, which determines its sharpness. The value of Q_f ranges between 30 and 150.

Step 5: Calculating the value of the resistance (R) from the predetermined Q_f.

$$R = \frac{X_n}{Q_f} \tag{6.6}$$

where

$$X_n = \sqrt{\frac{L}{C}} \tag{6.7}$$

From these equations, it is clear that filter performance, which depends on filter impedance, is affected by various parameters such as Q_F, Q_C, and t_f. These parameters should be selected by the designers to give specific filter characteristics. But, unfortunately there is no specific criterion for selecting these parameters, where their values depend on designer experience.

Numerical Example 6.1

Determining the main parameters (R, L, C) for the STF shown in Figure 6.1 based on the given data, as follows:
$t_f = 3$, ignoring the derating factor, nominal frequency = 50 Hz

Q_C= 300 kVAr, $Q_f = 100$; $V_L = 11$ Kv

Solution:
Calculating the capacitance of the filter capacitor:

$$X_C = \frac{\left(11\times10^3\right)^2}{300\times10^3} = 403.33 \ \ \Omega$$

$$C = \frac{1}{2\times3.14\times50\times403.33} = 7.896\mu F$$

Calculating the inductance of the filter reactor:

$$X_L = \frac{403.33}{9} = 44.814 \ \ \Omega$$

$$L = \frac{44.814}{2\times3.14\times50} = 0.1443 \ H$$

Calculating filter resistance:

$$X_n = \sqrt{\frac{0.14}{7.896}} = 0.13316\ \Omega$$

$$R = \frac{0.13316}{100} = 0.0013316\,\Omega$$

6.3 IMPACT OF FILTER PARAMETERS ON ITS CHARACTERISTICS CURVE

6.3.1 Impact of T_F (At Fixed Q_C and Q_F)

To study the effect of t_f on the filter characteristics curve, the values of Q_C and Q_f are taken to be 100 KVAR and 30, respectively, and different values of t_f are considered. By applying the pre-described design method and calculating Z_f at each case, the curves in Figure 6.2 are obtained, which show five filter characteristics curves each of a different tuned harmonic order.

From Figure 6.2, it is clear that by increasing the tuned harmonic order the sharpness of the curve is reduced and it becomes more flat, which means that the filter has its minimum impedance at the tuned frequency and has a low impedance for the surrounding harmonic order of the high-order tuned frequency.

6.3.2 Impact of Q_F (At Fixed Q_C and T_F)

To study the effect of Q_f on the filter characteristics curve, the values of Q_C and t_f are taken to be 100 KVAR and 7 respectively, and different values of Q_f are considered. By applying the pre-described design method and calculating Z_f at each case, the curves in Figure 6.3 are obtained, which show five filter characteristics curves each of a different tuned harmonic order.

From Figure 6.3, it is shown that the Q_f has a little effect on filter characteristics as the change in filter sharpness or the minimum impedance is limited. The only

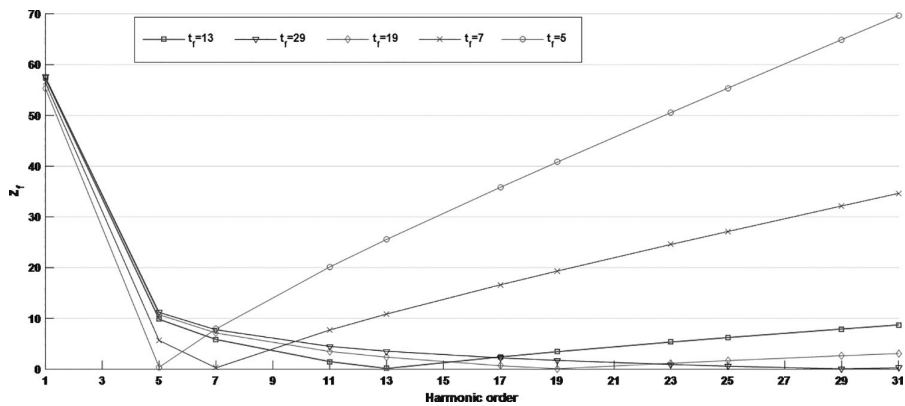

FIGURE 6.2 Effect of t_f on filter characteristics.

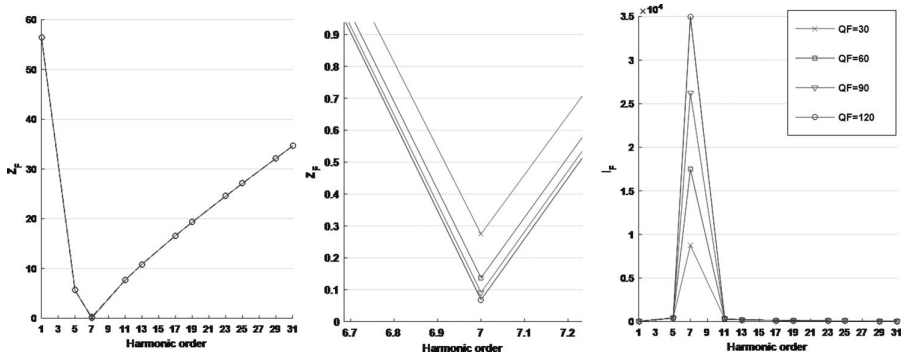

FIGURE 6.3 Effect of Q_f on filter characteristics.

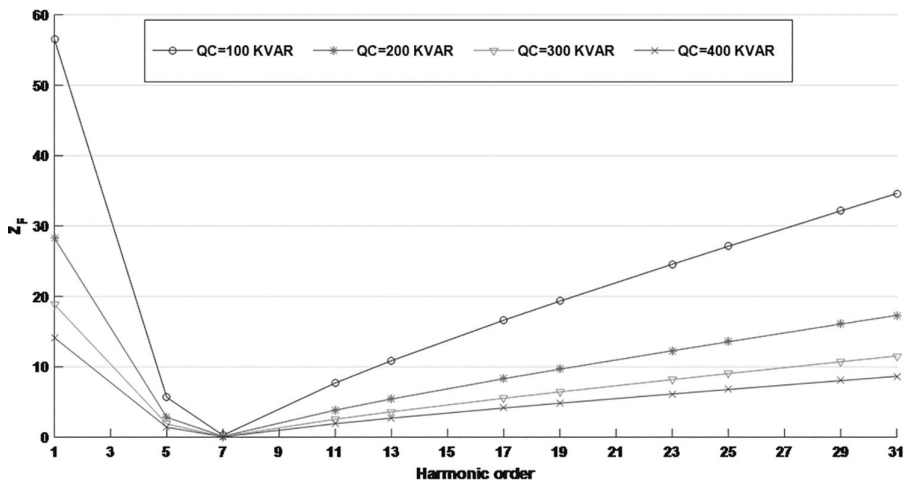

FIGURE 6.4 Effect of Q_C on filter characteristics.

significant effect is in the filter current, as the filter current is increased from 8 kA to 35 kA when increasing Q_f from 30 to 120.

6.3.3 Impact of Q_C (at Fixed Q_f and t_f)

To study the effect of Q_C on the filter characteristics curve, the values of Q_f and t_f are taken to be 30 and 7, respectively, and different values of Q_C are considered. By applying the pre-described design method and calculating Z_f at each case, the curves in Figure 6.4 are obtained, which show five filter characteristics curves each of a different tuned harmonic order around the tuned harmonic order.

From Figure 6.4, it is shown that with the increase in filter size, the characteristics curve of the filter becomes more flattened, which means that the filter has the ability to mitigate more harmonic orders.

6.4 SINGLE-TUNED FILTER PASSBAND

The passband can be defined as the harmonic frequencies that the filter can mitigate, and during this passband, the filter impedance has a value lower than $\sqrt{2} * Z_{min}$ as shown in Figure 6.5 where $2 * Z_{min}$ is the filter impedance at the tuned frequency.

However, this definition doesn't consider the relation between the system load impedances and the filter impedance. For example, when using the previous filter design steps for getting the impedance–frequency curve of two different tuned harmonic orders such as 5th and 13th order, with the same quality factor and filter size, the curves in Figures 6.6 and 6.7 are obtained. From these curves, by applying the passband criteria, both filters will eliminate the tuned harmonic order only. However, if the characteristics of the system are taken into consideration, the passband may be varied. For example, if the system which the filter will be implemented in, has a minimum load impedance of 50 ohm, the second filter (13th order) has more than one

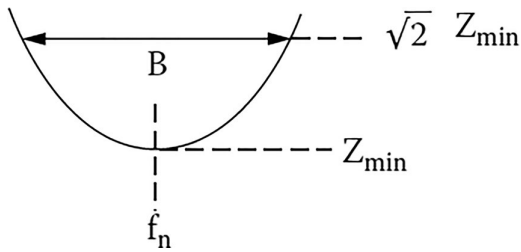

FIGURE 6.5 Passband of STF.

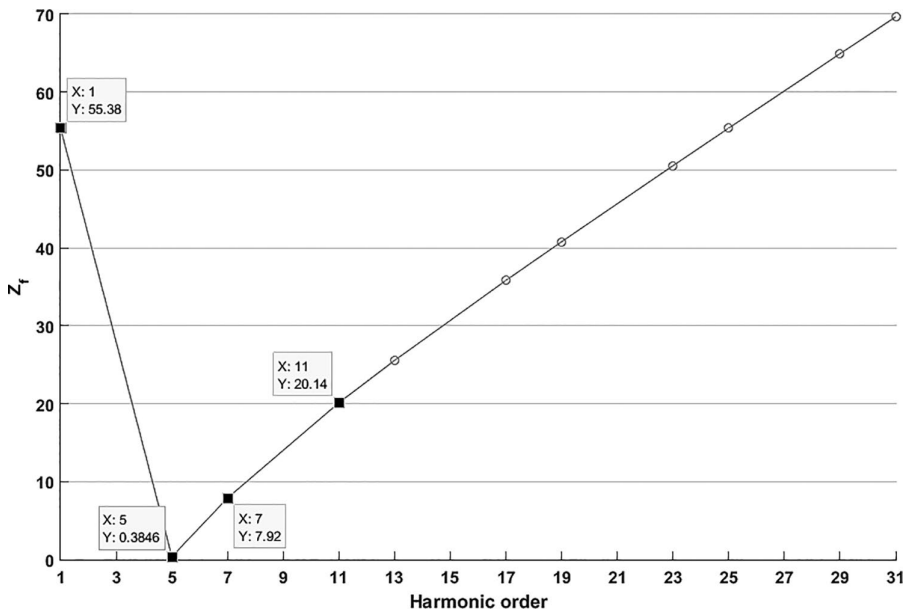

FIGURE 6.6 STF characteristics curve for the 5th tuned harmonic order.

harmonic order that has very low impedance compared with the system minimum load impedance.

Therefore, this chapter proposes new criteria for designing the filter and getting the practical passband that the filter can eliminate by considering the system characteristics.

Therefore, the passband can be defined as the band which contains the frequencies at which the filter impedance is very low compared with the system minimum impedance load. So, in this passband frequencies, all the load branches can be neglected in the harmonic load flow calculations if the filter impedance is lower than 1/10 of the system minimum impedance load.

So, it can be considered that any STF has the ability to mitigate a specific harmonic order if the filter impedance at this harmonic order satisfies the following condition:

$$Z_f < (1/10) * Z_{\text{system}}^{\min} \tag{6.7}$$

where $Z_{\text{system}}^{\min}$ is the minimum load impedance in the system.

From Figure 6.8, it is clear that with increasing filter size (Q_C), the passband of the filter is increased especially in the case of high harmonic orders (with fixed Q_f).

Figure 6.9, shows that at fixed value of Q_C (100 KVAR), the quality factor has no significant effect on the passband eliminated at different tuned harmonic orders. Also, this figure assures the ability of the higher-order tuned frequencies in eliminating large passbands compared with lower-order tuned frequencies.

For example: from Figure 6.9 at the 5th-order tuned harmonic frequency, the passband that the STF can eliminate is (373 Hz). However, at the 25th-order tuned harmonic frequency, the passband that the STF can eliminate is (9374 Hz).

Figure 6.10, shows that at a specific tuned harmonic order (5th), the quality factor has no significant effect on the passband eliminated at different filter sizes. Also,

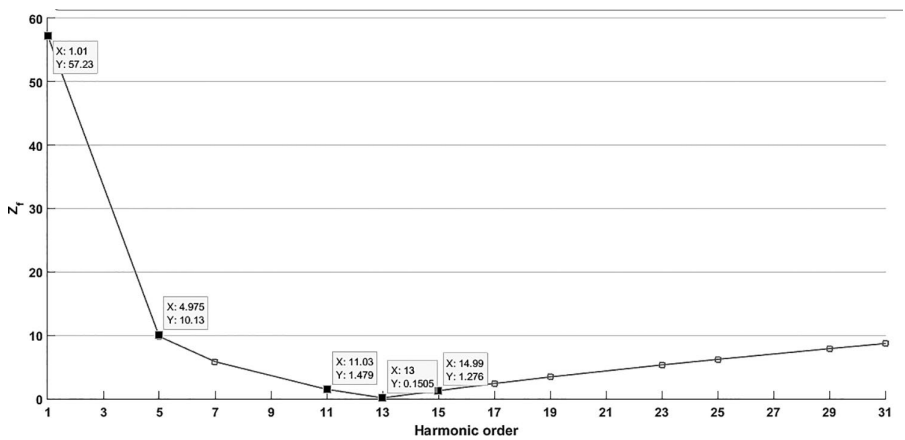

FIGURE 6.7 STF characteristics curve for the 13th tuned harmonic order.

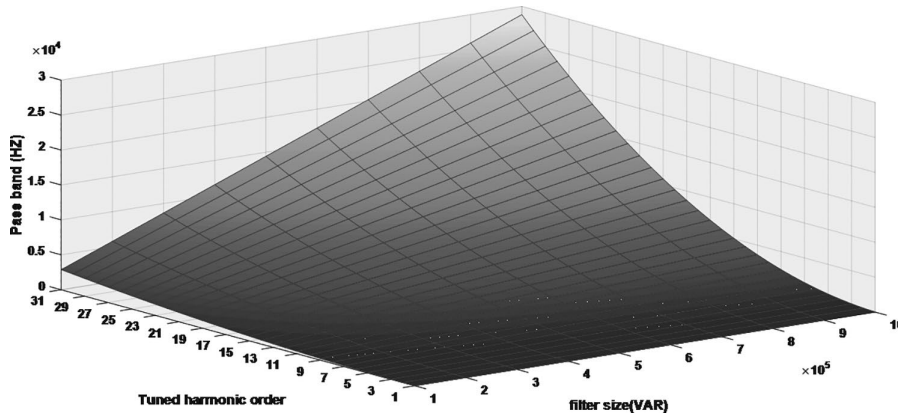

FIGURE 6.8 Effect of filter size and tuned harmonic order on filter passband.

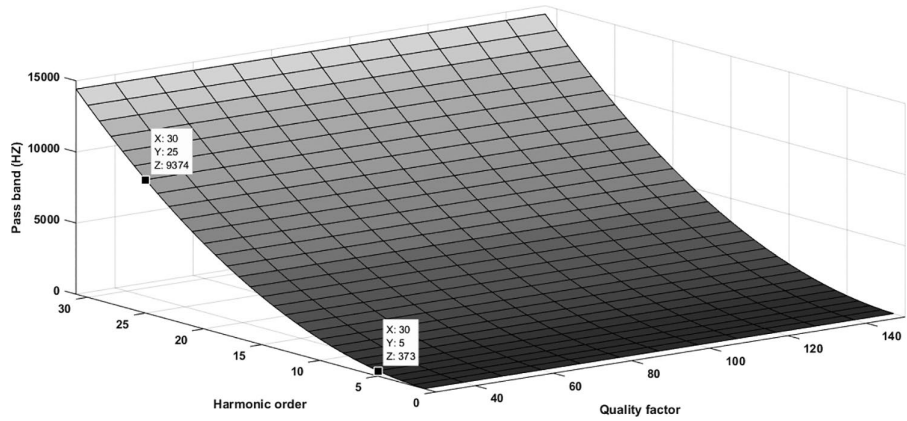

FIGURE 6.9 Effect of quality factor and tuned harmonic order on filter passband.

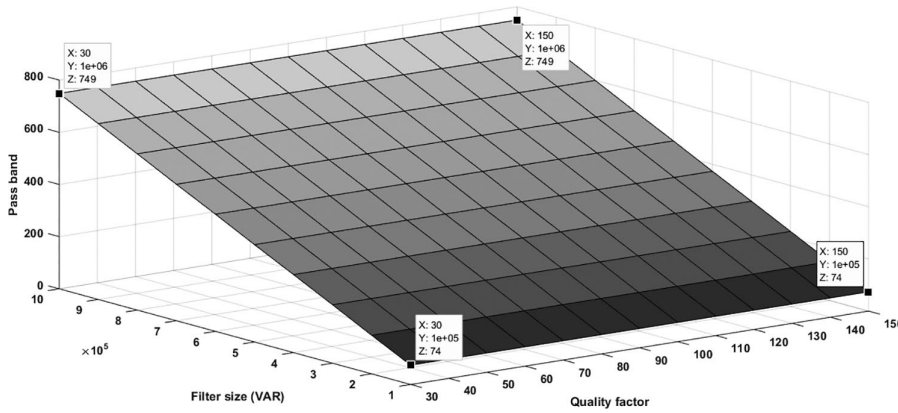

FIGURE 6.10 Effect of filter size and quality factor on filter passband.

this figure assures the ability of the higher filter sizes in eliminating large passbands compared with lower-order tuned frequencies.

For example: from Figure 6.10 when the filter size equals 100 kVAR, the passband that the STF can eliminate is only (74 Hz). However, at filter size equals 1 MVAR, the passband that the STF can eliminate is (749 Hz).

6.5 IMPACT OF SYSTEM CHARACTERISTICS ON FILTER PERFORMANCE

The main parameters that change from one distribution system to another are system base voltage and maximum load power. These parameters have a significant effect on the system minimum impedance load which may affect the filter passband. Figure 6.11 shows the effect of these system parameters on the system minimum impedance load (the impedance of maximum load power), which is calculated as follows:

$$Z_{\text{system}}^{\min} = \frac{V_{\text{base}}^2}{S_{\text{load}}^{\max}} \tag{6.8}$$

Therefore, the system minimum impedance will decrease when increasing the system maximum load power and decreasing the system voltage.

In Figure 6.11, the system minimum impedance seems to be zero and constant for large load power but if this part of the figure is zoomed out, the system minimum impedance will be as shown in Figure 6.12, which shows that the system minimum impedance decreases with increasing maximum load power and increases with increasing system voltage.

Figure 6.13 shows the effect of varying the system parameters on the filter passband for constant filter parameters (Q_C=300KVAR, Q_f =30, t_f =13). In this figure, the passband decreases with increasing system maximum load power because of decreasing system minimum impedance. Also, the passband doesn't depend on the

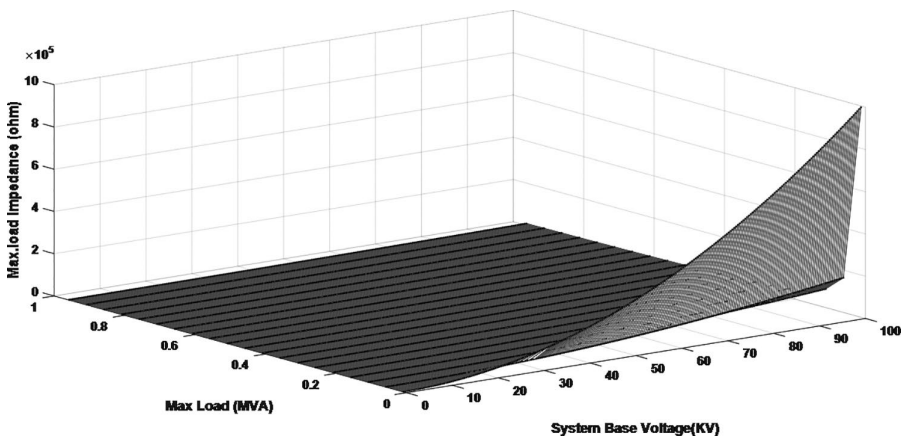

FIGURE 6.11 Effect of system parameters on the system minimum impedance load.

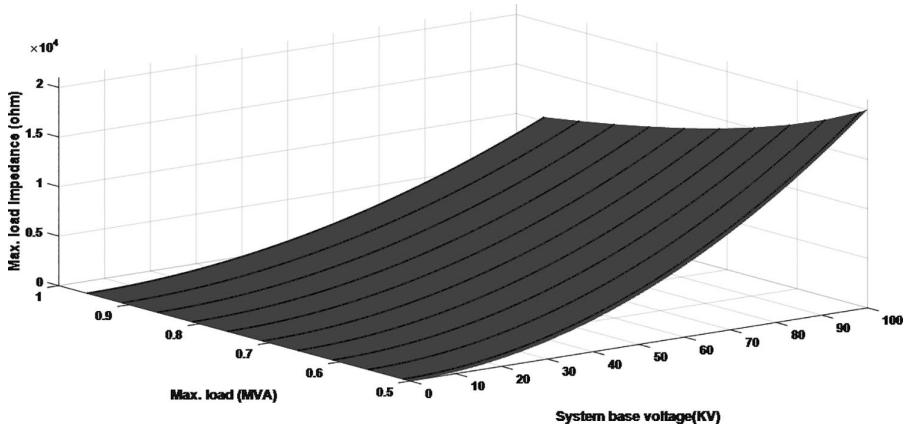

FIGURE 6.12 Effect of system parameters on the system minimum impedance load at large MVAs.

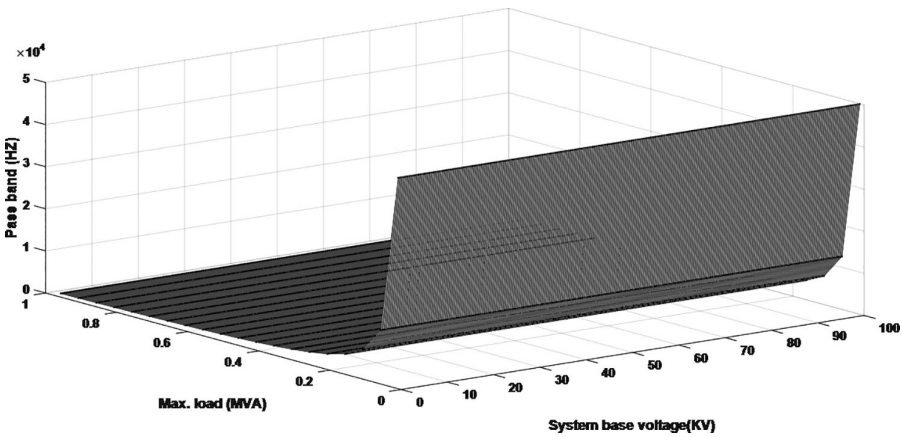

FIGURE 6.13 Effect of system parameters on filter passband.

system voltage because the filter impedance characteristics curve is dependent on the system voltage, as shown in Eq. (6.2).

In Figure 6.13, the passband seems to be zero and constant for large load power but if this part of the figure is zoomed out, the passband will be as shown in Figure 6.14, which shows that the filter passband is inversely proportional with maximum load power.

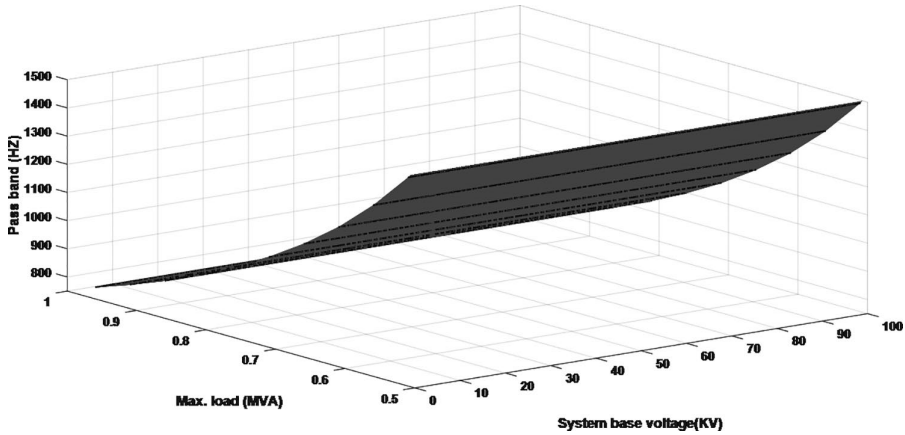

FIGURE 6.14 Effect of system parameters on filter passband at large MVAs.

6.6 CONCLUSION

In this chapter, the effectiveness of the STF parameters on filter performance has been studied through an analysis of each parameter such as Q_C, Q_f, and t_f. The analysis results show that the Q_f has less significant effect than the Q_C and t_f on the impedance–frequency characteristics curve. Also, a new practical criterion for the passband has been presented and applied to show the effect of the filter parameters on the passband that the filter can be eliminate. Also, the effect of changing the system parameters on the filter passband has been studied and the analysis results show that the passband decreases with increasing the system maximum load power but it doesn't depend on the system voltage.

7 Harmonic Mitigation for Distribution Systems with Inverter-Based DGs

7.1 INTRODUCTION

Nowadays, the power quality of distribution systems has become one of the most important challenges, especially after the widespread use of harmonic sources in distribution systems, which are considered as one of the most effective factors of power quality [92]. Harmonics presence in distribution systems can result in excessive losses and system equipment overheating and damage [13]. Consequently, to keep distribution systems reliable and working in high performance, harmonic levels should be kept within the allowable limits approved in the IEEE 519 standard [9]. However, due to the widespread use of power electronics devices and nonlinear loads in distribution systems, harmonics levels in distribution systems may exceed the standard limits. Hence, harmonic mitigation becomes a must in distribution systems to decrease distortion levels and enhance system performance [1]. On the other hand, huge efforts have been exerted for increasing the percentage of distributed generation units (DGs) in distribution systems, especially the renewable DGs that were dependent on inverters such as PV and wind generation sources [10] and [93]. The presence of DGs in distribution systems provides many technical, environmental, and economic merits [11, 94, 95], but on the other hand, the harmonic content of inverter-based DGs may increase the harmonic distortion problem in the distribution system [12, 96].

Further, to solve the harmonic distortion problem several methods have been presented for [15, 16], among these methods, single-tuned filter (STF) is still one of the most common methods for harmonic mitigation due to its effectiveness and economic benefits. Single-tuned passive filters are designed to trap the harmonic in the filter branch depending on the low impedance of the filter branch at the tuned harmonic order [17]. Various methods were developed for optimal design of passive harmonic filters based on optimization techniques such as particle swarm optimization [17], simulated annealing [97] and fuzzy linear programming [98]. The placement of harmonic filter in the system has a huge effect on the system harmonic mitigation. Authors in [18] presented a method for STF placement in small distribution systems based on genetic algorithm to reduce harmonic distortion. In [99], the authors presented a method for optimal allocation of passive filters in an industrial

DOI: 10.1201/9781003369448-7

distribution network based on the harmonic similarity metric. In [19], the authors introduced two sensitivity indices as a guide for the passive filter placement problem that can determine the sensitive buses for filter placement. In [20], a multi-objective optimization problem was considered for solving the optimal planning problem of passive filters considering specific harmonic orders without considering the harmonic distortion resulting from DG units. In [100], simultaneous planning of both inverter-based DGs and passive filters in distorted distribution system are considered for minimizing total harmonic distortion (THD) and power loss. In [101], the optimal placement and sizing of capacitor banks and inverter-based DGs were employed by biogeography-based optimization (BBO) algorithm considering the harmonic content of the DGs at different load levels. In [102], a comprehensive parametric analysis for STFs was presented. In [103], the design of STFs was carried out by using ETAP software in distribution systems with PV systems to eliminate the harmonics and their impact on the system. In this chapter, a new procedure is proposed for simultaneous optimal design, number, and placement of single-tuned harmonic filters by using WCA in distorted distribution system. The harmonic spectrums of the inverter-based DGs implemented in distribution systems are considered. The objectives of the proposed procedure are minimizing total harmonic distortion and filter investment cost and improving voltage profile. Harmonic load flow with and without a filter is implemented for analyzing system harmonics. The effects of harmonic spectrums of the DGs on the harmonic distortion in the system are studied through two cases studied.

7.2 PROBLEM FORMULATION

The proposed procedure aims to determine the optimal design, number, and placement of single-tuned harmonic filters in distorted distribution systems. The harmonic spectrum of the DG units in the system is considered. The proposed procedure aims to minimize THD and filter investment cost and improve the system voltage through the following objective functions.

7.2.1 Objective Functions

Three objective functions are considered in this optimization problem:

i. Minimizing the THD (f1)

THD of the system should be kept as low as possible according to the following equation [21]:

$$f_1 = \min \sum_{i=1}^{N} \left(\frac{1}{V_{1i}} \sqrt{\sum_{h=2}^{H} V_{hi}^2} \right) \tag{7.1}$$

where V_{1i} is the fundamental bus voltage, V_{hi} is the harmonic (h) voltage at bus I, and N is the total number of buses.

ii. Improving the Voltage Profile (f_2)

This objective function can be described as [98]

$$f_2 = \min \sum_{i=1}^{N} \left(\frac{v_i - v_i^{\text{spec}}}{v_i^{\max} - v_i^{\min}} \right)^2 \tag{7.2}$$

where v_i^{spec} is the specified voltage magnitude (1.0 p.u), $v_i^{\max}$ and $v_i^{\min}$ are the maximum and minimum fundamental voltages at bus i.

iii. Minimizing the Filter Investment Cost (f_3)

The filter investment cost is calculated as follows [102]:

$$f_3 = \min \sum_{i=1}^{n} (k_C.QC_i + k_L.QL_i + k_R.PR_i) \tag{7.3}$$

where n is the total number of filters; k_c, k_L, and k_R are the cost coefficients of the filter capacitor, inductor, and resistor, respectively, which are equal to 3 $ kVar [104].

This optimization problem is considered as a multi-objective function, which can be implemented using the weighting factors approach. So, the normalized fitness function (FF) can be formulated as

$$FF = \min \left(k_1 \frac{f_1}{f_{1\max}} + k_2 \frac{f_2}{f_{2\max}} + k_3 \frac{f_3}{f_{3\max}} \right) \tag{7.4}$$

where the weighting factors k_1, k_2, and k_3 are considered equal to 0.6, 0.2, and 0.2, respectively.

7.2.2 System Constraints

This optimization problem constraints include the following.

i. **Voltage Limits**

$$0.95 \le V_i \le 1.05,\ i = 1, 2, ...N \tag{7.5}$$

ii. **Harmonic Distortion Limits**

$$THD_i(x) \le THD_{\max} \tag{7.6}$$

$$IHD_{i,h}(x) \le IHD_{\max} \tag{7.7}$$

where $THD_{\max}$ and $IHD_{\max}$ are the maximum allowable total harmonic distortion and individual harmonic distortion at each bus, which have values equal to (5% and 3%), respectively, according to the IEEE-519 standard [9].

7.3 PROPOSED STF PLANNING PROCEDURE

The proposed filter allocation procedure for harmonic mitigation has the following steps:

Step 1: Randomly initialize the initial set of raindrops of size N_{pop}

$$RP = \begin{Bmatrix} 1 \\ \vdots \\ N_{\text{pop}} \end{Bmatrix} \begin{bmatrix} \text{filter}_1^{\text{place}} & \text{filter}_n^{\text{place}} & \text{filter}_1^{f_t} & \text{filter}_n^{f_t} & \text{filter}_1^{Q_c} & \text{filter}_n^{Q_c} \\ \vdots & \vdots & \vdots & \vdots & \vdots & \vdots \\ \vdots & \vdots & \vdots & \vdots & \vdots & \vdots \end{bmatrix} \tag{7.8}$$

Step 2: Check the following constraints:

$$f_t \in [\ 3 \quad 5 \quad 7 \quad \cdots \quad 25] \tag{7.9}$$

where f_t is the tuned harmonic order.

$$2 \le \text{filter}^{\text{place}} \le N \tag{7.10}$$

$$Q_c^{\min} \le Q_c \le Q_c^{\max} \tag{7.11}$$

Step3: Evaluate the fitness of each raindrop by the following steps:

I. Calculating filter parameters, which consist of (series of R, L, and C) from Eqs. (6.2–6.5).
II. Carrying out harmonic power flow calculation before and after insulating the filters in the system as described in Chapter 4.
III. Calculating FF using the harmonic load flow results.
IV. Checking the buses' voltage, THD, and IHD constraints. If a solution doesn't satisfy any of the constraints, putting the value of its FF equals infinity. So, it will not be selected as a minimum solution.

Step 4: Get the personal best data and store its controlled variables data:

$$P_{\text{best}} = \min(\text{fitness function matrix}) \tag{7.17}$$

Step 5: Apply the WCA described in Chapter 3 to generate a new set of solutions.
Step 6: Repeat steps 2–5 to complete the total number of iterations.

Numerical Example 7.1:

It is required to determine the optimal placement and planning of one STF in the modified 69-bus distribution system shown in Figure A.4. The objective function is to minimize the THD as in Eq. (7.1) with respect to the constraints mentioned in

Eqs. (7.5–7.8). For simplification, it is considered that there are no DG units in the system. Also, it is considered that, Q_F= 50, population number=100, and number of iterations= 5.

Solution:

Following the proposed STF planning procedure, The MATLAB M-file code for the optimal placement and planning of the STF on the distorted 69-bus distribution system is developed as follows:

```
clc;
clear all
%---------------------------

fl_max=10;
npop=100;  itt=5;   ;v_base=12.66*1000/sqrt(3);
run(itt,n_run)=0; % store matrix personal pest fitness function for all itt
personal_best(itt,n_run)=0;

for run_number=1:n_run
n_filter=run_number;
Q_F=50;
n_variables=2*n_filter;
databestl(n_run,n_variables)=0;
best_busesl(n_run,n_filter)=0;
 maxg=zeros(n_variables);
 ming=zeros(n_variables);

selected_harmonic=[3  5  7  9  11  13  17  19  23  25  29    31 ];
n_selected_harmonic=length(selected_harmonic);


  maxg(1:n_filter)=1;
  maxg(n_filter+1:n_variables)=1000000; %VAR 3 PHASE
% min limit
ming(1:n_filter)=min(selected_harmonic);
 ming(n_filter+1:n_variables)=1000; %VAR 3 PHASE
  best_buses=zeros(1,n_filter);

%---------------------------
filter_matrix=zeros(n_filter,5);
dr(1,1)=0;%booo;2
dmax=1*10^-3;%evaporation and raining process factor


r11=rand(1);          %a random number with the range of [0, 1]
c11=2;                %the acceleration constant
pbest(itt,1)=0;  %matrix of personal pest fitness function of raindrops
%matrix of fitness functions
THD(npop,1)=0;
fitness(npop,1)=0;
gbest=inf;   %min ploss of fitness function matrix
u(npop,1)=0;
for i=1:npop
   u(i,1)=1;
end;
```

```
% step1  Randomly initialize the initial set of raindrops of size Npop,
%where each rains is of dimensions [ pg1 pg2 .....pgng, qg1 qg2 .....qgng]
for jj1=1:npop

c(jj1,i)=selected_harmonic(int16(rand*(n_selected_harmonic-1)+1));

end

for i=n_filter+1:n_variables
    c(:,i)=ming(i)*u+rand(npop,1)*(maxg(i)-ming(i));
end


%~~~~~~~~~~~~~~~~~~~~~~~~~~~~~~~~~~~~~~~~~~~~~~~~~~~~~~~~~~~~~~~~~~~~~~~~~~~~
for z=1:itt
    z

for abc=1:1
for jj=1:npop
    for i=1:n_variables
        if(c(jj,i)<ming(i))
           c(jj,i)=ming(i);
        end
        if(c(jj,i)>maxg(i))
           c(jj,i)=maxg(i);
        end
    end

  x8=find(selected_harmonic==c(jj,ii));
  if (length(x8)==0)
      x8=find(selected_harmonic<c(jj,ii));
    c(jj,ii)=selected_harmonic(length(x8));
  end

 end

end

end
c;

% Evaluate the fitness of each raindrop and keep the position of
for j=1:npop
   %                location   r     l        c
 filter_matrix(:,1)=DG_location(j,1:n_filter)';
 for ii4=1:n_filter
 xc=(v_base)^2/c(j,ii4+n_filter);
 cap=1/(2*pi*50*xc);
 xl=xc/(c(j,ii4))^2;
 l=xl/(2*pi*50);
 r=sqrt(l/cap)/(Q_F);
 filter_matrix(ii4,2)=r;
 filter_matrix(ii4,3)=l;
 filter_matrix(ii4,4)=cap;
 filter_matrix(ii4,5)=c(j,ii4);
 end
```

```
   %cheek the constrain of voltage on buses
  max_volt=max(V_normal_freqency);
  min_volt=min(V_normal_freqency);

  if (min_volt<0.9)
  fitness(j,1) = inf;
  end;
  if (max_volt>1.1)
  fitness(j,1) = inf;
  end;
  for ww=1:n_bus
  if (max(v_harmonics_percentage1(ww,:))>3)
  fitness(j,1) = inf;break;
  end;
  if (max(v_harmonics_percentage2(ww,:))>3)
  fitness(j,1) = inf;break;
  end;
  if (max(v_harmonics_percentage3(ww,:))>3)
  fitness(j,1) = inf;break;
  end;
  end
   if (max(thd1)>5)
   fitness(j,1) = inf;
   end;
   if (max(thd2)>5)
   fitness(j,1) = inf;
   end;
   if (max(thd3)>5)
   fitness(j,1) = inf;
   end;
% start WCA xxxxxxxxxxxxxxxxxxxxxxxxxxxxxxxxxxxxxxxxxxxxxxxxxxxxxxxxxxxxxxxxxxx
% xxxxxxxxxxxxxxxxxxxxxxxxxxxxxxxxxxxxxxxxxxxxxxxxxxxxxxxxxxxxxxxxxxxxxxxxxxxxx
% End WCA xxxxxxxxxxxxxxxxxxxxxxxxxxxxxxxxxxxxxxxxxxxxxxxxxxxxxxxxxxxxxxxxxxxxx
%xxxxxxxxxxxxxxxxxxxxxxxxxxxxxxxxxxxxxxxxxxxxxxxxxxxxxxxxxxxxxxxxxxxxxxxxxxxx
if(z==itt)
    break;
end
%%%%%%%%%%%%%%%%%%%%%%%%

end

run(:,run_number)=pbest(:,1);
best_buses1(run_number,:)=best_buses;
databest1(run_number,:)=databest;

end
best_run=min(run(itt,:))
 for j7=1:n_run
     if(run(itt,j7)==best_run)
         k3=j7;
     end
 end
 %*********************************
```

```
%+++++++++++++++
matrix2_1=thd1;
matrix2_2=thd2;
matrix2_3=thd3;
volt_after=V_normal_freqency;
max_volt=max(V_normal_freqency);
 min_volt=min(V_normal_freqency);
bbus=1:length(matrix2_1);
subplot(1,3,1);
matrix_D=matrix_1;
matrix_D(:,2)=matrix2_1;

bar(matrix_D);
title('THD')

subplot(1,3,2);
plot(bbus,volt_after,'b-',bbus,volt_befor,'r-')
title('voltages')
it=[1:itt];
best_run_data=k3
subplot(1,3,3);
plot(it,personal_best(:,k3))
title('convergance')
```

TABLE 7.1
Results of the Optimal Planning of a STF.

				Filter Parameters		
THD %	**Filter Placement**	**Size (kVAr)**	t_f	**R (Ω)**	**L (H)**	**C (μF)**
2.529	44	271.7	7	0.5618	0.0128	16.189

The developed M-file code determines the optimal placement, size, tuned frequency, and parameters of a single-tuned harmonic filter in the IEEE 69-bus distribution system using WCA. The obtained results are shown in Table 7.1.

7.4 APPLICATIONS

The proposed procedure is applied considering two studied cases as follows:

Case 1: optimal planning of STFs without considering the harmonic spectrum of the DG units.

Case 2: optimal planning of STFs considering the harmonic spectrum of the DG units.

The nonlinear load is assumed to be a six-pulse inverter that has a harmonic spectrum as shown in Table 7.2 [105]. Also, the harmonic spectrum of the inverter-based DGs is considered as shown in Table 7.3 [101]. DGs are placed near the heavy loads

TABLE 7.2
Harmonic Spectrum of Six-pulse Nonlinear Loads

Harmonic order	1	5	7	11	13	17	19	23	25
Value (%)	100	42	14.3	7.9	3.2	3.7	2.3	2.3	1.4

TABLE 7.3
Harmonic Spectrum of the Inverter Based on DGs

Harmonic Order	Magnitude (%)	Phase (Deg.)	Harmonic Order	Magnitude (%)	Phase (Deg.)
1	100	–2.34	9	8	140.36
3	20	–15.29	11	5	65.54
5	15	–20.74	13	3	42.62
7	10	–30.85	15	2	153.28

TABLE 7.4
Inverter-Based DGs Characteristics

DG location	DG Size	
	Active Power (kW)	Reactive Power (kVAR)
27	190.1	134.7
43	190.1	134.7
46	190.1	134.7
52	190.1	134.7

to reduce power losses and improve the voltage profile [11]. The total capacity of the DGs is assumed to be 40% from the total demand and divided equally into four units. The proposed procedure considered all the odd harmonic orders from 3rd up to 25th harmonic orders. To analyze the test system and evaluate the harmonic distortion, fundamental and harmonic power flows described in Chapter 4 are applied.

7.5 SIMULATION RESULTS AND DISCUSSIONS

7.5.1 Test Distribution System

The proposed procedure is applied to modified IEEE 69-bus distribution system [11]: The total active and reactive loads of this system are 3.802 MW and 2.694 MVAr, respectively, where the total active power loss in the initial case is 225 kW. The number of nonlinear loads are six loads located at buses [11, 26, 27, 43, 49, 53, 63] as shown in Figure A.4. The considered DGs characteristics are described in Table 7.4.

7.5.2 Simulation Results

7.5.2.1 Results of Case 1

The results of the filter planning in the first case are shown in Tables 7.5 and 7.6. The results show that the proposed procedure effectively reduced the maximum THD from 6.87% to 2.32% to meet the IEEE-519 standard. Also, the results show that only one filter is needed for mitigating the 7th harmonic order and keep the THD within limits. The objective function values are obtained in Table 7.6. The THD of the system buses before and after applying the proposed procedure is shown in Figure 7.1. The figure shows that the filters have a great effect in minimizing the

TABLE 7.5
Results of Control Variables for Filter Planning in Case 1

Filter no.	1
Placement (Bus)	43
f_t	7
Q_c (k_{Var})	277.2
R (Ω)	0.5506
L(H)	0.0125
C(μF)	16.516

TABLE 7.6
Results of Objective Functions in Case 1

Parameter	Without Filter	With Filter
Filter cost ($)	—	12303
V max. (pu)	1.0	1.0
Vmin (pu)	0.953	0.966
Max-THD %	6.872	2.328

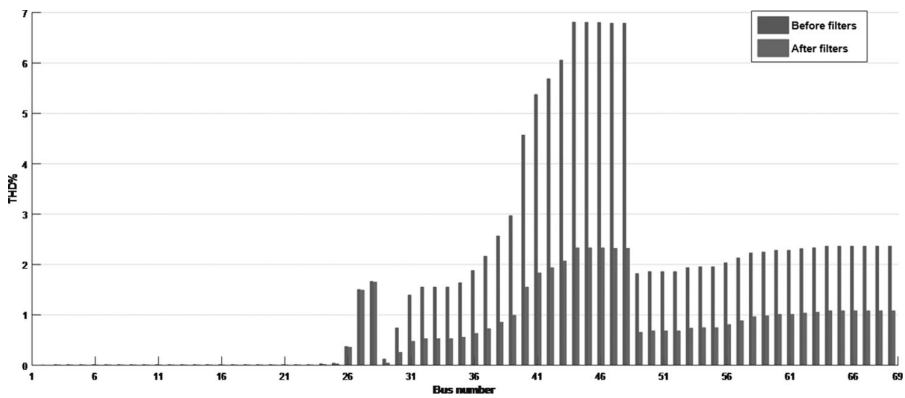

FIGURE 7.1 THD of the system buses with and without filters in case 1.

THD and enhancing system performance. Moreover, the installed filters have the ability to improve system the voltage profile as shown in Figure 7.2.

7.5.2.2 Results of Case 2

Tables 7.7 and 7.8 show the results of the filter planning considering the harmonic spectrum of DGs in case 2. The results show that, four STFs are placed to eliminate the 3rd, 7th, 17th, and 23th harmonics orders. These filters reduce the maximum THD from 8.83% to 2.92% to meet the IEEE-519 standard. The THD of the system buses before and after applying the proposed procedure is shown in Figure 7.3. This figure shows that the DG units harmonics have a harmful effect in increasing the

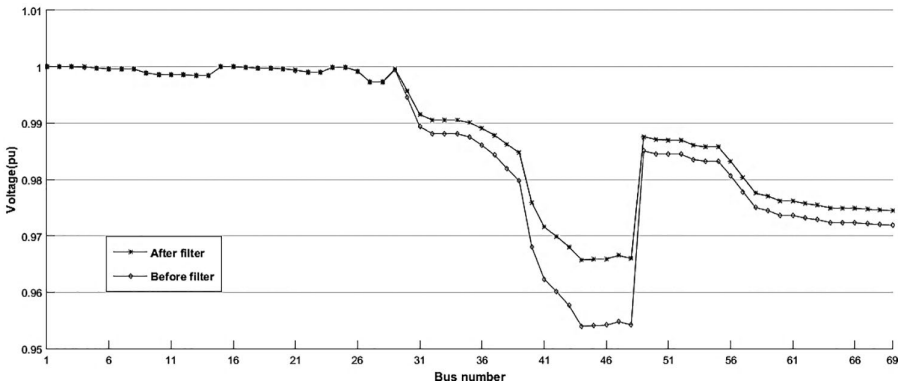

FIGURE 7.2 The system fundamental voltage profile with and without filters in case 1.

TABLE 7.7
Results of Control Variables for Filter Planning in Case 2

Filter No.	Filter 1	Filter 2	Filter 3	Filter 4
Placement (Bus)	45	31	34	69
f_t	7	23	17	3
Qc (kVar)	165.06	51.03	804.51	202.07
R (Ω)	0.9248	0.9103	0.0781	1.7626
L(H)	0.0210	0.0063	0.0007	0.0935
C(μF)	9.83	3.04	47.93	12.04

TABLE 7.8
Results of Objective Functions in Case 2

Parameter	Without Filter	With Filter
Filter cost ($)	zero	2.0122e+04
Vmax (pu)	1.0	1.0
Vmin (pu)	0.953	0.971
Max-THD%	8.832	2.9271

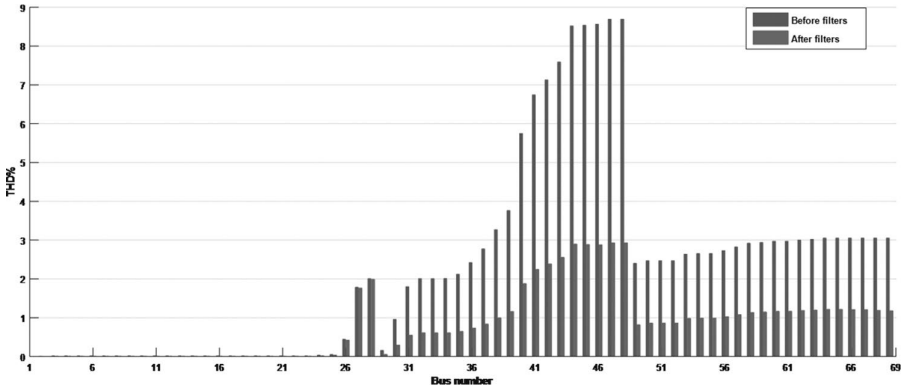

FIGURE 7.3 The THD of the system buses with and without filters in case 2.

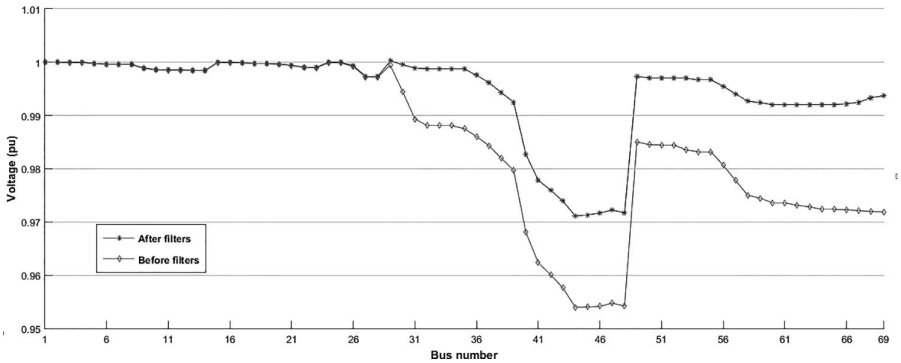

FIGURE 7.4 Fundamental voltage of the system buses with and without filters in case 2.

THD of the system. The system THD is increased by 28.5% when the DGs harmonic spectrum is considered. Moreover, the installed filters have the ability to improve system voltage profile as shown in Figure 7.4.

7.6 CONCLUSION

In this chapter, the optimal planning of passive single-tuned harmonic filters in distorted distribution systems has been proposed. The proposed procedure considers the harmonic content of the inverter-based DGs in the distribution system. The optimal planning problem has been solved by the proposed procedure using WCA optimization technique with the aid of fundamental and harmonic backward/forward sweep power flow. Minimizing THD and investment cost and improving the voltage profile have been considered as the objective functions. The simulation results approve the effectiveness of the proposed procedure in determining the optimal design, number, and placement of the STF in the radial distribution system. Also, the results indicate that the harmonic spectrum of the DG units should be considered while designing harmonic filters to prevent maximization of harmonic distortion in the system.

8 Conclusions

8.1 CONCLUSIONS

In this book, various proposed procedures have been presented to solve the power quality problems of distribution systems in the presence of distributed generation (DG) units. The proposed procedures are based on water cycle algorithm (WCA) as a modern optimization technique, since the power quality problems can be formulated as optimization problems. To study the power distribution systems and analyze their power quality problems, fundamental and harmonic load flows have been presented and formulated based on the backward/forward sweep power flow method in radial distribution systems. To test the effectiveness of the presented WCA, a comparative study for solving the problem of placement and sizing of both DGs and capacitor banks (CBs) in distribution systems is presented. The results approve that the WCA is more efficient and accurate than other competitive optimization techniques such as BFOA, CSA, PSO, etc. As the harmonic distortion has a destructive effect on the system, a comprehensive study has been carried out to analyze and propose a solution for the harmonic distortion problem in distribution systems.

The salient findings of this book are summarized as follows:

- A proposed procedure for obtaining the optimal placement and sizing of both DGs and CBs in distribution systems has been efficiently presented. This proposed procedure aims to enhance the voltage profile, the voltage deviation, and the voltage stability index of the system, besides achieving other technical, economic, and environmental benefits. Five different operational case studies are considered to assess the performance of the proposed procedure.
- The simulation results show that the proposed procedure succeeds in improving the voltage profile and minimizing the voltage deviation and the voltage stability index besides achieving more emission reduction up to 58%, more power loss reduction up to 86%, and more energy cost reduction up to 18%, as in case 5 for the 33-bus system.
- Also, the simulation results show that more improvement in distribution system performance has been achieved using DGs with controllable power factor than the case of fixed power factor of the DGs.
- For analyzing the harmonic distortion problem, the distribution system has been analyzed in the presence of nonlinear loads and DG units using fundamental and harmonic power flows. Two cases are considered to study the effect of DGs harmonic spectrum on the system distortion.
- The two cases show that the DGs' harmonics can increase harmonic distortion in the system to values that exceed the allowable limits. The simulation

DOI: 10.1201/9781003369448-8

results show that the total harmonic distortion (THD) of the system increased by 30% due to the DGs where the penetration level of the DGs was 40% from the total demand.

- Single-tuned filters (STFs) have been used for mitigating the harmonic distortion in the distribution system; therefore, the effectiveness of the STF parameters on filter performance has been studied through an analytical study of each parameter such as Q_C, Q_f, and t_f. The analysis results showed that the Q_f has less significant effect than Q_C and t_f on the impedance–frequency characteristics curve.
- Moreover, a new practical criterion for the passband has been presented and applied to show the effect of the filter parameters on the passband that the filter can eliminate. In addition, the effect of the distribution system characteristics on the filter performance has been studied. The results show that the system voltage has no effect on STF performance, whereas the system load impedances have a significant effect in determining the passband that the filter can eliminate.
- In addition to that, a proposed procedure has been efficiently presented for harmonic mitigation as well as improving the power quality in distribution systems. The proposed procedure is based on WCA for simultaneously determining the optimal number, sizing, and placement of single-tuned harmonic filters in the presence of inverter-based DGs. The simulation results approve that the proposed procedure succeeds in mitigating the harmonics and reducing the maximum THD from 8.83% to 2.92% to meet the IEEE-519 standard.
- From the simulation results in this book, it is shown that DGs have positive and negative effects on power quality, since DGs can reduce power loss, emissions, energy cost, and voltage deviation. On the other hand, DGs may increase harmonic distortion in the system due to their harmonic spectrum, especially of the inverter-based DGs.
- The proposed procedures have been applied to various distribution systems, such as
  1. IEEE 33-bus balanced test system
  2. IEEE 69-bus balanced test system
  3. East Delta 30-bus network as a real part of the Egyptian system

References

[1] S. Santoso, M. McGranaghan, R. Dugan and H. Beaty, *Electrical power systems quality*. New York: McGraw-Hill, 2012.

[2] J.A. Momoh, *Smart grid: Fundamentals of design and analysis*. Hoboken, NJ: Wiley, 2012.

[3] A. Kumar, B. Jha, D. Singh, and R. Misra, "A New Current Injection Based Power Flow Formulation", *Electric Power Components and Systems*, vol. 48, no. 3, pp. 268–280, 2020. Available: 10.1080/15325008.2020.1758846.

[4] R. Jabr and I. Dzafic, "A Compensation-Based Conic OPF for Weakly Meshed Networks", *IEEE Transactions on Power Systems*, vol. 31, no. 5, pp. 4167–4168, 2016. Available: 10.1109/tpwrs.2015.2505508.

[5] S. Ghosh, "A New Technique for Load-Flow Analysis of Radial Distribution Networks", *International Journal of Engineering and Technology*, vol. 1, no. 1, pp. 75–81, 2009. Available: 10.7763/ijet.2009.v1.14.

[6] W. Forst and D. Hoffmann, *Optimization-Theory and Practice*. New York: Springer, 2010.

[7] M. Cavazzuti, "*Optimization methods: From theory to design", scientific and technological aspects in mechanics*. Springer Science & Business Media, London, 2012.

[8] A. Jabbar and S. Zainudin, "Water Cycle Algorithm for Attribute Reduction Problems in Rough Set Theory," *Journal of Theoretical Application and Information Technology*, vol. 61, no. 1, 2014.

[9] C. Duffey, and R. Stratford, Update of Harmonic standard IEEE-519-IEEE recommended practices and requirements for harmonic control in Electric Power Systems, *Conference Record of the IEEE Industry Applications Society Annual Meeting* [Preprint]. Available at: https://doi.org/10.1109/ias.1989.96858.

[10] S. Sakar, M. Balci, S. Abdel Aleem and A. Zobaa, "Increasing PV Hosting Capacity in Distorted Distribution Systems Using Passive Harmonic Filtering", *Electric Power Systems Research*, vol. 148, pp. 74–86, 2017.

[11] A. El-Ela, R. El-Sehiemy and A. Abbas, "Optimal Placement and Sizing of Distributed Generation and Capacitor Banks in Distribution Systems Using Water Cycle Algorithm", *IEEE Systems Journal*, vol. PP, no. 99, pp. 1–8, 2018.

[12] R. Langella, A. Testa, J. Meyer, F. Moller, R. Stiegler and S. Djokic, "Experimental-Based Evaluation of PV Inverter Harmonic and Interharmonic Distortion Due to Different Operating Conditions", *IEEE Transactions on Instrumentation and Measurement*, vol. 65, no. 10, pp. 2221–2233, 2016.

[13] J. Arrillaga, *Power system harmonic analysis*. Chichester: Wiley, 2000.

[14] T. Jen-Hao and C. Chuo-Yean, "Backward/Forward Sweep Based Harmonic Analysis Method for Distribution Systems," *IEEE Transactions on Power Delivery*, vol. 22, pp. 1665–1672, 2007.

[15] R. Abdollahi, "Harmonic Mitigation Using 36-Pulse AC-DC Converter for Direct Torque Controlled Induction Motor Drives", *Journal of Applied Research and Technology*, vol. 13, no. 1, pp. 135–144, 2015. Available: 10.1016/s1665-6423(15)30012-2.

[16] U. N. Khan and T. S. Sidhu, "A Phase-Shifting Transformer Protection Technique Based on Directional Comparison Approach, " *IEEE Transactions on Power Delivery*, vol. 29, pp. 2315–2323, 2014.

[17] M. Azab, "Multi-objective Design Approach of Passive Filters for Single-phase Distributed Energy Grid Integration Systems Using Particle Swarm Optimization", *Energy Reports*, vol. 6, pp. 157–172, 2020. Available: 10.1016/j.egyr.2019.12.015.
[18] E. Kazemi-Robati and M. Sepasian, "Passive Harmonic Filter Planning Considering Daily Load Variations and Distribution System Reconfiguration", *Electric Power Systems Research*, vol. 166, pp. 125–135, 2019. Available: 10.1016/j.epsr.2018.09.019.
[19] M. Aghaei and A. Dastfan, "A Graph Search Algorithm: Optimal Placement of Passive Harmonic Filters in a Power System", *Journal of Artificial Intelligence and Data Mining*, vol. 3, no. 2, 2015. Available: 10.5829/idosi.jaidm.2015.03.02.11.
[20] Y. Chang, C. Low and S. Hung, "Integrated Feasible Direction Method and Genetic Algorithm for Optimal Planning of Harmonic Filters with Uncertainty Conditions", *Expert Systems with Applications*, vol. 36, no. 2, pp. 3946–3955, 2009.
[21] A. Abbas et al., "Optimal Harmonic Mitigation in Distribution Systems with Inverter Based Distributed Generation", *Applied Sciences*, vol. 11, no. 2, p. 774, 2021. Available: 10.3390/app11020774.
[22] B. Nasiri, C. Wagner, U. Häger and C. Rehtanz, "Distribution Grid Planning Considering Smart Grid Technologies", *CIRED - Open Access Proceedings Journal*, vol. 2017, no. 1, pp. 2228–2232, 2017. Available: 10.1049/oap-cired.2017.0991.
[23] European Smart Grids Technology Platform: Vision and Strategy for Europe's Electricity. Available via Online. https://ec.europa.eu/info/index_en. Cited 21 Nov 2022.
[24] Department of Energy and Climate Change, UK. (2009) Smarter Grids: The Opportunity. Available via Online. http://www.decc.gov.uk/. Cited 01 Feb 2021.
[25] J. Momoh, *Smart grid*. Hoboken, NJ: Wiley, 2012.
[26] T. Ackermann, G. Andersson and L. Söder, "Distributed Generation: A Definition", *Electric Power Systems Research*, vol. 57, pp. 195–204, 2001.
[27] S. Santoso, *Fundamentals of electric power quality.* Austin, TX: Published by Surya Santoso through CreateSpace, 2012.
[28] P. Kang, W. Guo, W. Huang, J. Le and T. Mao, "Power Quality Problem and Key Improvement Technology for Regional Power Grids", *International Journal of Emerging Electric Power Systems*, vol. 21, no. 3, 2020. Available: 10.1515/ijeeps-2019–0243.
[29] De la Rosa, F. *Harmonics and power systems*. Boca Raton: CRC press, pp. 1–184, 2006.
[30] S. Kasthala, Krishnapriya and R. Saka "Design and Development of Protective Circuit against Voltage Disturbances", *International Journal of Recent Trends in Engineering and Research*, vol. 4, no. 1, pp. 25–29, 2018. Available: 10.23883/ijrter.2018.4005.cejxl.
[31] F II, I. *IEEE recommended practices and requirements for harmonic control in electrical power systems*. New York, NY: IEEE, p. 1, 1993.
[32] J. Arrillaga and N. Watson, *Power system harmonics*. Chichester: John Wiley & Sons, 2004.
[33] T. Dhadbanjan and S. Vanjari, "Linear Programming Approach for Power System State Estimation Using Upper Bound Optimization Techniques", *International Journal of Emerging Electric Power Systems*, vol. 11, no. 3, 2010. Available: 10.2202/1553-779x.2464.
[34] P. Fortenbacher and T. Demiray, "Linear/Quadratic Programming-based Optimal Power Flow Using Linear Power Flow and Absolute Loss Approximations", *International Journal of Electrical Power & Energy Systems*, vol. 107, pp. 680–689, 2019. Available: 10.1016/j.ijepes.2018.12.008.
[35] D. Simon, *Evolutionary optimization algorithms*. Hoboken, NJ: John Wiley & Sons Inc, 2013.
[36] S. Morgan, *The water cycle*. New York: Rosen Pub. Group/PowerKids Press, 2009.

[37] M. Ameca-Alducin, E. Mezura-Montes and N. Cruz-Ramírez, "Dynamic Differential Evolution with Combined Variants and a Repair Method to Solve Dynamic Constrained Optimization Problems: An Empirical Study", *Soft Computing*, vol. 22, no. 2, pp. 541–570, 2016. Available: 10.1007/s00500-016-2353-1

[38] A. Mortazavi, V. Togan and A. Nuhoglu, "An Integrated Particle Swarm Optimizer for Optimization of Truss Structures with Discrete Variables", *Structural Engineering and Mechanics*, vol. 61, no. 3, pp. 359–370, 2017. Available: 10.12989/sem.2017.61.3.359.

[39] K. Mistry and R. Roy, "Enhancement of Loading Capacity of Distribution System Through Distributed Generator Placement Considering Techno-economic Benefits with Load Growth", *International Journal of Electrical Power & Energy Systems*, vol. 54, pp. 505–515, 2014.

[40] T. Chen and N. Yang, "Three-phase Power-flow by Direct ZBR Method for Unbalanced Radial Distribution Systems", *IET Generation, Transmission & Distribution*, vol. 3, no. 10, pp. 903–910, 2009.

[41] D. Xia and G. T. Heydt, "Harmonic Power Study Part I – Formulation and Solution", *IEEE Transmission Power Application System*, vol. PAS-101, no. 6, pp. 1257–1265, Jun. 1982.

[42] D. Xia and G. T. Heydt, "Harmonic Power Study Part II – Implementation and Practical Application", *IEEE Transmission Power Application System*, vol. PAS-11, no. 6, pp. 1266–1270, Jun. 1982.

[43] S. Mekhamer, A. Abdelaziz and S. Ismael, "Design Practices in Harmonic Analysis Studies Applied to Industrial Electrical Power Systems", *Engineering, Technology & Applied Science Research*, vol. 3, no. 4, pp. 467–472, 2013. Available: 10.48084/etasr.309.

[44] S. Herraiz, L. Sainz, and J. Clua, "Review of Harmonic Load Flow Formulations," *IEEE Transmission Power Deletion*, vol. 18, no. 3, pp. 1079–1087, Jul. 2003.

[45] C. Kocaman and M. Özdemir, "Determining Five Kinds of Power Quality Disturbances by Using Statistical Methods and Wavelet Energy Coefficients", *Renewable Energy and Power Quality Journal*, vol. 1, no. 15, pp. 745–750, 2017. Available: 10.24084/repqj15.455.

[46] A. Sedighi, "Classification of Transient Phenomena in Distribution System Using Wavelet Transform", *Journal of Electrical Engineering*, vol. 65, no. 3, pp. 144–150, 2014. Available: 10.2478/jee-2014–0022.

[47] J. Teng and C. Chang, "Backward/Forward Sweep-Based Harmonic Analysis Method for Distribution Systems", *IEEE Transactions on Power Delivery*, vol. 22, no. 3, pp. 1665–1672, 2007.

[48] S. Saha and V. Mukherjee, "Optimal Placement and Sizing of DGs in RDS Using Chaos Embedded SOS Algorithm", *IET Generation Transmission Distribution*, vol. 10, no. 14, pp. 3671–3680, Apr. 2016.

[49] M. Khalid, U. Akram and S. Shafiq, "Optimal Planning of Multiple Distributed Generating Units and Storage in Active Distribution Networks", *IEEE Access*, vol. 6, pp. 55234–55244, 2018. Available: 10.1109/access.2018.2872788.

[50] A. Abou El-Ela, R. El-Sehiemy, A.-M. Kinawy, and E. S. Ali, "Optimal placement and sizing of distributed generation units using different cat swarm optimization algorithms," in *Proceedings of the IEEE 2016 18th International Middle East Power System Conference*, Cairo, Egypt, 2016, pp. 975–981.

[51] A. Ghaweta, "Optimal Distribution Feeder Reconfiguration with Optimal Planning of Distributed Generation for Loss Reduction and Voltage Improvement using Deferential Evolution Algorithm", *International Journal of Forensic Software Engineering*, vol. 1, no. 1, p. 1, 2019. Available: 10.1504/ijfse.2019.10024915.

[52] S. Remha, "Optimal DG Location and Sizing for Minimum Active Power Loss in Radial Distribution System using Firefly Algorithm", *International Journal of Energetica*, vol. 2, no. 1, p. 6, 2017. Available: 10.47238/ijeca.v2i1.20.

[53] M. H. Amini, M. P. Moghaddam, and O. Karabasoglu, "Simultaneous Allocation of Electric Vehicles' Parking Lots and Distributed Renewable Resources in Smart Power Distribution Networks," *Sustainable Cities Society*, vol. 28, pp. 332–342, 2017.

[54] A. Elsayed, M. Mishref and S. Farrag, "Optimal Allocation and Control of Fixed and Switched Capacitor Banks on Distribution Systems Using Grasshopper Optimisation Algorithm with Power Loss Sensitivity and Rough Set Theory", *IET Generation, Transmission & Distribution*, vol. 13, no. 17, pp. 3863–3878, 2019. Available: 10.1049/iet-gtd.2018.5494.

[55] A. Shaheen, R. El-Sehiemy and S. Farrag, "Adequate Planning of Shunt Power Capacitors Involving Transformer Capacity Release Benefit", *IEEE Systems Journal*, vol. 12, no. 1, pp. 373–382, 2018. Available: 10.1109/jsyst.2015.2491966.

[56] M. Doostan, S. Navaratnan, S. Mohajeryami, and V. Cecchi, "Concurrent Placement of Distributed generation resources and capacitor banks in distribution systems," in Proc. 2016 North Amer. Power Symp., Nov. 2016,pp. 1–6.

[57] J. Vuletić and M. Todorovski, "Optimal Capacitor Placement in Distorted Distribution Networks with Different Load Models Using Penalty Free Genetic Algorithm", *International Journal of Electrical Power & Energy Systems*, vol. 78, pp. 174–182, 2016. Available: 10.1016/j.ijepes.2015.11.065.

[58] O. Mahela, "Optimal Capacitor Placement Techniques in Transmission and Distribution Networks to Reduce Line Losses and Voltage Stability Enhancement: A Review", *IOSR Journal of Electrical and Electronics Engineering*, vol. 3, no. 4, pp. 01–08, 2012. Available: 10.9790/1676–0340108.

[59] A. Kaur, "Different Tactics of Capacitor Placement in Distribution System. A Retrospection", *International Journal of Advance Engineering and Research Development*, vol. 2, no. 12, 2015. Available: 10.21090/ijaerd.021272.

[60] A. M. Shaheen, R. A. El-Sehiemy, and S. M. Farrag, "A Novel Adequate Bi-level Reactive Power Planning Strategy," *International Journal of Electronic Power Energy System*, vol. 78, pp. 897–909, 2016.

[61] A. K. Saonerkar and B. Y. Bagde, "Optimized DG Placement in Radial Distribution System with Reconfiguration and Capacitor Placement Using Genetic Algorithm," in *Proc. 2014 Int. Conf. Adv. Commun. Contr. Comput.Technol*., May 2014, pp. 1077–1083.

[62] M. Jannat and A. Savi´c, "Optimal Capacitor Placement in Distribution Networks Regarding Uncertainty in Active Power Load and DG Units Production," *IET Generation Transmission Distribution*, vol. 10, pp. 3060–3067, 2016.

[63] A. M. Imran, M. Kowsalya, and D. P. Kothari, "A Novel Integration Technique for Optimal Network Reconfiguration and Distributed Generation Placement in Power Distribution Networks," *International Journal of Electronic Power Energy System*, vol. 63, pp. 461–472, 2014.

[64] M. Kefayat, A. L. Ara, and S. N. Niaki, "A Hybrid of Ant Colony Optimization and Artificial Bee Colony Algorithm for Probabilistic Optimal Placement and Sizing of Distributed Energy Resources," *Energy Conversation Management*, vol. 92, pp. 149–161, 2015.

[65] C. Lee, H. Ayala and L. Coelho, "Capacitor Placement of Distribution Systems Using Particle Swarm Optimization Approaches", *International Journal of Electrical Power & Energy Systems*, vol. 64, pp. 839–851, 2015. Available: 10.1016/j.ijepes.2014.07.069.

[66] A. Abou El-Ela, M. Mouwafi, A. Kinawy and R. El-Sehiemy, "Optimal Capacitor Placement in Distribution Systems for Power Loss Reduction and Voltage Profile Improvement", *IET Generation, Transmission & Distribution*, vol. 10, no. 5, pp. 1209–1221, 2016.

[67] A. Abou El-Ela, A. Kinawy, M. Mouwafi and R. El-Sehiemy, "Optimal Sitting and Sizing of Capacitors for Voltage Enhancement of Distribution Systems," in *Proc. 2015 50th Int. Univ. Power Eng. Conf.*, 2015, pp. 1–6.

[68] Energy licenses and licensing procedures. (no date) *Public-Private-Partnership Legal Resource Center.* Available via Online. https://ppp.worldbank.org/public-private-partnership/library/egyptian-electric-utility-and-consumer-protection-regulatory-agency-egyptera. Cited 22 Nov 2022.

[69] M. Kowsalya, "Optimal Distributed Generation and Capacitor Placement in Power Distribution Networks for Power Loss Minimization," in *Proc. 2014 Int. Conf. Adv. Electr. Eng.*, Jan. 2014, pp. 1–6.

[70] A. Askarzadeh, "Capacitor placement in distribution systems for power loss reduction and voltage improvement: A new methodology," *IET Generation, Transmission & Distribution*, vol. 10, no. 14, pp. 3631–3638, 2016.

[71] R. S. Rao, K. Ravindra, K. Satish, and S. V. L. Narasimham, "Power Loss Minimization in Distribution System Using Network Reconfiguration in the Presence of Distributed Generation," *IEEE Transmission Power System*, vol. 28, no. 1, pp. 317–325, Feb. 2013.

[72] N. K. Meena, A. Swarnkar, N. Gupta, and K. R. Niazi, "A Taguchi-based Approach for Optimal Placement of Distributed Generations for Power Loss Minimization in Distribution System," in *Proc. 2015 IEEE Power Energy Soc. Gen. Meet.*, Jul. 2015, pp. 1–5.

[73] M. H. Moradi and M. Abedini. "A Combination of Genetic Algorithm and Particle Swarm Optimization for Optimal DG Location and Sizing in Distribution Systems," *International Journal of Electronic Power Energy System*, vol. 34, no. 1, pp. 66–74, 2012.

[74] S. Salimon, A. Baruwa, S. Amuda and H. Adeleke, "Optimal Placement and Sizing of Capacitors in Radial Distribution Systems: A Two-Stage Method", *Journal of Engineering Research and Reports*, pp. 31–43, 2020. Available: 10.9734/jerr/2020/v19i217229.

[75] Ivanov, Neagu, Grigoras and Gavrilas, "Optimal Capacitor Bank Allocation in Electricity Distribution Networks Using Metaheuristic Algorithms", *Energies*, vol. 12, no. 22, p. 4239, 2019. Available: 10.3390/en12224239.

[76] A. El-Fergany and A. Abdelaziz, "Capacitor Allocations in Radial Distribution Networks Using Cuckoo Search Algorithm," *IET Generation, Transmission & Distribution*, vol. 8, no. 2, pp. 223–232, 2014.

[77] S. Sultana and P. Roy, "Optimal Capacitor Placement in Radial Distribution Systems Using Teaching Learning Based Optimization," *International Journal of Electronic Power Energy System* , vol. 54, pp. 387–398, 2014.

[78] Y. Shuaib, M. Kalavathi, and C. Rajan, "Optimal Capacitor Placement in Radial Distribution System Using Gravitational Search Algorithm," *International Journal of Electronic Power Energy System*, vol. 64, pp. 384–397, 2015.

[79] M. Raju, K. Murthy, and K. Ravindra, "Direct Search Algorithm for Capacitive Compensation in Radial Distribution Systems," *International Journal of Electronic Power Energy System*, vol. 42, no. 1, pp. 24–30, 2012.

[80] C. Wang and Y. Gao, "Determination of Power Distribution Network Configuration Using Non-Revisiting Genetic Algorithm", *IEEE Transactions on Power Systems*, vol. 28, no. 4, pp. 3638–3648, 2013. Available: 10.1109/tpwrs.2013.2238259.

[81] A. Abubakar, K. Ekundayo and A. Olaniyan, "Optimal Reconfiguration of Radial Distribution Networks Using Improved Genetic Algorithm", *Nigerian Journal of Technological Development*, vol. 16, no. 1, p. 10, 2019. Available: 10.4314/njtd.v16i1.2.

[82] A. Gantayet and S. Mohanty, "An Analytical Approach for Optimal Placement and Sizing of Distributed Generation Based on a Combined Voltage Stability Index," in *Proc. 2015 IEEE Power, Commun. Inf. Technol. Conf.*, Oct. 2015, pp. 762–767

[83] Z. Juan, G. Yi-nan and Z. Shu-ying, "Optimal Design of Passive Power Filters of an Asymmetrical System Based on Genetic Algorithm", *Procedia Earth and Planetary Science*, vol. 1, no. 1, pp. 1440–1447, 2009.
[84] Q. Zheng and J. Lu, "Passive Filter Design Based on Non-dominated Sorting Genetic Algorithm II", *Computer Measure & Control*, vol. 15, pp. 135–137, 2007.
[85] S. Zhao and J. Li, "Adaptive Evolutionary Design of Passive Power Filters in Hybrid Power Filter System", *Automation of Electric Power Systems*, vol. 28, pp. 54–57, 2004.
[86] C. Tu, "Passive Filter's Optimization Design of the Multi-objective", *CSEE*, vol. 22, pp. 17–21, 2002.
[87] X. Zhu, Simulated Annealing Based Multi-Object Optimal Planning of Passive Power Filters, *2005 IEEE/PES Transmission and Distribution Conference & Exhibition*, 2005.
[88] M. Balci, "Optimal C-Type Filter Design to Maximize Transformer's Loading Capability under Non-sinusoidal Conditions", *Electric Power Components and Systems*, vol. 42, no. 14, pp. 1565–1575, 2014.
[89] S. Abdel Aleem, A. Zobaa and M. Abdel Aziz, "Optimal C-Type Passive Filter Based on Minimization of the Voltage Harmonic Distortion for Nonlinear Loads", *IEEE Transactions on Industrial Electronics*, vol. 59, no. 1, pp. 281–289, 2012.
[90] A. Zobaa and S. Aleem, "A New Approach for Harmonic Distortion Minimization in Power Systems Supplying Nonlinear Loads", *IEEE Transactions on Industrial Informatics*, vol. 10, no. 2, pp. 1401–1412, 2014.
[91] M. ZAGIRNYAK, "An Analytical Method for Calculation of Passive Filter Parameters with the Assuring of the Set Factor of the Voltage Supply Total Harmonic Distortion", *PRZEGLĄD ELEKTROTECHNICZNY*, vol. 1, no. 12, pp. 197–200, 2017.
[92] A. Bracale, P. Caramia, G. Carpinelli, A. Russo and P. Verde, "Site and System Indices for Power-Quality Characterization of Distribution Networks With Distributed Generation", *IEEE Transactions on Power Delivery*, vol. 26, no. 3, pp. 1304–1316, 2011.
[93] P. Paliwal, N. Patidar and R. Nema, "Planning of Grid Integrated Distributed Generators: A Review of Technology, Objectives and Techniques", *Renewable and Sustainable Energy Reviews*, vol. 40, pp. 557–570, 2014.
[94] L. Li, H. Mu, N. Li and M. Li, "Economic and Environmental Optimization for Distributed Energy Resource Systems Coupled with District Energy Networks", *Energy*, vol. 109, pp. 947–960, 2016.
[95] R. Walling, R. Saint, R. Dugan, J. Burke and L. Kojovic, "Summary of Distributed Resources Impact on Power Delivery Systems", *IEEE Transactions on Power Delivery*, vol. 23, no. 3, pp. 1636–1644, 2008.
[96] H. Hu, Q. Shi, Z. He, J. He and S. Gao, "Potential Harmonic Resonance Impacts of PV Inverter Filters on Distribution Systems", *IEEE Transactions on Sustainable Energy*, vol. 6, no. 1, pp. 151–161, 2015.
[97] M. Ertay, S. Tosun, and A. Zengin, "Simulated Annealing Based Passive Power Filter Design for a Medium Voltage Power System", *Innovations in Intelligent Systems and Applications (INISTA)*, pp. 1–5, 2012.
[98] A. Abou El-Ela, S. Allam and H. El-Arwash, "An Optimal Design of Single Tuned Filter in Distribution Systems", *Electric Power Systems Research*, vol. 78, no. 6, pp. 967–974, 2008.
[99] P. Stone, J. Wang, Y. Shin and R. Dougal, "Efficient Harmonic Filter Allocation in an Industrial Distribution System", *IEEE Transactions on Industrial Electronics*, vol. 59, no. 2, pp. 740–751, 2012.

[100] M. Mohammadi, A. Rozbahani and M. Montazeri, "Multi Criteria Simultaneous Planning of Passive Filters and Distributed Generation Simultaneously in Distribution System Considering Nonlinear Loads with Adaptive Bacterial Foraging Optimization Approach", *International Journal of Electrical Power & Energy Systems*, vol. 79, pp. 253–262, 2016.

[101] N. Ghaffarzadeh and H. Sadeghi, "A New Efficient BBO Based Method for Simultaneous Placement of Inverter-based DG Units and Capacitors Considering Harmonic Limits", *International Journal of Electrical Power & Energy Systems*, vol. 80, pp. 37–45, 2016.

[102] A. Abbas, E. Ali, R. El-Sehiemy, A. Abou El-Ela and K. Fetyan, "Comprehensive Parametric Analysis of Single Tuned Filter in Distribution Systems", in *2019 21st International Middle East Power Systems Conference (MEPCON)*, Cairo, 2019.

[103] M. El -Sayed, A. Abou El-Ela and R. El-Sehiemy, "Effect of Photovoltaic System on Power Quality in Electrical Distribution Networks", in *International Middle East Power Systems*, Cairo, pp. 1005–1012, 2016.

[104] J. Cabral Leite, I. Pérez Abril and M. Santos Azevedo, "Capacitor and Passive Filter Placement in Distribution Systems by Non-dominated Sorting Genetic Algorithm-II", *Electric Power Systems Research*, vol. 143, pp. 482–489, 2017.

[105] A. Ulinuha, M. Masoum and S. Islam, "Hybrid Genetic-fuzzy Algorithm for Volt/var/total Harmonic Distortion Control of Distribution Systems with High Penetration of Non-linear Loads", *IET Generation, Transmission & Distribution*, vol. 5, no. 4, p. 425, 2011.

Appendix A: Test Systems

A.1 IEEE 33-BUS DISTRIBUTION TEST SYSTEM

The configuration of the 33-bus test system is shown in Figure A.1 (with IEEE numbering) and Figure A.2 (with the numbering used in this book). The total active and reactive loads of the system are 3.715+j2.3 MVA. The system data is listed in Table A.1.

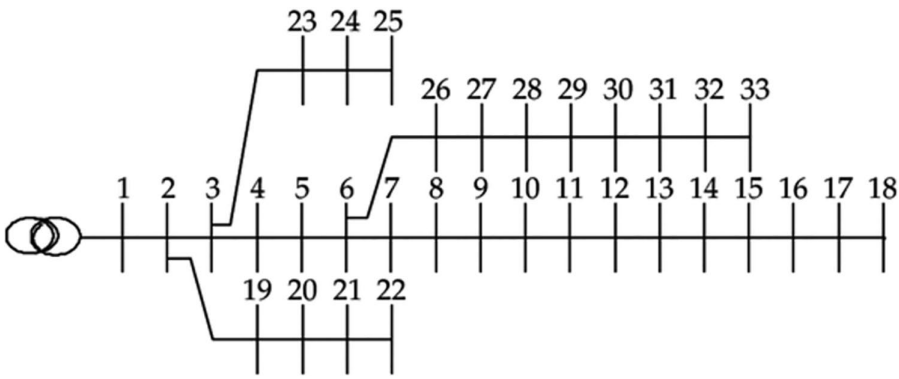

FIGURE A.1 IEEE 33-bus test system with IEEE numbering.

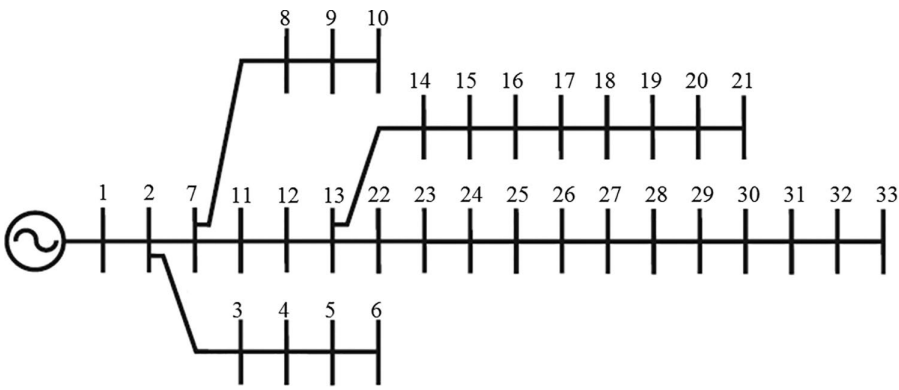

FIGURE A.2 IEEE 33-bus test system with the numbering of the load flow.

TABLE A.1
IEEE 33-Bus Test System Data

Line Number	From	To	R (Ω)	X (Ω)	P_{load} (MW)	Q_{load} (MVAR)
1	1	2	0.0922	0.0470	0.1000	0.0600
2	2	3	0.4930	0.2511	0.0900	0.0400
3	3	4	0.3660	0.1864	0.1200	0.0800
4	4	5	0.3811	0.1941	0.0600	0.0300
5	5	6	0.8190	0.7070	0.0600	0.0200
6	6	7	0.1872	0.6188	0.2000	0.1000
7	7	8	1.7114	1.2351	0.2000	0.1000
8	8	9	1.0300	0.7400	0.0600	0.0200
9	9	10	1.0440	0.7400	0.0600	0.0200
10	10	11	0.1966	0.0650	0.0450	0.0300
11	11	12	0.3744	0.1238	0.0600	0.0350
12	12	13	1.4680	1.1550	0.0600	0.0350
13	13	14	0.5416	0.7129	0.1200	0.0800
14	14	15	0.5910	0.5260	0.0600	0.0100
15	15	16	0.7463	0.5450	0.0600	0.0200
16	16	17	1.2890	1.7210	0.0600	0.0200
17	17	18	0.7320	0.5740	0.0900	0.0400
18	2	19	0.1640	0.1565	0.0900	0.0400
19	19	20	1.5042	1.3554	0.0900	0.0400
20	20	21	0.4095	0.4784	0.0900	0.0400
21	21	22	0.7089	0.9373	0.0900	0.0400
22	3	23	0.4512	0.3083	0.0900	0.0500
23	23	24	0.8980	0.7091	0.4200	0.2000
24	24	25	0.8960	0.7011	0.4200	0.2000
25	6	26	0.2030	0.1034	0.0600	0.0250
26	26	27	0.2842	0.1447	0.0600	0.0250
27	27	28	1.0590	0.9337	0.0600	0.0200
28	28	29	0.8042	0.7006	0.1200	0.0700
29	29	30	0.5075	0.2585	0.2000	0.6000
30	30	31	0.9744	0.9630	0.1500	0.0700
31	31	32	0.3105	0.3619	0.2100	0.1000
32	32	33	0.3410	0.5302	0.0600	0.0400

A.2 IEEE 69-BUS TEST SYSTEM

The configuration of the 69-bus test system is shown in Figure A.3 (with IEEE numbering) and Figure A.4 (with the numbering used in this book). The total active and reactive loads of the system are 3.802+j2.694 MVA. The system data is listed in Table A.2. The data is listed according to the IEEE numbering.

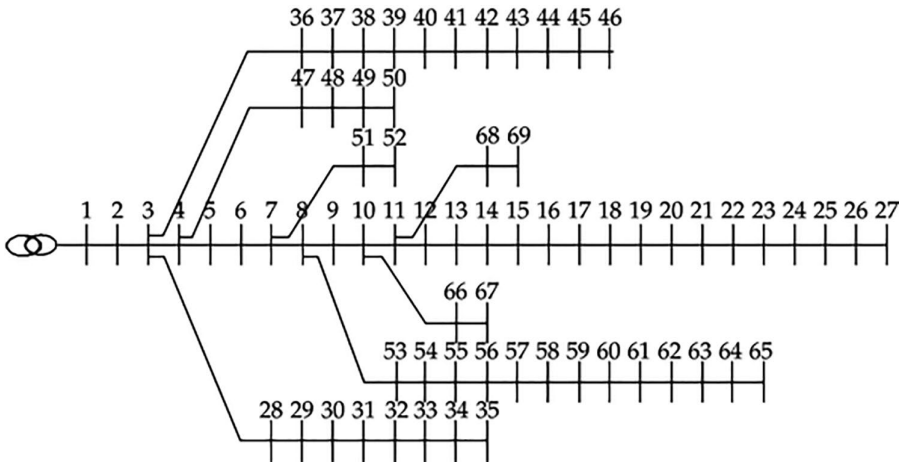

FIGURE A.3 IEEE 69-bus test system with IEEE numbering.

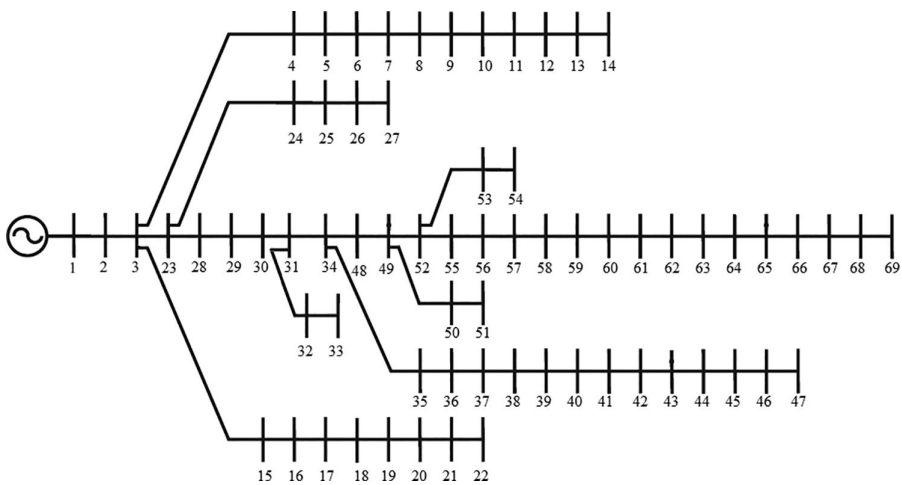

FIGURE A.4 IEEE 69-bus test system with the numbering of the load flow.

TABLE A.2
IEEE 69-Bus Test System Data

Line Number	From	To	R (Ω)	X (Ω)	P_{load} (MW)	Q_{load} (MVAR)
1	1	2	0.0005	0.0012	0	0
2	2	3	0.0005	0.0012	0	0
3	3	4	0.0015	0.0036	0	0
4	4	5	0.0251	0.0294	0	0
5	5	6	0.366	0.1864	0.0026	0.0022
6	6	7	0.381	0.1941	0.0404	0.03
7	7	8	0.0922	0.047	0.075	0.054
8	8	9	0.0493	0.0251	0.03	0.022
9	9	10	0.819	0.2707	0.028	0.019
10	10	11	0.1872	0.0619	0.145	0.104
11	11	12	0.7114	0.2351	0.145	0.104
12	12	13	1.03	0.34	0.008	0.005
13	13	14	1.044	0.345	0.008	0.0055
14	14	15	1.058	0.3496	0	0
15	15	16	0.1966	0.065	0.0455	0.03
16	16	17	0.3744	0.1238	0.06	0.035
17	17	18	0.0047	0.0016	0.06	0.035
18	18	19	0.3276	0.1083	0	0
19	19	20	0.2106	0.069	0.001	0.0006
20	20	21	0.3416	0.1129	0.114	0.081
21	21	22	0.014	0.0046	0.005	0.0035
22	22	23	0.1591	0.0526	0	0
23	23	24	0.3463	0.1145	0.028	0.02
24	24	25	0.7488	0.2475	0	0
25	25	26	0.3089	0.1021	0.014	0.01
26	26	27	0.1732	0.0572	0.014	0.01
27	3	28	0.0044	0.0108	0.026	0.0186
28	28	29	0.064	0.1565	0.026	0.0186
29	29	30	0.3978	0.1315	0	0
30	30	31	0.0702	0.0232	0	0
31	31	32	0.351	0.116	0	0
32	32	33	0.839	0.2816	0.014	0.01
33	33	34	1.708	0.5646	0.0195	0.014
34	34	35	1.474	0.4873	0.006	0.004
35	3	36	0.0044	0.0108	0.026	0.0186
36	36	37	0.064	0.1565	0.026	0.0186
37	37	38	0.1053	0.123	0	0

Line Number	From	To	R (Ω)	X (Ω)	P_{load} (MW)	Q_{load} (MVAR)
38	38	39	0.0304	0.0355	0.024	0.017
39	39	40	0.0018	0.0021	0.024	0.017
40	40	41	0.7283	0.8509	0.0012	0.001
41	41	42	0.31	0.3623	0	0
42	42	43	0.041	0.0478	0.006	0.0043
43	43	44	0.0092	0.0116	0	0
44	44	45	0.1089	0.1373	0.0392	0.0263
45	45	46	0.0009	0.0012	0.0392	0.0263
46	4	47	0.0034	0.0084	0	0
47	47	48	0.0851	0.2083	0.079	0.0564
48	48	49	0.2898	0.7091	0.3847	0.2745
49	49	50	0.0822	0.2011	0.3847	0.2745
50	8	51	0.0928	0.0473	0.0405	0.0283
51	51	52	0.331	0.1114	0.0036	0.0027
52	9	53	0.174	0.0886	0.0043	0.0035
53	53	54	0.203	0.1034	0.0264	0.019
54	54	55	0.2842	0.1447	0.024	0.0172
55	55	56	0.2813	0.1433	0	0
56	56	57	1.59	0.5337	0	0
57	57	58	0.7837	0.263	0	0
58	58	59	0.3042	0.1006	0.1	0.072
59	59	60	0.3861	0.1172	0	0
60	60	61	0.5075	0.2585	1.244	0.888
61	61	62	0.0974	0.0496	0.032	0.023
62	62	63	0.145	0.0738	0	0
63	63	64	0.7105	0.3619	0.227	0.162
64	64	65	1.041	0.5302	0.059	0.042
65	11	66	0.2012	0.0611	0.018	0.013
66	66	67	0.0047	0.0014	0.018	0.013
67	12	68	0.7394	0.2444	0.028	0.02
68	68	69	0.0047	0.0016	0.028	0.02

A.3 REAL EAST DELTA NETWORK (EDN)

EDN is a real part of the Egyptian distribution network. It consists of 30-bus with total active and reactive loads of 22.441 MW and 14.162 MVAR, respectively. The configuration of the EDN test system is shown in Figure A.5. Total active power loss in the initial case equals 805.73kW. The system data is listed in Table A.3.

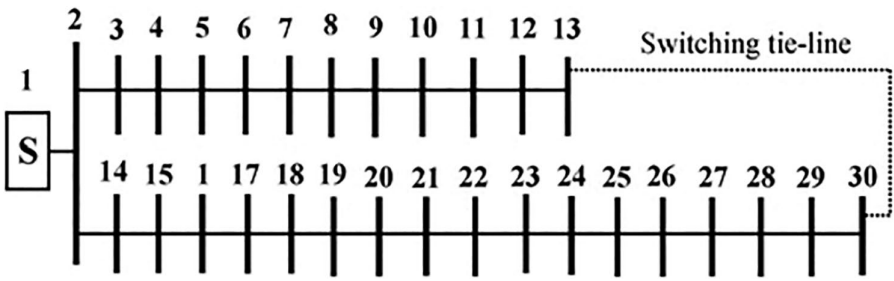

FIGURE A.5 Single line diagram of the EDN distribution system.

TABLE A.3
Bus and Line Data for EDN Distribution System

Line No.	Sending Bus	Receiving Bus	R (Ω)	X (Ω)	Load at Receiving Bus	
					P (kW)	Q (kVAR)
1	1	2	0.05630	0.031500	2875	1814
2	2	3	0.07155	0.025974	1100	695
3	3	4	0.01855	0.006734	1058	669
4	4	5	0.05565	0.020202	899	568
5	5	6	0.05300	0.019240	770	486
6	6	7	0.05300	0.019240	668	423
7	7	8	0.02120	0.007696	598	378
8	8	9	0.10070	0.036556	546	345
9	9	10	0.04505	0.016354	380	240
10	10	11	0.03975	0.014430	210	132
11	11	12	0.11130	0.040404	94.586	59.368
12	12	13	0.01325	0.004810	34.423	21.518
13	2	14	0.06360	0.023088	1772	1118
14	14	15	0.07155	0.025974	1640	1035
15	15	16	0.02650	0.009620	1452	915
16	16	17	0.01060	0.003848	1434	904
17	17	18	0.09275	0.033670	1212	765
18	18	19	0.01060	0.003848	1086	685
19	19	20	0.02650	0.009620	953	602
20	20	21	0.04505	0.016354	827	521
21	21	22	0.05300	0.019240	716	452
22	22	23	0.05300	0.019240	550	347
23	23	24	0.0663	0.0240	434	273
24	24	25	0.2253	0.0818	346	218
25	25	26	0.0265	0.0096	316	199
26	26	27	0.0265	0.0096	184	116
27	27	28	0.0133	0.0048	139	87.911
28	28	29	0.1723	0.0625	113	71.734
29	29	30	0.0080	0.0029	34.25	21.734